FDL-TDR-64-13,
Vol. I

FEASIBILITY STUDY OF NEW TECHNIQUES FOR CONTROL OF RE-ENTRY VEHICLES

Vol. I. Calculation of Optimal Trajectories and Synthesis of Control Functions

TECHNICAL DOCUMENTARY REPORT NO. FDL-TDR-64-13, Vol. I.
March 1964

Flight Dynamics Laboratory
Research and Technology Division
Air Force Systems Command
Wright-Patterson Air Force Base, Ohio

Project No. 8225, Task No. 822181

[Prepared under Contract No. AF33(657)-7383 by the Research Department, Military Products Group, Minneapolis-Honeywell Regulator Company, Minneapolis, Minnesota; D. K. Scharmack, G. D. Swanlund, M. D. Ward, R. G. Johnson, and E. R. Rang, authors]

NOTICES

When Government drawings, specifications, or other data are used for any purpose other than in connection with a definitely related Government procurement operation, the United States Government thereby incurs no responsibility nor any obligation whatsoever; and the fact that the Government may have formulated, furnished, or in any way supplied the said drawings, specifications, or other data, is not to be regarded by implication or otherwise as in any manner licensing the holder or any other person or corporation, or conveying any rights or permission to manufacture, use, or sell any patented invention that may in any way be related thereto.

Qualified requesters may obtain copies of this report from the Defense Documentation Center (DDC), (formerly ASTIA), Cameron Station, Bldg. 5, 5010 Duke Street, Alexandria 4, Virginia

This report has been released to the Office of Technical Services, U.S. Department of Commerce, Washington 25, D.C., in stock quantities for sale to the general public.

Copies of this report should not be returned to the Aeronautical Systems Division unless return is required by security considerations, contractual obligations, or notice on a specific document.

FDL-TDR-64-13,
Vol. I

FEASIBILITY STUDY OF NEW TECHNIQUES FOR CONTROL OF RE-ENTRY VEHICLES

Vol. I. Calculation of Optimal Trajectories and Synthesis of Control Functions

TECHNICAL DOCUMENTARY REPORT NO. FDL-TDR-64-13, Vol. I.
March 1964

Flight Dynamics Laboratory
Research and Technology Division
Air Force Systems Command
Wright-Patterson Air Force Base, Ohio

Project No. 8225, Task No. 82181

[Prepared under Contract No. AF33(657)-7383 by the Research Department, Military Products Group, Minneapolis-Honeywell Regulator Company, Minneapolis, Minnesota; D. K. Scharmack, G. D. Swanlund, M. D. Ward, R. G. Johnson, and E. R. Rang, authors]

FOREWORD

This document is the first of two volumes comprising the final report on a feasibility study of techniques for the control of re-entry vehicles. The research was sponsored by the Flight Dynamics Laboratory, RTD, under Task No. 82181 of Project No. 8225 and Contract No. AF33(657)-7383 with the Minneapolis-Honeywell Regulator Company, Minneapolis, Minnesota. Lt. E. B. Stear was the RTD project officer for this program. Work at Honeywell was performed by the Systems Techniques group of the Military Products Research department under the supervision of J. T. Van Meter. Project personnel were: G. D. Swanlund and D. K. Scharmack, principal investigators, and M. D. Ward, R. G. Johnson, L. D. Dolid, D. L. Lukes, W. C. Marshall, and E. R. Rang.

The first volume of this report, "Calculation of Optimal Trajectories and Synthesis of Control Functions", presents the mathematical models, the development of theory and the results of the numerical calculations for a two-year study of controlled re-entry vehicles. The digital computer programs developed and used in this effort are documented in Volume 2, "Computer Programs". These reports are designated as Honeywell MPG Documents 1535-TR2, Volumes 1 and 2.

The encouragement, assistance, and direction provided by Lt. Edwin B. Stear is gratefully acknowledged.

Some of the digital computation was conducted at the RTD computation center.

ABSTRACT

Optimization techniques are used to synthesize the control programs and compute the corresponding flight paths for controllable re-entry vehicles. Linear perturbation control about these reference trajectories is investigated.

A large portion of the theory of the calculus of variations is modified and extended to apply to this problem. Many details of computational techniques, necessary in the adaptation of the theory to large scale digital calcuation, are reported. The optimization method which evolves is a modification of a Newton-Raphson iteration, although gradient procedures are also studied.

The criteria for re-entry trajectories are functionals of the motion related to the heating of the vehicle. It is found that these criteria are relatively insensitive to the flight path, and this fact leads to computational problems which must be handled carefully. The paths and control authority are constrained by reasonable physical requirements.

The linear perturbational control is found by requiring the integral of the square of the control deviation to be minimum. The vehicle position is the object of control in the cases studied. It is found that this form of control can be used throughout the entire re-entry corridor. Various modifications of the control gain program at the end of the trajectory are considered.

This technical documentary report has been reviewed and is approved.

Technical Director
Flight Dynamics Laboratory

CONTENTS

ILLUSTRATIONS

ILLUSTRATIONS (Continued)

ILLUSTRATIONS (Continued)

TABLES

SYMBOLS

a_t	acceleration along velocity axis, ft/sec^2
a_n	acceleration normal to velocity axis, ft/sec^2
a_p	total acceleration due to aerodynamic force, ft/sec^2
A	terminal altitude, ft.
A_4	positive-definite matrix in Newton-Raphson method
B	specified maximum value for a_p, ft/sec^2
C_D	coefficient of drag
C_L	coefficient of lift
C_{DO}, C_{DL}, C_{LO}	aerodynamic coefficient constants
f_o	integrand in J
E(t)	feedback gain matrix
F	generalized Lagrangian for optimization problem
g	function of terminal state in J
g_o	nominal gravity at surface of earth, ft/sec^2
G	inequality constraint vector
h	altitude, ft.
H	Hamiltonian
J	function to be minimized
m	vehicle mass
p	multiplier, or adjoint, vector
p_o	initial multiplier vector
$\dot{q}$	heating rate, a function of the path, $BTU/ft^2/sec$
$\dot{Q}$	specified constant heating rate, $BTU/ft^2/sec$
$\dot{q}_c$	corrective heating rate
$\dot{q}_r$	radiative heating rate
R	radius of the earth, ft.
$\tilde{R}$	terminal range, ft.
S	aerodynamic reference area, ft^2
T	terminal time, sec.

SYMBOLS (Cont'd.)

u	control vector for optimal trajectory
U	any admissible control vector
v	velocity, ft/sec.
V	terminal velocity, ft/sec.
x	state vector
x_o	initial value of state vector
$Y(T, a)$	influence matrix
Z	zero matrix
α	angle-of-attack, deg., measured positively upward
β	atmosphere exponent coefficient, ft.$^{-1}$
γ	flight path angle, deg., measured positively upward
δ	perturbation operator (time independent)
ζ	great circle range, ft.
μ	multiplier vector for inequality constraint
ξ	dimensionless altitude
ρ	atmospheric density, slug/ft.^{3}
σ	slack variable
φ	roll angle, degrees
ψ	terminal surface vector
∇_x	gradient with respect to the control vector, x (If the operand is a vector, the result is a matrix)
∇_u	gradient with respect to the control vector, u
Δ	first variation, increment
$(\cdot)$	differentiation with respect to time
$(')$	matrix transpose

SECTION I
INTRODUCTION

COMPENDIUM

Synthesis of control for a re-entry vehicle presents many difficulties in the form of nonlinearities, constraints on the dynamical state, constraints on the control and questions of controllability and observability. These are of such importance they must be directly incorporated into the design process and cannot be considered secondary, as is done in most engineering methods. Further, there is good physical justification for minimizing certain functionals of the motion, such as heat input and acceleration effects. The re-entry problem, therefore, provides an excellent proving ground for the new optimization design techniques.

The goal of this study is to demonstrate the efficacy of these new techniques by actual synthesis and simulation of the mechanization of an automatic re-entry control scheme developed through their use. This has not yet been achieved. However, a method of automatically computing optimal re-entry trajectories has been developed and demonstrated; and a careful study of a scheme of linear control about a reference trajectory has been conducted, serving to point out sensitivities and difficulties which must be anticipated in a mechanization attempt. Many details, concerning the application of the theory of the calculus of variations to this problem and of the use of a large digital computer in trajectory and control calculations, have been studied and are reported here.

Manuscript released by authors, October 14, 1963, for publication as an FDL Technical Documentary Report.

Model for Re-entry Studies

The model chosen for these re-entry studies is two-dimensional and assumes a spherical, non-rotating earth and an exponential atmosphere. The model differential equations are a great simplification of the actual equations of motion but do represent the essential phenomena found in re-entry flights.

The velocity v, flight path angle γ, the dimensionless altitude $\xi = h/R$, and the great circle range $\zeta = R\theta$, are chosen as the components of the state x. The control is represented by the function u and is manifested by authority over the vehicle aerodynamic coefficients.

In this notation, the model equations of motion are

$$\frac{dv}{dt} = -\frac{S}{2m}\rho v^2 C_D(u) - \frac{g_o \sin\gamma}{(1+\xi)^2}$$

$$\frac{d\gamma}{dt} = \frac{S}{2m}\rho v C_L(u) + \frac{v\cos\gamma}{R(1+\xi)} - \frac{g_o\cos\gamma}{v(1+\xi)^2} \qquad (1.1)$$

$$\frac{d\xi}{dt} = \frac{v}{R}\sin\gamma$$

$$\frac{d\zeta}{dt} = \frac{v}{1+\xi}\cos\gamma \quad ,$$

where R is the radius of the earth, S and m the vehicle frontal area and mass, respectively, ρ the atmospheric density, and C_L and C_D are the aerodynamic lift and drag coefficients.

For convenience, the system (1.1) is usually represented by the vector equation

$$\dot{x} = f(x, u) . \tag{1.2}$$

Vehicles

Three vehicles are considered in these studies. The first is a high lift-drag-ratio vehicle, for which the control function is the angle of attack α. The aerodynamic coefficients, based on flat plate Newtonian flow, are

$$\begin{aligned} C_D &= C_{DO} + C_{DL} \, |\sin^3 \alpha| \\ C_L &= C_{LO} \sin\alpha \cos\alpha \, |\sin\alpha| \end{aligned} \tag{1.3}$$

in which C_{DO}, C_{DL} and C_{LO} are constants. The other two vehicles are low lift-drag-ratio Apollo-type bodies. One has a variable angle of attack, for which the coefficients are

$$\begin{aligned} C_D &= C_{DO} + C_{DL} \cos u \, , \\ C_L &= C_{LO} \sin u \quad , \quad u = e\alpha, \ e \text{ - constant.} \end{aligned} \tag{1.4}$$

The other assumes a fixed angle of attack, but uses a roll angle φ out of the plane of motion as the control function:

$$\begin{aligned} C_D &= C_{DO} \\ C_L &= C_{LO} \cos\varphi \, . \end{aligned} \tag{1.5}$$

The criteria for those optimal trajectory calculations which were studied are the minimum of the integral of heating rate deviation from a prescribed value

$$\frac{1}{T}\int_0^T (\dot{Q} - \dot{q})^2 \, dt \tag{1.6}$$

and the minimum of total heat, represented by

$$\int_0^T \dot{q} \, dt \ , \tag{1.7}$$

where $\dot{q}$ is the heating rate for the vehicle, and $\dot{Q}$ is a given constant. The vehicle described by Equations (1.3) was used with criterion (1.6), whereas the vehicle represented by (1.4) was used for the minimum total heat problem.

Studies Conducted

A considerable body of theory, based on the calculus of variations, was developed to facilitate the solution of the control optimization problem on the computer. The objective of these studies was the development of an automatic optimization method. A gradient scheme and the second-order Newton-Raphson method, using the first and second variations, are described in detail in Section II. Also presented is a Newton-Raphson scheme for the two-point boundary value problem associated with the minimization problem. Experiences with these methods, together with computer results, are given in Section III.

Linear control about a reference trajectory, found experimentally for the roll-modulated vehicle, and about an extremal trajectory for the variable angle-of-attack vehicle is derived by requiring the quadratic integral of control deviation Δu,

$$\int_0^T (\Delta u)^2 \, dt \,, \tag{1.8}$$

to be minimum. The theory and results for these studies, along with results of navigation and configuration investigations, are given in Section IV. A detailed error analysis and a sensitivity study of the controlled systems also are outlined.

This volume ends with conclusions and recommendations in Section V. The computer programs used are documented in Volume Two.

BACKGROUND

Previous Studies

Re-entry into earth atmosphere by vehicles launched from the earth or from an orbit about the earth is a problem which has received extensive analysis during the past several years. Allen, Eggers, Gazely, Lees, and Chapman (References 1 through 7) have made pioneering contributions to the understanding of re-entry. Their important work has been augmented by a multitude of studies, most significantly those of Robinson and Besonis (Ref. 8), Wong and Slye (Ref. 9), Young and Eggleston (Ref. 10), and Luidens (Ref. 11). A comprehensive list of re-entry literature would be extremely extensive.

The primary concern of the early studies was aerodynamic heating and deceleration, with the object of showing the feasibility of safe descent through the atmosphere from orbital initial velocity. The earliest studies concentrated on ballistic vehicles. Later, the effects of constant lift-drag ratios were evaluated. More recently, careful consideration has been given to modulated aerodynamic coefficients, produced by varying the angle of attack according to some stated objective (maintenance of constant deceleration for example). References 12 through 17 are examples of this work.

Many trajectories have been calculated for a wide variety of initial velocities and flight-path angles. Attempts to generalize solutions through non-dimensionalization, notably the work of Chapman (Ref. 6 and 7), and more recently Loh (Ref. 18), have been particularly rewarding.

The Safe Flight Corridor

These numerous studies resulted in clarification of the concept of a safe flight corridor. This corridor is usually described in a plot of altitude versus velocity, bounded on the lower side by heating and/or deceleration limits and on the upper side by sustained flight at maximum lift (negative lift for super-orbital velocities and positive lift for suborbital velocities). Corridor depth is used to evaluate the guidance requirements for separation of the perigees of two vacuum conic trajectories, one initiated at the upper corridor bound and the other at the lower; this is described by Chapman (Ref. 7) and Luidens (Ref. 11).

As a result of this work, the kinematics and aerodynamics of re-entry are now quite well understood.

Vehicle Dynamics and Control

Recently, attention has been given to vehicle dynamics and control during re-entry (aside from a few early studies of the oscillatory stability of re-entry bodies). Several relatively simple range and cross-range schemes have been proposed for landing-point control. References 16 and 17 are examples of this kind of investigation, based on currently established concepts and equipment mechanization.

Credit for the use of optimization techniques in determining re-entry trajectories seems due Bryson, et al (Ref. 19). This paper pointed out the possibility of using more sophisticated control over the vehicle (to minimize functionals of the motion) while still satisfying given end-point conditions. Linear control techniques were, again, first published by Bryson (Refs. 20 and 21). These methods provide the vernier adjustments to the control function made necessary by model variations, such as atmospheric density deviations and winds.

The control scheme envisioned in this report makes use of both optimal trajectories and linear control. Since Bryson's and similar calculations are not automatic but require the intervention of the person making the calculation to produce convergence of the iterations, these methods are not suitable, without modification, for on-board mechanization. The studies reported here were aimed at finding a calculation which would be automatic, converge rapidly and ensure an actual minimum for the functional.

SECTION II
OPTIMAL TRAJECTORY CALCULATIONS - THEORY

PROBLEM STATEMENT (A)

The problem considered here is a special form of the problem of Bolza as formulated by Bliss (Ref. 22) and extended to include inequality constraints by Valentine (Ref. 23). It is: Find that path which minimizes the function

$$J = (T, x(T)) + \int_0^T f_0(x, u)\, d\tau \tag{2.1}$$

subject to differential equations of the form

$$\dot{x} = f(x, u), \qquad x(0) = x_0, \tag{2.2}$$

inequality constraints

$$G(x, u) \geq 0, \tag{2.3}$$

and terminal surface equations

$$\psi(T, x(T)) = 0. \tag{2.4}$$

In the above, x and u are n and m dimensional state and control column vectors, and $(\cdot)$ represents differentiation with respect to the independent variable t. The dimension of vector Equation (2.3) is q, and that of (2.4) is r, where $r \leq n + 1$.

Following Valentine (Ref. 23), Equations (2.3) are rewritten in the form

$$\dot{\sigma}^2 = G(x, u) \tag{2.5}$$

where the components of the vector $\dot{\sigma}^2$ are $\dot{\sigma}_j^2$, $j = 1, \ldots, q$. The σ's are slack variables, introduced to complete the set of differential equations for the problem of Bolza. No more than m of the $\dot{\sigma}$'s may be zero at any point on the path.

It is assumed that $f_o(x, u)$ and the differential Equations (2.2) and (2.5) have continuous partial derivatives of at least third order in all variables in an open region S_1 about the minimizing path. Furthermore, the matrix made up of the partial derivatives of the differential equations, with respect to all derivatives and the control functions, must have rank $n + q$ at each point of the minimizing path. This ensures that the differential equations are independent. The matrix has the form

$$\begin{bmatrix} -I & \nabla_u f & Z \\ Z' & \nabla_u G & -\Sigma \end{bmatrix} \tag{2.6}$$

where I is the nxn identity matrix, Z is an nxq zero matrix, Z' is the transpose of Z, and Σ is a qxq diagonal matrix whose elements are $2\dot{\sigma}_j$.

The solution $x(t)$ of the differential Equations (2.2) and (2.5) is supposed to be continuous, with, at least, absolutely continuous first derivatives. In some instances, it will be possible to consider corners, i.e., points at which the derivatives are discontinuous. The control functions are treated as derivatives in (2.6) so they can be discontinuous, as in the bang-bang problem. Potential corners are those points at which inequality constraints change from greater than to equality states or vice versa.

They may also be defined by switching points, as in the bang-bang problem where the equality sign holds in the constraint relation. A subarc is defined as that part of the path between corners or potential corners.

Finally, the functions $g(T, x(T))$ and (2.4) are assumed to have continuous partial derivatives of at least third order in an open set S_2 of points $(T, x(T))$, and the matrix

$$\nabla\psi = \begin{bmatrix} \frac{\partial\psi_1}{\partial T} & \frac{\partial\psi_1}{\partial x_1} & \cdots & \frac{\partial\psi_1}{\partial x_n} \\ \cdot & \cdot & & \cdot \\ \cdot & \cdot & & \cdot \\ \cdot & \cdot & & \cdot \\ \frac{\partial\psi_r}{\partial T} & \frac{\partial\psi_r}{\partial x_1} & \cdots & \frac{\partial\psi_r}{\partial x_n} \end{bmatrix} \tag{2.7}$$

is assumed to have rank r. An admissible arc is defined to be a path having all of its elements $(t, x, \dot{x}, u)$ and $(T, x(T))$ lying in S_1 and S_2, respectively.

Differential equations and inequality constraints containing t, explicitly, can easily be brought to the form of Equations (2.2) and (2.5). The independent variable is changed from t to s by adding the differential equation

$$\frac{dt}{ds} = 1, \qquad s_o = t_o = 0 \tag{2.8}$$

and noting that

$$\frac{dx}{dt} = \frac{dx}{ds}\frac{ds}{dt} = \frac{dx}{ds} \tag{2.9}$$

Then t becomes a dependent variable, and the resulting n + q + 1 differential equations are in the desired form. Observe that the order of the system has been increased by one.

NECESSARY CONDITIONS (B)

The necessary conditions for this problem are stated here without proof. The reader is referred to References 22, 23, and 24, for their derivation. The first necessary condition is

The Multiplier Rule

An admissible arc E, defined on an interval $[0, T]$ is said to satisfy the multiplier rule if there exist constants $p_o = 1$, $e' = [e_1, \ldots, e_r]$, not all zero, and a function

$$F(t, x, u, \dot{x}, p, \mu, \dot{\sigma}) = f_o + p'(f - \dot{x}) + \mu'(G - \dot{\sigma}^2) \tag{2.10}$$

with multipliers $p'(t) = [p_1(t), \ldots, p_n(t)]$, continuous on $[0, T]$ and $\mu'(t) = [\mu_1(t), \ldots, \mu_q(t)]$ continuous on $[0, T]$ except possibly at corners of E where unique right and left hand limits exist, and satisfying the Euler-Lagrange equations

$$-\dot{p}' = \nabla_x f_o + p' \nabla_x f + \mu' \nabla_x G \tag{2.11}$$

$$0 = \nabla_u f_o + p' \nabla_u f + \mu' \nabla_u G \tag{2.12}$$

$$0 = \mu_j G_j, \qquad j = 1, \ldots, q \tag{2.13}$$

where

$$0 \geq \mu \ , \tag{2.14}$$

and differential equations

$$\dot{x} = f; \qquad x(0) = x_o \tag{2.15}$$

$$\dot{\sigma}^2 = G \geq 0 \tag{2.16}$$

along E, and furthermore, such that the equations

$$\left(f_o + p'f + \frac{\partial g}{\partial T} + e' \frac{\partial \psi}{\partial T} \right)\Big|_T dT \tag{2.17}$$

$$+ \quad (\nabla_x g + e' \nabla_x \psi - p')\Big|_T dx(T) = 0, \qquad \psi = 0$$

hold for every choice of the differentials dT, $dx(T)$. The multipliers p_o, p, μ do not vanish simultaneously at any point of the interval $[0, T]$ for an arc E satisfying the multiplier rule. Furthermore, the function

$$H \equiv f_o + p'f \tag{2.18}$$

is a constant on E. Every minimizing arc E for the given form of the problem of Bolza must satisfy the multiplier rule. In the above, the vector $\frac{\partial \psi}{\partial T}\Big|_T$ is the first column of the matrix (2.7).

The vanishing of the coefficients of dT and $dx(T)$ in equation (2.17) constitutes the transversality condition on the arc E. Thus,

$$H = (f_o + p'f)_t = (f_o + p'f)_T = -\left(\frac{\partial g}{\partial T} + e' \frac{\partial \psi}{\partial T} \right)\Big|_T \tag{2.19}$$

$$p'(T) = (\nabla_x g + e' \nabla_x \psi)\Big|_T . \tag{2.20}$$

The Hamiltonian, Equation (2.19), is often called a first integral for this problem. It has further significance in the second necessary condition:

The Necessary Condition of Weierstrass (The Minimum Principle)

An admissible arc E satisfying the multiplier rule with multipliers $p_o = 1, p, \mu$, is said to satisfy the necessary condition of Weierstrass with these multipliers if the condition

$$H(t, x, p, u) \leq H(t, x, p, U) \tag{2.21}$$

is valid at every element $(t, x, \dot{x}, u)$ of E for all admissible points $(t, x, \dot{X}, U) \neq (t, x, \dot{x}, u)$ satisfying the Equations (2.2) and (2.3). Every minimizing arc E for the given form of the problem of Bolza must satisfy this condition.

A consequence of the Weierstrass condition is:

The Necessary Condition of Clebsch

At each point of E let $\tilde{G}$ be a vector whose components are those components of G which vanish, and $\tilde{\mu}$ the corresponding multipliers. Then the inequality

$$\pi' \nabla_u^2 (H + \tilde{\mu}\tilde{G}) \pi \geq 0 \tag{2.22}$$

must be satisfied for every vector $\pi \neq 0$ where $\pi' = [\pi_1, \ldots, \pi_m]$ and satisfies the equations

$$\nabla_u \tilde{G}\, \pi = 0. \tag{2.23}$$

Every minimizing arc for the given form of the problem of Bolza must satisfy this condition.

EXTREMALS AND THE EQUIVALENT MINIMIZATION PROBLEM (C)

The paths considered here are supposed to satisfy the Equations (2.11) through (2.16), as well as the Weierstrass and Clebsch necessary conditions. Such paths will be called extremals. The paths are further supposed to consist of a finite number of subarcs. On each subarc a given subset of the inequality constraints are equality constraints, and all the rest are greater than zero, except possibly at a finite number of points. It is shown in Appendix A that such paths can be generated by integrating sets of differential equations of the form

$$\dot{x} = f(x, p), \qquad x(0) = x_o \tag{2.24}$$

$$-\dot{p} = \nabla_x' F(x, p) \tag{2.25}$$

These differential equations change from subarc to subarc, but the solutions are continuous at the junction of two subarcs.* It is further shown in Appendix A that the solutions can be represented as functions of the initial conditions on the multipliers $p(0) = p_o$, and the terminal value of the independent variable, T; i.e., a solution is defined by specifying a particular set (T, p_o). Continuous partial derivatives of at

---

*Junction points are potential corner points and are also referred to as breakpoints.

least second order in these variables exist. The optimization problem can then be reformulated as: Minimize the function

$$J = J(y) \tag{2.26}$$

in the variables $y = (T, p_o)$, subject to the constraint equations

$$\psi(y) = 0. \tag{2.27}$$

This is the equivalent minimization problem. Necessary and sufficient conditions for a relative minimum for this problem are well known. First, form the function

$$F(y, \lambda) = J(y) + \lambda' \psi(y) \ , \tag{2.28}$$

where λ is an r dimensional vector of Lagrange undetermined multipliers. Then assuming that y is defined over an open region R, that the necessary partial derivatives exist in the neighborhood of the critical point $y = c$, and that the critical point is normal (Ref. 22, pp. 210-213), the necessary and sufficient conditions may be written:

If a critical point $y = c$ has a set of multipliers λ for which the function F satisfies the conditions

$$\nabla_y F(c) = 0 \tag{2.29}$$

and

$$\Delta y' \ \nabla_y^2 F(c) \ \Delta y > 0 \tag{2.30}$$

for all vectors Δy satisfying

$$\nabla_y \psi(c) \ \Delta y = 0 \ , \quad \Delta y \neq 0 \ , \tag{2.31}$$

then c is a minimizing point.

It should be remarked that the Equations (2, 29) and (2, 27) are $n + r + 1$ equations in the $n + r + 1$ variables y and λ. They may be solved, in principle at least, for the critical value $y = c$ and the corresponding set of multipliers, if the matrix

$$\begin{bmatrix} (\nabla_y^2 F)' & (\nabla_{y\lambda}^2 F)' \\ \nabla_y \psi & Z \end{bmatrix} = \begin{bmatrix} \nabla_y^2 F & (\nabla_y \psi)' \\ \nabla_y \psi & Z \end{bmatrix} \qquad (2, 32)$$

is non-singular.

The sufficiency condition, Equations (2, 30) and (2, 31) is rather awkward to test numerically. However, a more convenient test, showing that a matrix is positive-definite, is easily derived. There are two ways in which this can be done.

The most obvious method is to solve (2, 31) for a set of r dependent components of Δy in terms of the $(n + 1 - r)$ others, and to substitute back into (2, 30). The resulting $(n + 1 - r) \times (n + 1 - r)$ matrix must be positive-definite. The other method is to complete the set of constraint Equations (2, 27) with $(n + 1 - r)$ equations of the form

$$\psi_1(y) = \psi_1(c) + z \qquad (2, 33)$$

chosen such that the matrix

$$\begin{bmatrix} \nabla_y \psi \\ \nabla_y \psi_1 \end{bmatrix} = \nabla_y \psi_2 \qquad (2, 34)$$

is non-singular.

Then the equations

$$\nabla_y \psi_2 \, \Delta y = \begin{bmatrix} 0 \\ \Delta z \end{bmatrix} \qquad (2.35)$$

may be thought of as a transformation relating arbitrary Δz to values of Δy satisfying the constraint Equations (2.31). Substitution of (2.35) into the sufficiency condition (2.30), followed by the indicated multiplication then gives the result

$$\Delta z' \, A_4 \, \Delta z > 0 \, . \qquad (2.36)$$

Since Δz is arbitrary, the $(n + 1 - r) \times (n + 1 - r)$ matrix A_4 must be positive-definite.

COMPUTATIONAL METHODS FOR FINDING A RELATIVE MINIMUM (D)

Three of the many numerical schemes for finding a minimum are discussed here. These are the Newton-Raphson method, a modification of the Newton-
ıethod and the method of steepest descent. Reference 31 gives a
other methods. It is assumed that the required partial derivatives are available. Methods for obtaining them are given in subsections E and F.

Consider first the case in which r , the dimension of terminal surface Equations (2.4) is less than (n + 1). Expansion of Equations (2.26) and (2.27) through second-order terms about a point y_o gives

$$J(y) = J(y_o) + \nabla_y J(y_0) \, \Delta y + \frac{1}{2} \, \Delta y' \, \nabla_y^2 \, J(y_o) \, \Delta y + \ldots \qquad (2.37)$$

$$\psi(y) = \psi(y_o) + \nabla_y \psi(y_o) \, \Delta y + \frac{1}{2} \Delta y' \, \nabla_y^2 \, \psi(y_o) \, \Delta y + \ldots \, , \qquad (2.38)$$

where

$$\Delta y = y - y_o .$$

In the Newton-Raphson scheme, the point y_o is assumed to be so close to the minimizing point that (2.37) and (2.38) adequately approximate behavior at the minimizing point. The function F of Equation (2.28) is formed with these expressions and differentiated with respect to y, the assumed minimizing point. Setting the result to zero gives

$$\nabla_y F(y, \lambda) = 0 = \nabla_y F(y_o, \lambda) + \nabla_y^2 F(y_o, \lambda) \Delta y. \tag{2.39}$$

The iterative solution of Equations (2.39) and (2.38) (with $\psi(y) = 0$) for Δy and λ then constitutes the Newton-Raphson method, provided the matrix

$$\nabla_y^2 F(y_o, \lambda) \tag{2.40}$$

satisfies the sufficiency condition. Otherwise, the solution would be driven toward a saddle point or, worse, a maximizing point.

If the sufficiency condition is not met, some other iterative scheme, such as steepest descent, should be used. This situation will generally arise if the point y_o is too far from the minimizing point for the second order expansions (2.37) and (2.38) to be accurate. In steepest descent, the point y is assumed to be closer to the minimizing value than the present estimate y_o. The expansions (2.37) and (2.38) are truncated after first-order terms and written in the form

$$\begin{bmatrix} dJ \\ d\psi \end{bmatrix} = \begin{bmatrix} J(y) - J(y_o) \\ \psi(y) - \psi(y_o) \end{bmatrix} = \begin{bmatrix} \nabla_y J(y_o) \\ \nabla_y \psi(y_o) \end{bmatrix} \Delta y = \theta(y_o) \Delta y \tag{2.41}$$

A change Δy in the gradient, or steepest descent, direction is made by the choice

$$\Delta y = \theta'(y_o) K, \tag{2.42}$$

where K is an $(r + 1) \times 1$ constant vector to be determined. Substitution of (2.42) into (2.41) to determine K, and insertion of the result back into (2.42) gives

$$\Delta y = \theta'(\theta\ \theta')^{-1} \begin{bmatrix} dJ \\ d\psi \end{bmatrix}; \tag{2.43}$$

that is, the desired change in y_o is given in terms of the $\theta(y_o)$ matrix, and specified small changes dJ and $d\psi$. The latter are chosen to make J and ψ smaller at the completion of the next step. Reference (19) provides a more complete description of the use of the method. It should be pointed out that the method blows up as a critical point is approached, since the $(r + 1) \times (n + 1)$ matrix θ is necessarily of rank r at such a point. Otherwise the gradient vector could not be the zero vector. The inverse matrix of Equation (2.43) does not exist under this condition. Hopefully, the critical point is a minimizing point, so the computational equations can be switched to those of the Newton-Raphson method as the point is approached.

Now, suppose $r = (n + 1)$. In this case, the $(n + 1)$ Equations (2.38) completely specify the (fixed) end-point and, hence, Δy, without reference to the minimization criterion (2.37). Truncation of (2.38) after first-order terms and rearrangement then gives

$$\Delta y = [\nabla_y \psi(y_o)]^{-1} (\psi(y) - \psi(y_o)), \tag{2.44}$$

provided the problem is normal. If the choice

$$\psi(y) - \psi(y_o) = -C\,\psi(y_o) \tag{2.45}$$

is made, a gradient-like iterative equation results:

$$\Delta y = -C\,[\nabla_y \psi(y_o)]^{-1}\,\psi(y_o) \;, \quad 0 < C \leq 1 \tag{2.46}$$

Use of an equation of this form to find the minimizing path will be termed the "modified Newton-Raphson method."

The scalar constant C is the only experience factor required for this scheme. If C = 1, Equation (2.46) is recognized as the ordinary Newton-Raphson method for finding a root. Usually, the initial guess of y_o is so far from the minimizing point that some smaller value for C will be required; hence, the bounds $0 < C \leq 1$. As the solution approaches the critical value, it is normally found that acceptable values of C become larger and larger. It is possible to automate the proper selection of C on the computer.

There is no guarantee that the method will converge to a minimizing solution. However, the second variation test described in Appendix B can be used to determine whether or not a solution does minimize.

The modified Newton-Raphson method can also be used for the class of control optimization problems for which the terminal surface Equations (2.4) assume either the form

$$\psi_i = x_i(T) - X_i = 0 \;, \qquad i = 1, \ldots, r < (n+1) \tag{2.47}$$

or the form

$$\psi_j = x_j(T) - X_j = 0, \quad j = 1, \ldots, (r-1) < n \tag{2.48}$$

$$\psi_r = T - D = 0, \tag{2.49}$$

after a suitable renumbering of the state coordinates.* In these equations, X_i, X_j and D are specified constants. A large number of optimization problems fall into this category. The advantage of using the modified Newton-Raphson method over the method of steepest descent is faster convergence.

When the terminal conditions (2.47) are substituted into the transversality conditions (2.19) and (2.20), there results

$$H(x_o, p_o) = (f_o + p'f)\big|_{t=0} = 0 \tag{2.50}$$

$$p_i(T) = e_i, \quad i = 1, \ldots, r \tag{2.51}$$

$$p_j(T) = 0, \quad j = r+1, \ldots, n \tag{2.52}$$

Since the Hamiltonian is constant along the entire path it is evaluated in (2.50) at the instant $t = 0$, which allows simpler computation. Equation (2.51) specify the constants e_i and hence give no new information. When the solutions are considered to be functions of the vector y, Equations (2.47), (2.50) and (2.52) become the set

$$\begin{aligned} x_i(y) - X_i &= 0, \quad i = 1, \ldots, r \\ H(y) &= 0, \\ p_j(y) &= 0, \quad j = r+1, \ldots, n \end{aligned} \tag{2.53}$$

*The function g of Equation (2.1) is taken to be zero here for convenience

This is the two-point boundary value problem, based on the necessary conditions of the minimization problem. When the set (2.53) is expanded about the point y_o and rearranged as in the development of Equation (2.46) there results

$$\Delta y = - C \Omega^{-1}(y_o) \begin{bmatrix} \tilde{x}(y_o) - \tilde{X} \\ H(y_o) \\ \tilde{p}(y_o) \end{bmatrix} \qquad 0 < C \leq 1, \tag{2.54}$$

where $(\tilde{x} - \tilde{X})$ and $\tilde{p}$ are the vector forms of x_i and p_j in (2.53). Let f(0) be the right-hand side of Equation (2.2) evaluated at $t = 0$. Then the matrix Ω is

$$\Omega(y_o) = \begin{bmatrix} \nabla_y \tilde{x}(y_o) \\ 0 \ , \ f'(0) \\ \nabla_y \tilde{p}(y_o) \end{bmatrix} \tag{2.55}$$

Again, there is no guarantee that the iterative Equation (2.54) will converge to a minimizing solution. However, the sufficiency condition of Subsection C may be used to determine if an optimal trajectory has been obtained.

When the terminal value of the independent variable is specified as in Equations (2.48) and (2.49), a reduction in the size of the system is found. The boundary value problem for the terminal surface becomes that of solving the system

$$\begin{aligned} x_j(p_o) - X_j &= 0 , \qquad j = 1, \ldots , (r - 1) \\ p_k(p_o) &= 0 , \qquad k = r, \ldots , n \end{aligned} \tag{2.56}$$

for the minimizing p_o. The iterative equation is

$$\Delta p_o = - C\, w^{-1}(p_o) \begin{bmatrix} \hat{x}(p_o) - \hat{X} \\ \\ \hat{p}(p_o) \end{bmatrix}, \quad 0 \leq C \leq 1, \tag{2.57}$$

where $(\hat{x} - \hat{X})$ and $\hat{p}$ are the vector forms of the left-hand side of system (2.56), and

$$w(p_o) = \begin{bmatrix} \nabla_{p_o} \hat{x}(p_o) \\ \\ \nabla_{p_o} \hat{p}(p_o) \end{bmatrix} \tag{2.58}$$

THE PARTIAL DERIVATIVES I (E)

When Equations (2.26) and (2.27) are differentiated with respect to the variable $y = (T, p_o)$, there results

$$\dot{J} = \frac{\partial g(T, x(T))}{\partial T} + \nabla_x g(T, x(T))\ \dot{x}(T) + f_o(T) \tag{2.59}$$

$$\nabla_{p_o} J = \nabla_x g(T, x(T))\ \nabla_{p_o} x(T) + \nabla_{p_o} x_{n+1}(T) \tag{2.60}$$

$$\dot{\psi} = \frac{\partial \psi(T, x(T))}{\partial T} + \nabla_x \psi(T, x(T))\ \dot{x}(T) \tag{2.61}$$

$$\nabla_{p_o} \psi = \nabla_x \psi(T, x(T))\ \nabla_{p_o} x(T) \tag{2.62}$$

where

$$x_{n+1}(t) = \int_0^t f_o \, d\tau \,, \tag{2.63}$$

the integral term of Equation (2.1), has been introduced as a new variable (see Appendix A).

The symbol $\dot{J}$ in Equation (2.59) represents the partial derivative of Equation (2.26) with respect to the variable T. This variable appears both explicitly and implicitly (in the variables x), as indicated on the right-hand side of (2.59). A similar interpretation holds for Equation (2.61).

Since all terms of Equations (2.59) and (2.61) are available after a path has been found, $\dot{J}$ and $\dot{\psi}$ are readily evaluated. The other partials may be estimated or they may be computed if $\nabla_{p_o} x(T)$ and $\nabla_{p_o} x_{n+1}(T)$ are known.

Consider, first, the estimation of the partial derivatives. Since the solutions are continuous functions of p_o, the function J may be expanded in a Taylor's series expansion through second-order terms in one of the variables p_{i_o}:

$$J(p_{i_o} + \delta p_{i_o}) = J_o + \frac{\partial J}{\partial p_{i_o}} \delta p_{i_o} + \frac{1}{2} \frac{\partial^2 J}{\partial p_{i_o}^2} (\delta p_{i_o})^2 \tag{2.64}$$

The left-hand side notation of (2.64) indicates that only one component of p_o has been changed by the small positive amount δp_{i_o}

Note that the terminal value of the independent variable T is also held constant. The quantities J_o, $\frac{\partial J}{\partial p_{i_o}}$ and $\frac{\partial^2 J}{\partial p_{i_o}^2}$ correspond to the extremal generated with the initial conditions p_o. Substitution of $-\delta p_{i_o}$ into (2.64) results in

$$J(p_{i_o} - \delta p_{i_o}) = J_o - \frac{\partial J}{\partial p_{i_o}} \delta p_{i_o} + \frac{1}{2} \frac{\partial^2 J}{\partial p_{i_o}^2} (\delta p_{i_o})^2 . \qquad (2.65)$$

Subtraction of (2.65) from (2.64) and rearrangement gives the desired result

$$\frac{\partial J}{\partial p_{i_o}} = \frac{J(p_{i_o} + \delta p_{i_o}) - J(p_{i_o} - \delta p_{i_o})}{2 \delta p_{i_o}} ; \qquad (2.66)$$

that is, the partial derivative is obtained from two solutions with slightly different initial conditions in one of the components of p_o. A complete set of first partials is obtained from 2n perturbed solutions. Since values of ψ can be determined for these perturbed solutions, the obvious changes in Equation (2.66) may be made to calculate $\nabla_{p_o} \psi$.

If the Newton-Raphson method is used, second partials must also be estimated. The form of the matrix of second partial derivatives for the function J is

$$\begin{bmatrix} J & \nabla_{p_o} J \\ \nabla_{p_o}^{-1} J & \nabla_{p_o}^2 J \end{bmatrix} .$$

Of these, only $\ddot{J}$ can be calculated explicitly. The computational equation, from differentiation of Equation (2.59), is

$$\ddot{J} = \frac{\partial^2 g(T, x(T))}{\partial T^2} + 2 \frac{\partial}{\partial T} (\nabla_x g(T, x(T)) \dot{x}(T) + \nabla_x g(T, x(T)) \ddot{x}(T) + \dot{x}'(T) \nabla_x^2 g(T, x(T)) \dot{x}(T) + \dot{f}_o(T), \tag{2.67}$$

where

$$\dot{f}_o = \nabla_x f_o \dot{x} + \nabla_u f_o (\nabla_x u \dot{x} + \nabla_p u \dot{p}), \tag{2.68}$$

and where $\nabla_x f_o$ and $\nabla_u f_o$ are partials with respect to explicit appearance of x and u in f_o. Similar equations may be written for $\ddot{x} = \dot{f}$. The components of $\nabla_{p_o} \dot{J}$ are computed from application of (2.66) to the function $\dot{J}$.

The diagonal elements of $\nabla_{p_o}^2 J$ are estimated from

$$\frac{\partial^2 J}{\partial p_{i_o}^2} = \frac{J(p_{i_o} + \delta p_{i_o}) + J(p_{i_o} - \delta p_{i_o}) - 2J_o}{(\delta p_{i_o})^2} \tag{2.69}$$

Equation (2.69) is derived by adding Equation (2.64) to (2.65) and rearranging the result.

The off-diagonal terms of $\nabla^2_{p_o} J$ are estimated from

$$\frac{\partial^2 J}{\partial p_{i_o} \partial p_{j_o}} = \frac{J(p_{i_o} + \delta p_{i_o}, p_{j_o} + \delta p_{j_o}) + J_o - J(p_{i_o} + \delta p_{i_o}) - J(p_{j_o} + \delta p_{j_o})}{\delta p_{i_o} \delta p_{j_o}} , \tag{2.70}$$

where $J(p_{i_o} + \delta p_{i_o}, p_{j_o} + \delta p_{j_o})$ is the solution which results when the elements p_{i_o} and p_{j_o} are perturbed by the small positive amounts δp_{i_o} and δp_{j_o}, respectively.

Equation (2.70) was derived by expanding J in a Taylor's series expansion through second-order terms in the variables p_{i_o}, p_{j_o} about the solution for p_o. Substitution of (2.66) and (2.69) into the result, followed by some rearrangement, then gives (2.70).

Equations similar to (2.70) can be found for either or both of δp_{i_o} and δp_{j_o} considered negative. It is recommended that cross partials be computed for the perturbations δp_{i_o}, δp_{j_o} taken in the direction of expected change in the solution. This can be found from the direction of steepest descent. The partials (2.70) require an additional $\frac{n(n-1)}{2}$ solutions. The grand total of solutions for a Newton-Raphson step rises to $\frac{n(n+3)}{2}$, not counting the unperturbed solution

Finally, second derivatives of ψ are computed by substituting components of ψ for J in the above equations, with the exception that

$$\ddot{\psi}_i = \frac{\partial^2 \psi_i}{\partial T^2} + 2 \frac{\partial}{\partial T} \left[\nabla_x \psi_i \right] \dot{x} + \nabla_x \psi_i \ddot{x} + \dot{x}' \nabla_x^2 g \dot{x}$$

There are several disadvantages associated with estimated partial derivatives. The biggest problem involves the integration accuracy. Since the partial derivatives are approximated by differencing integrated solutions, the random error generated by the integration algorithm may result in bad predictions of the minimizing point. Closely related to this problem is the one of picking the perturbations, δp_o. If these are too small, the partial derivatives will reflect the integration error alone. If they are too large, the partial derivatives will not reflect the nature of the surface in the vicinity of the point (T, p_o). Intermediate values must be chosen by experience. Even then, there are errors in the estimating equations, since these correspond to differentiated (quadratic) three-point fits. It generally takes longer to estimate the partials on the computer than to compute them explicitly (see Subsection E). The total number of equations integrated per step is $n(n + 1)(n + 2)$ for estimated partials, whereas it is $2n(n + 1)$ for explicit computation. It took about three times longer to estimate the partials than it did to compute them explicitly for a particular problem ($n = 3$).

In spite of these difficulties it may be wise to estimate the partial derivatives for some problems rather than to calculate them explicitly. The set of differential equations for estimated partials is much smaller and easier to set up than the corresponding set for the explicit computation of partials. Even if the partials are to be computed explicitly it is helpful, for program checkout purposes, to have estimates of the partial derivatives.

The value of the Hamiltonian is theoretically constant, so it may be used to detect large truncation and round-off errors.

THE PARTIAL DERIVATIVES II (F)

Now consider the explicit computation of partial derivatives. For this purpose it is convenient to shift to the Hamiltonian formulation of the problem. It may readily be verified that the equations

$$\dot{x} = \nabla'_p H_1 (x, u, p, \mu) \tag{2.72}$$

$$-\dot{p} = \nabla'_x H_1 (x, u, p, \mu) \tag{2.73}$$

$$0 = \nabla_u H_1 (x, u, p, \mu) \tag{2.74}$$

$$H_1 = H(x, u, p) + \mu G(x, u) \ , \tag{2.75}$$

where H is defined by Equation (2.18), are identical with Equations (2.15), (2.11) and (2.12), respectively. According to the arguments of Appendix A, each subarc of a path has its own set of reduced differential equations of the extremals of the form

$$\dot{x} = \nabla'_p H_1 (x, p) \tag{2.76}$$

$$-\dot{p} = \nabla'_x H_1 (x, p) \tag{2.77}$$

where, of course,

$$u = u(x, p) \tag{2.78}$$

$$\mu = \mu(x, p) , \tag{2.79}$$

Now, in the solutions of Equations (2.76) and (2.77), x, p, are functions of the independent variable t and the initial conditions x_1, p_1, on the subarc. Consequently, $\dot{x}$ and $\dot{p}$ are also functions of these quantities. Differentiation of Equations (2.76) and (2.77) with respect to a typical initial value a, followed by an interchange of the order of differentiation on the left-hand sides (which is permissible) gives

$$\frac{d}{dt}\left(\frac{\partial x}{\partial a}\right) = \nabla^2_{px} H_1 \frac{\partial x}{\partial a} + \nabla^2_p H_1 \frac{\partial p}{\partial a} \tag{2.80}$$

$$\frac{d}{dt}\left(\frac{\partial p}{\partial a}\right) = -\nabla^2_x H_1 \frac{\partial x}{\partial a} - \nabla^2_{xp} H_1 \frac{\partial p}{\partial a} \ . \tag{2.81}$$

Equations (2.80) and (2.81) are a set of 2n linear first-order homogeneous differential equations with time-varying coefficients. They have a maximal set of 2n independent (column) vector solutions. Only n of these solutions are of interest for the control optimization problem; namely, those representing partial derivatives with respect to the initial values of the multipliers p_o. These solutions are represented in matrix form by

$$\begin{bmatrix} \nabla_{p_o} x \\ \\ \nabla_{p_o} p \end{bmatrix} \tag{2.82}$$

where $\nabla_{p_o} x$ and $\nabla_{p_o} p$ are both n x n matrices. Linear combinations of the solutions (2.82) of the form

$$\delta x(t) = \nabla_{p_o} x(t)\, dp_o \tag{2.83}$$

$$\delta p(t) = \nabla_{p_o} p(t)\, dp_o \tag{2.84}$$

for small dp_o represent all possible neighboring extremals about the extremal whose initial conditions are x_o and p_o at $t = 0$ (holding x_o fixed). The equations of these extremals are

$$x(t, p_o + dp_o) = x(t, p_o) + \nabla_{p_o} x(t)\, dp_o \tag{2.85}$$

$$p(t, p_o + dp_o) = p(t, p_o) + \nabla_{p_o} p(t)\, dp_o \tag{2.86}$$

Initial conditions for the solution (2.82) of the differential Equations (2.80) and (2.81) must be determined. For the first subarc, these are

$$\nabla_{p_o} x(0) = Z \ , \qquad \nabla_{p_o} p(0) = I \ , \tag{2.87}$$

since the initial conditions on the path are $t = 0$, and

$$x(0) = x_o \ , \qquad p(0) = p_o \ . \tag{2.88}$$

Differentiation of (2.88) with respect to p_o results in (2.87).

The initial conditions at the junction point t_1 of two subarcs are determined from continuity considerations. These require (see Appendix A)

$$x(t_1, p_o) = x(t_1, x_1, p_1) \tag{2.89}$$

$$p(t_1, p_o) = p(t_1, x_1, p_1) \ . \tag{2.90}$$

Differentiating and noting that $\nabla_{x_1} x(t_1) = I$, $\nabla_{p_1} p(t_1) = 0$, $\nabla_{x_1} p(t_1) = 0$, and $\nabla_{p_1} p(t_1) = I$ then gives

$$\nabla_{p_o} x_1 = \nabla_{p_o} x(t_1) + \left[\dot{x}^-(t_1) - \dot{x}^+(t_1)\right] \nabla_{p_o} t_1 \tag{2.91}$$

$$\nabla_{p_o} p_1 = \nabla_{p_o} p(t_1) + \dot{p}^-(t_1) - \dot{p}^+(t_1) \quad \nabla_{p_o} t_1 \ . \tag{2.92}$$

Here, the matrices $\nabla_{p_o} x(t_1)$ and $\nabla_{p_o} p(t_1)$ are terminal values for the previous subarc, and $\dot{x}^-(t_1)$, $\dot{p}^-(t_1)$ and $\dot{x}^+(t_1)$, $\dot{p}^+(t_1)$ are limits of the time derivatives from the left and from the right, respectively. If the control functions are continuous, the partial derivatives are continous in time at t_1; if discontinuous, the row vector $\nabla_{p_o} t_1$ must be computed.

It is determined from either (A.28) or (A.35) of Appendix A, depending on whether a constraint is being added or subtracted. If (A28) is the subarc terminal surface, it is found from the implicit function theorem that

$$\nabla_{p_o} t_1 = -\frac{1}{\dot{G}_1}\left[\nabla_x G_1 \; \nabla_{p_o} x(t_1) + \nabla_p G_1 \; \nabla_{p_o} p(t_1)\right], \tag{2.93}$$

where $\dot{G}_1$ is defined by the equation following (A.28).

The differential Equations (2.80) and (2.81) are usually integrated right along with the set of Equations (2.76) and (2.77). In this manner, the time-varying coefficients of (2.80) and (2.81) are easily calculated at each point along the path.

The terminal surface of a path is usually described by one, but not necessarily all, of the components of (2.4) being zero. On the surface, the first partial derivatives are evaluated from Equations (2.59) - (2.62). Examination of these equations now shows that only $\nabla_{p_o} x_{n+1}(T)$ is still undetermined. This may be evaluated in one of two ways. The first is to add the differential equation

$$\frac{d}{dt}\left(\frac{\partial x_{n+1}}{\partial a}\right) = \nabla_x f_o \; \frac{\partial x}{\partial a} + \nabla_p f_o \; \frac{\partial p}{\partial a} \tag{2.94}$$

To the set (2.80) and (2.81) and to integrate it along with the others. The initial conditions for the first subarc and at breakpoints are, respectively,

$$\nabla_{p_o} x_{n+1}(0) = 0 \tag{2.95}$$

$$\left(\nabla_{p_o} x_{n+1}\right)_1 = \nabla_{p_o} x_{n+1}(t_1) + \dot{x}_{n+1} \; \nabla_{p_o} t_1 \; . \tag{2.96}$$

The second method of evaluating $\nabla_{p_o} x_{n+1}$ stems from a theorem in the calculus of variations concerning the differential of x_{n+1} for a one-parameter family of extremals (Ref. 22, p. 237). Here,

$$dx_{n+1}(T) = (f_o + p'f)\Big|_T dT - p'(T)\, dx(T). \tag{2.97}$$

Substitution of

$$d\,x(T) = \dot{x}(T)\, dT + \nabla_{p_o} x(T)\, dp_o \tag{2.98}$$

into (2.97), and rearranging, then gives

$$d\,x_{n+1}(T) = f_o\, dT - p'(T)\, \nabla_{p_o} x(T)\, dp_o , \tag{2.99}$$

from which it follows that

$$\nabla_{p_o} x_{n+1}(T) = - p'(T)\, \nabla_{p_o} x(T) . \tag{2.100}$$

Integration of (2.94) and evaluation of (2.100) give the same result theoretically. However, for numerical accuracy it is better to perform the integration than to evaluate the identity. Equation (2.100) is useful for program check-out and for checking the integration accuracy, since it is true for all values of the independent variable.

The second derivatives come from application of the second variation, see Ref. 22, p. 226. For the control optimization problem, this may be written

$$d^2J = d^2V - \left[\dot{p}'(T)\,\dot{x}(T)\,dT^2 + 2\,\dot{p}'(T)\,\delta x(T)\,dT\right] + \int_0^T 2\omega\,d\tau \qquad (2.101)$$

where

$$V = g + e'\psi \qquad (2.102)$$

$$d^2V = \left[\frac{\partial^2 V}{\partial T^2} + 2\nabla_x\left(\frac{\partial V}{\partial T}\right)\dot{x}(T) + \dot{x}'(T)\,\nabla_x^2 V\,\dot{x}(T)\right]dT^2$$

$$+ 2\left[\nabla_x\,\frac{\partial V}{\partial T} + \dot{x}'(T)\,\nabla_x^2 V\right]\delta x(T)\,dT + \delta x'(T)\,\nabla_x^2 V\,\delta x(T)\,, \qquad (2.103)$$

and

2ω = quadratic form in second partials of (2.10) in all variables.

The definition of the δ-operation is given on P. 195 in Bliss' book. The expression (2.101) assumes that the transversality conditions (2.19) and (2.20) are satisfied, so it is generally an approximation during the iterative process. The terms required to make it exact are usually too complex to compute. They are neglected here on the grounds that the transversality conditions are nearly satisfied, and the Newton-Raphson method is known to be insensitive to errors in the coefficient matrix.

When the comparison curves are restricted to the neighboring extremals (2.85) and (2.86), the integral of (2.101) can be reduced to (Ref. 22, p. 245)

$$\int_0^T 2\omega\,dt = -\delta\,p'(T)\,\delta x(T)\,, \qquad (2.104)$$

where δp and δx are defined by (2.83) and (2.84), respectively. Substitution into (2.101) then gives

$$d^2J = \begin{bmatrix} dT, & dp_o' \end{bmatrix} \begin{bmatrix} \ddot{W} & \nabla_{p_o} \dot{W} \\ \nabla'_{p_o} \dot{W} & \nabla^2_{p_o} W \end{bmatrix} \begin{bmatrix} dT \\ dp_o \end{bmatrix} , \tag{2.105}$$

where the (usually approximate) partial derivatives are computed from

$$\ddot{W} = -\dot{p}'(T)\,\dot{x}(T) + \left[\frac{\partial^2 V}{\partial T^2} + 2\nabla_x \left(\frac{\partial V}{\partial T} \right) \dot{x}(T) + \dot{x}'(T)\,\nabla_x^2 V\,\dot{x}(T) \right] , \tag{2.106}$$

$$\nabla_{p_o} \dot{W} = -\dot{p}'(T)\,\nabla_{p_o} x(T) + \left[\nabla_x \left(\frac{\partial V}{\partial T} \right) + \dot{x}'(T)\,\nabla_x^2 V \right] \nabla_{p_o} x(T) , \tag{2.107}$$

and

$$\nabla^2_{p_o} W = -\left[\nabla'_{p_o} p(T)\,\nabla_{p_o} x(T) \right]_{sym} + \nabla'_{p_o} x(T)\,\nabla_x^2 V\,\nabla_{p_o} x(T) . \tag{2.108}$$

Note that (2.100) may be substituted into (2.107) and that the partials simplify considerably if (2.101) is a linear function.

It was tacitly assumed above that breakpoints contributed nothing to either the first or the second variation. This point can be checked by splitting the integral of Equation (2.1) into several integrals, one for each subarc, and expanding each through second-order terms. It is found that breakpoints contribute nothing to the first variation because of continuity of all the elements across such a point. The second variation contributions are zero if the breakpoint is not a corner. Corner points, apparently, require further examination for individual problems.

SECTION III

OPTIMAL TRAJECTORY CALCULATIONS - APPLICATIONS AND RESULTS

AN EXAMPLE PROBLEM (A)

The following simple analytical example illustrates the concepts presented in Section II. The problem chosen is the two-dimensional harmonic oscillator with a single control function. The problem was found in Reference 27. The equations of motion are

$$\frac{dx_1}{dt} = x_2, \qquad x_1(0) = x_{1_o} \tag{3.1}$$

$$\frac{dx_2}{dt} = -x_1 + u, \; x_2(0) = x_{2_o}. \tag{3.2}$$

It is desired to minimize the control effort over the path. This may be expressed in integral form as

$$J = \int_o^T u^2 \, d\tau. \tag{3.3}$$

The terminal surface is specified by a given terminal time and by $x_1(T) = 0$. Thus,

$$\psi_1 = T - K = 0 \tag{3.4}$$

$$\psi_2 = x_1(T) = 0, \tag{3.5}$$

where T is the value of t on the terminal surface. The Hamiltonian for this system is

$$H = p_1 x_2 + p_2 (-x_1 + u) + u^2 . \tag{3.6}$$

The Euler-Lagrange equations are, thus,

$$\dot{p}_1 = p_2 \tag{3.7}$$

$$\dot{p}_2 = - p_1 \tag{3.8}$$

$$p_2 + 2u = 0 . \tag{3.9}$$

The optimal control function, from (3.9), is seen to be

$$u = - \frac{p_2}{2} . \tag{3.10}$$

This control function automatically satisfies the minimum principle and the Clebsch necessary condition. Equations (3.7) and (3.8) are linear equations with constant coefficients and may be solved directly. In terms of initial conditions,

$$\begin{bmatrix} p_1(t) \\ p_2(t) \end{bmatrix} = \begin{bmatrix} \cos t & \sin t \\ - \sin t & \cos t \end{bmatrix} \begin{bmatrix} p_{1_o} \\ p_{2_o} \end{bmatrix} , \tag{3.11}$$

where p_{1_o} and p_{2_o} are the initial conditions on p_1 and p_2.

The homogeneous part of Equations (3.1) and (3.2) is the same as that for Equations (3.7) and (3.8). The system is thus self-adjoint. The solution

of Equations (3.1) and (3.2) can then be written as

$$\begin{bmatrix} x_1(t) \\ x_2(t) \end{bmatrix} = \begin{bmatrix} \cos t & \sin t \\ -\sin t & \cos t \end{bmatrix} \begin{bmatrix} x_{1_o} \\ x_{2_o} \end{bmatrix} \tag{3.12}$$

$$- \begin{bmatrix} \cos t & \sin t \\ -\sin t & \cos t \end{bmatrix} \int_{t_o}^{t} \begin{bmatrix} \cos \tau & -\sin \tau \\ \sin \tau & \cos \tau \end{bmatrix} \begin{bmatrix} 0 \\ 1 \end{bmatrix} \frac{p_2(\tau)\, d\tau}{2} .$$

After substitution and integration,

$$\begin{bmatrix} x_1(t) \\ x_2(t) \end{bmatrix} = \begin{bmatrix} \cos t & \sin t \\ -\sin t & \cos t \end{bmatrix} \begin{bmatrix} x_{1_o} \\ x_{2_o} \end{bmatrix} \tag{3.13}$$

$$- \frac{1}{4} \begin{bmatrix} (t \cos t - \sin t) & t \sin t \\ -t \sin t & (\sin t + t \cos t) \end{bmatrix} \begin{bmatrix} p_{1_o} \\ p_{2_o} \end{bmatrix} .$$

Finally, the evaluation of expression (3.3) is

$$J(t) = \frac{1}{8} \left[p_{1_o}^2 (t - \sin t \cos t) - 2 p_{1_o} p_{2_o} \sin^2 t \right. \tag{3.14}$$

$$\left. + p_{2_o}^2 (t + \sin t \cos t) \right] .$$

On the terminal surface, then,

$$J(T) = \frac{1}{8}\left[p_{1_o}^2 (T - \sin T \cos T) - 2 p_{1_o} p_{2_o} \sin^2 T + p_{2_o}^2 (T + \sin T \cos T) \right], \tag{3.15}$$

$$\begin{bmatrix} x_1(T) \\ x_2(T) \end{bmatrix} = \begin{bmatrix} \cos T & \sin T \\ -\sin T & \cos T \end{bmatrix} \begin{bmatrix} x_{1_o} \\ x_{2_o} \end{bmatrix}$$

$$-\frac{1}{4} \begin{bmatrix} (T \cos T - \sin T) & T \sin T \\ -T \sin T & (\sin T + T \cos T) \end{bmatrix} \begin{bmatrix} p_{1_o} \\ p_{2_o} \end{bmatrix}. \tag{3.16}$$

The function $\bar{F}$ of Equation (2.28) for the equivalent minimization problem may be written, from (3.15), (3.4) and (3.5), as

$$\bar{F} = J(T) + e_1(T - K) + e_2 x_1(T) . \tag{3.17}$$

The first necessary condition then gives

$$\frac{\partial \bar{F}}{\partial T} = 0 = \frac{1}{4}(p_{1_o} \sin T - p_{2_o} \cos T)^2 + e_1 + e_2 \left\{ -x_{1_o} \sin T + x_{2_o} \cos T + \frac{1}{4}\left[p_{1_o} T \sin T - p_{2_o}(\sin T + T \cos T) \right] \right\}. \tag{3.18}$$

$$\frac{\partial F}{\partial p_{1_o}} = 0 = \frac{1}{4}\left[p_{1_o}(T - \sin T \cos T) - p_{2_o} \sin^2 T \right]$$

$$- \frac{e_2}{4} (T \cos T - \sin T) \tag{3.19}$$

$$\frac{\partial F}{\partial p_{2_o}} = 0 = \frac{1}{4}\left[- p_{1_o} \sin^2 T + p_{2_o} (T + \sin T \cos T) \right]$$

$$- \frac{e_2}{4} T \sin T \,. \tag{3.20}$$

These, together with (3.4) and (3.5) are to be solved for T, p_{1_o}, p_{2_o}, e_1 and e_2. The solutions are

$$T = K \tag{3.21}$$

$$p_{1_o} = A \cos K \tag{3.22}$$

$$p_{2_o} = A \sin K \tag{3.23}$$

$$e_1 = \frac{A\left[x_{1_o} K \sin K - x_{2_o} (K \cos K - \sin K)\right]}{(K - \sin K \cos K)} \tag{3.24}$$

$$e_2 = A = \frac{4\left[x_{1_o} \cos K + x_{2_o} \sin K\right]}{(K - \sin K \cos K)} \,, \tag{3.25}$$

provided $K \neq 0$.

The point defined by Equations (3.21) through (3.25) is truly a minimizing point. This will now be shown by constructing the matrix A_4 of Equation (2.36). The set (3.4) and (3.5) is first completed by adding the equation

$$\psi_3 = x_2(T) + y. \tag{3.26}$$

Then the Equation (2.35) may be written, for the critical point, as

$$\begin{bmatrix} 1 & 0 & 0 \\ \dot{x}_1 & x_{11} & x_{12} \\ \dot{x}_2 & x_{21} & x_{22} \end{bmatrix} \begin{bmatrix} \Delta T \\ \Delta p_{1_o} \\ \Delta p_{2_o} \end{bmatrix} = \begin{bmatrix} 0 \\ 0 \\ \Delta y \end{bmatrix}, \tag{3.27}$$

where

$$x_{11} = \frac{\partial x_1}{\partial p_{1_o}}, \quad x_{12} = \frac{\partial x_1}{\partial p_{2_o}}, \quad x_{21} = \frac{\partial x_2}{\partial p_{1_o}}, \quad x_{22} = \frac{\partial x_2}{\partial p_{2_o}}.$$

Equation (3.27) may be rewritten

$$\begin{bmatrix} \Delta T \\ \Delta p_{1_o} \\ \Delta p_{2_o} \end{bmatrix} = \begin{bmatrix} 1 & 0 & 0 \\ a_{21} & a_{22} & a_{23} \\ a_{31} & a_{32} & a_{33} \end{bmatrix} \begin{bmatrix} 0 \\ 0 \\ \Delta y \end{bmatrix} \tag{3.28}$$

where

$$a_{21} = C(x_{12}\dot{x}_2 - x_{22}\dot{x}_2), \quad a_{22} = Cx_{22}, \quad a_{23} = -Cx_{12}$$

$$a_{31} = C(x_{21}\dot{x}_1 - x_{11}\dot{x}_2), \quad a_{32} = Cx_{21}, \quad a_{33} = Cx_{11}$$

$$\frac{1}{C} = (x_{11}\,x_{22} - x_{21}\,x_{12}).$$

Also, at the critical point,

$$\nabla^2 F = \begin{bmatrix} 0 & \frac{A}{4} K \sin K & -\frac{A}{4}(\sin K + K \cos K) \\ \frac{A}{4} K \sin K & \frac{1}{4}(K - \sin K \cos K) & -\frac{\sin^2 K}{4} \\ -\frac{A}{4}(\sin K + K \cos K) & -\frac{\sin^2 K}{4} & \frac{1}{4}(K + \sin K \cos K) \end{bmatrix}$$

(3.29)

After all the substitutions have been made, it is found that the matrix A_4 of Equation (2.36) is the scalar

$$A_4 = \frac{(K - \sin K \cos K)}{4(K^2 - \sin^2 K)} .$$

Since $K > \sin K$ for all $K > 0$, $A_4 > 0$. It is, thus, concluded that the solution is indeed a minimizing solution, since there is only one critical point.

The accessory differential Equations (2.80) and (2.81) for this problem can be written

$$\frac{d}{dt} \begin{bmatrix} \frac{\partial x_1}{\partial a} \\ \frac{\partial x_2}{\partial a} \\ \frac{\partial p_1}{\partial a} \\ \frac{\partial p_2}{\partial a} \end{bmatrix} = \begin{bmatrix} 0 & 1 & 0 & 0 \\ -1 & 0 & 0 & -\frac{1}{2} \\ 0 & 0 & 0 & 1 \\ 0 & 0 & -1 & 0 \end{bmatrix} \begin{bmatrix} \frac{\partial x_1}{\partial a} \\ \frac{\partial x_2}{\partial a} \\ \frac{\partial p_1}{\partial a} \\ \frac{\partial p_2}{\partial a} \end{bmatrix} . \qquad (3.30)$$

It can readily be verified that the solution of (3.30) is

$$\nabla_{p_o} x = \begin{bmatrix} \frac{\partial x_1}{\partial p_{1_o}} & \frac{\partial x_1}{\partial p_{2_o}} \\ \frac{\partial x_2}{\partial p_{1_o}} & \frac{\partial x_2}{\partial p_{2_o}} \end{bmatrix} = \begin{bmatrix} \frac{\sin t - t \cos t}{4} & \frac{-t \sin t}{4} \\ \frac{t \sin t}{4} & \frac{-(\sin t + t \cos t)}{4} \end{bmatrix}, \quad \nabla_{p_o} x(0) = Z \tag{3.31}$$

$$\nabla_{p_o} p = \begin{bmatrix} \frac{\partial p_1}{\partial p_{1_o}} & \frac{\partial p_1}{\partial p_{2_o}} \\ \frac{\partial p_2}{\partial p_{1_o}} & \frac{\partial p_2}{\partial p_{2_o}} \end{bmatrix} = \begin{bmatrix} \cos t & \sin t \\ -\sin t & \cos t \end{bmatrix}, \quad \nabla_{p_o} p(0) = I \tag{3.32}$$

The first derivative of (3.3) with respect to p_o, from (2.100), is

$$\nabla_{p_o} J = -p'(T) \nabla_{p_o} x(T) = \frac{1}{4}\Big[(p_{1_o}(T - \sin T \cos T) - p_{2_o} \sin^2 T), \; (-p_{1_o} \sin^2 T + p_{2_o}(T + \sin T \cos T))\Big] \tag{3.33}$$

It is seen that this corresponds to the results of differentiating Equation (3.14).

Since the constraint Equations (3.4) and (3.5) are linear, it is seen that the matrix (2.105) of second partials reduces to

$$\nabla^2_{p_o} J = \nabla'_{p_o} x(T)\ \nabla_{p_o} p(T) = \begin{bmatrix} \dfrac{T - \sin T \cos T}{4} & \dfrac{-\sin^2 T}{4} \\ \dfrac{-\sin^2 T}{4} & \dfrac{T + \sin T \cos T}{4} \end{bmatrix} \tag{3.34}$$

This agrees with the corresponding terms of (3.29) when the identification $T = K$ is made.

THE HIGH LIFT-DRAG RATIO VEHICLE OPTIMIZATION STUDY (B)

The Problem Statement (B-1)

A trajectory is sought which minimizes the functional (1.6) for a flat-plate vehicle with aerodynamic coefficients represented by Equations (1.3). The data for these formulas is $C_{LO} = 1.82$, $C_{DO} = 0.042$, and $C_{DL} = 1.40$. The motion is assumed to be governed by equations of the form (1.1) and the atmosphere is specified by the relation

$$\rho = \rho_o\ e^{-\beta R \xi}. \tag{3.35}$$

The terminal surface is represented by the single equation

$$\psi_1 = T - K = 0, \tag{3.36}$$

where K is a specified constant. The pilot's acceleration, computed from the formula

$$a_p = \frac{S \rho v^2}{2 m g_o} \sqrt{C_D^2 + C_L^2}, \tag{3.37}$$

is constrained by the inequality

$$B + a_p \geq 0 \ , \tag{3.38}$$

(The constant B is generally taken as 10 g.) Initial conditions for the path are

$$v_o = 35,000 \text{ feet per second}$$

$$\gamma_o = -5 \text{ degrees}$$

$$h_o = 400,000 \text{ feet}$$

$$\zeta_o = 0 \ .$$

The criterion (1, 6) is chosen to correspond to a vehicle which radiates heat most efficiently at a specified temperature. The constant $\dot{Q} = 195$ BTU/sq. ft./second fixes this temperature around 3000° R for this particular vehicle, and, since the trajectory is selected by the criterion, the heating rate of the vehicle deviates in the mean-square sense as little as possible from this constant. To simplify the computations, the heating law is taken, following Chapman (Ref. 6) as

$$\dot{q} = C \rho^{1/2} v^3 \ , \qquad (C = 2 \times 10^{-8}) \ . \tag{3.39}$$

A more realistic formula, which includes a radiative heating term in addition to this formula representing convective heating, is used in the next subsection.

Since T is a constant by (3.36), it may be omitted from the criterion; so the integrand f_o of Equation (2.1) may be identified with the integrand of (1.6):

$$f_o = (\dot{Q} - \dot{q})^2 \ . \tag{3.40}$$

The function g of (2.1) is taken as zero. Thus, Equation (2.10) for this application reads

$$F = f_o + p\,(f - \dot{x}) + \mu\,(B - a_p - \dot{\sigma}^2)\,, \tag{3.41}$$

where the terms on the right-hand side correspond to relations (3.40), (1.1), and (3.38), respectively. The range coordinate ζ does not appear explicitly in these terms and, hence, is a cyclic (or ignorable) coordinate. The corresponding Euler-Lagrange Equation (2.11) is $\dot{p}_4 = 0$; hence, p_4 must be a constant. This constant is zero in order that the transversality condition (2.20) is satisfied on the terminal surface (3.36). Hence, the fourth equation of system (1.1) may be eliminated. Further evaluation of the transversality condition gives

$$p_1(T) = p_2(T) = p_3(T) = 0\,,$$

and

$$H = e\,,$$

where e is a constant which is yet to be determined. To compress the notation, the remaining three coordinates are written as

$$x_1 = v\,, \quad x_2 = \gamma\,, \quad x_3 = \xi\,.$$

The Unconstrained Subarc (B-2)

The multiplier μ in expression (3.41) is zero on any subarc which is not limited by equality in the constraint relation. This follows from (2.13)

with $G \geq 0$. The Euler-Lagrange Equations (2.11) and (2.12) become

$$
\begin{aligned}
-\dot{p}_1 &= \frac{\partial f_o}{\partial x_1} + p_1 \frac{\partial f_1}{\partial x_1} + p_2 \frac{\partial f_2}{\partial x_1} + p_3 \frac{\partial f_3}{\partial x_1} \\
-\dot{p}_2 &= p_1 \frac{\partial f_1}{\partial x_2} + p_2 \frac{\partial f_2}{\partial x_2} + p_3 \frac{\partial f_3}{\partial x_2} \qquad (3.42) \\
-\dot{p}_3 &= \frac{\partial f_o}{\partial x_3} + p_1 \frac{\partial f_1}{\partial x_3} + p_2 \frac{\partial f_2}{\partial x_3}
\end{aligned}
$$

$$
0 = p_1 \frac{\partial f_1}{\partial \alpha} + p_2 \frac{\partial f_2}{\partial \alpha} . \qquad (3.43)
$$

The last equation becomes, when substitutions from (1.1) and (1.3) are made,

$$
\frac{S \rho v}{2m} \cdot |\sin\alpha| \cdot \left[-3 C_{DL} p_1 v \sin\alpha \cos\alpha + C_{LO} p_2 (3\cos^2\alpha - 1) \right] = 0 . \qquad (3.44)
$$

Assuming re-entry conditions, the leading terms of (3.41) are non-zero if $|\sin\alpha| \neq 0$. The bracketed terms may then be rewritten in the form

$$
\tan^2\alpha + \frac{3C_{DL}}{C_{LO}} \frac{p_1 v}{p_2} \tan\alpha - 2 = 0 . \qquad (3.45)
$$

This leads to the equation

$$\tan\alpha = -a \pm \sqrt{a^2 + 2} \quad , \tag{3.46}$$

where

$$a = \frac{3C_{DL}}{2C_{LO}} \frac{p_1 v}{p_2} \quad .$$

Note that the sign of $\tan\alpha$ is determined by the choice of the $\pm$ sign in Equation (3.46)

The lift-drag polar is traversed once as α ranges through π radians. It is thus advisable to limit the control function to a range of π radians to avoid double values. Furthermore, the points $\alpha = 0, \pi$ are singular points, since $\frac{\partial^2 F}{\partial \alpha^2}$ (the determinant R_1 of (A.13) in Appendix A) is zero at these points. The range $0 < \alpha < \pi$ is chosen here, since then, $|\sin\alpha| = \sin\alpha$, and the proper sign for the equation is most easily chosen. The singular points are removed by defining $\alpha = 0$ at these points. Thus, the range of α is

$$0 \leq \alpha < \pi \quad . \tag{3.47}$$

The proper choice of sign is determined by considering the minimum principle which yields the inequality

$$\begin{aligned} &\sin\alpha \left[-C_{DL}\, p_1 v \sin^2\alpha + C_{LO}\, p_2 \sin\alpha \cos\alpha \right] \\ &\leq \sin A \left[-C_{DL}\, p_1 v \sin^2 A + C_{LO}\, p_2 \sin A \cos A \right] , \end{aligned} \tag{3.48}$$

where A is any value of the control function satisfying Inequalities (3.47) and (3.38). Substitution of (3.45) into (3.48) and rearranging, then gives

$$p_2 \sin\alpha \tan\alpha \leq p_2 \sin A \tan A \quad , \tag{3.49}$$

providing $\tan A$ satisfies Equation (3.45) .

Since $\sin\alpha \geq 0$ and the sign of $\tan\alpha$ is determined by the $\pm$ sign of Equation (3.46), it is seen that (3.49) is satisfied by the choices:

If $p_2 > 0$, choose - sign $(\frac{\pi}{2} < \alpha < \pi)$;

if $p_2 < 0$, choose + sign $(0 < \alpha < \frac{\pi}{2})$.

The behavior where $p_2 = 0$ is examined by a limiting process, since p_1, p_2 and v are continuous functions of time. The binomial series expansion, assuming large a, gives

$$a^2 + 2 = |a| + \frac{1}{|a|} .$$

If $a > 0$ and the minus sign were chosen, then

$$\tan\alpha = \lim_{a \to \infty} -2|a| , \qquad \alpha \to \frac{\pi}{2} \text{ (from the left)} .$$

If $a < 0$ and the plus sign chosen,

$$\tan\alpha = \lim_{a \to \infty} 2|a| , \qquad \alpha \to \frac{\pi}{2} \text{ (from the right)} .$$

On the other hand, if $a < 0$ and the minus sign chosen,

$$\tan\alpha = \lim_{a \to \infty} -\frac{1}{|a|} = 0 , \quad \alpha \to \pi \text{ (from the right)} .$$

Finally, with $a > 0$ and the plus sign,

$$\tan\alpha = \lim_{a \to \infty} \frac{1}{|a|} = 0, \quad \alpha \to 0 \text{ (from the left)} .$$

The last two cases show that it is possible for α to be discontinuous. For example, if p_2 passes through zero and α was near π, then α will jump to zero as p_2 goes through zero. This difficulty is cleared up if the proper interpretation is made. Since $\tan(\pi + \alpha) = \tan\alpha$, α may be thought of as being continuous across jumps, but in the dis-allowed region $\pi \leq \alpha < 2\pi$. The control function discontinuity will be retained since computer results can properly be interpreted, and since it allows $|\sin\alpha| = \sin\alpha$ in all equations. Finally, although of little practical importance, if p_1 and p_2 are simultaneously zero at a point, the limit ratio p_1/p_2 is $\dot{p}_1/\dot{p}_2$ at that point by L'Hospital's rule.

To sum up, the reduced differential equations of the extremals for subarcs having $a_p < B$ are the first three of (1.1) and system (3.42). The control function is computed from Equation (3.46) in the range $0 \leq \alpha < \pi$ according to the rules following Equation (3.49). The subarc terminal surface is $a_p = B$, provided that $\dot{a}_p \neq 0$.

The Constrained Subarc (B-3)

When $a_p = B$ the multiplier μ of (3.41) may be different from zero. The Euler-Lagrange Equations (3.42) and (3.43), modified for this event, are

$$
\begin{aligned}
-\dot{p}_1 &= \frac{\partial f_o}{\partial x_1} + p_1\frac{\partial f_1}{\partial x_1} + p_2\frac{\partial f_2}{\partial x_1} + p_3\frac{\partial f_3}{\partial x_1} - \mu\frac{\partial a_p}{\partial x_1} \\
-\dot{p}_2 &= p_1\frac{\partial f_1}{\partial x_2} + p_2\frac{\partial f_2}{\partial x_2} + p_3\frac{\partial f_3}{\partial x_2} \qquad (3.50) \\
-\dot{p}_3 &= \frac{\partial f_o}{\partial x_3} + p_1\frac{\partial f_1}{\partial x_3} + p_2\frac{\partial f_2}{\partial x_3} - \mu\frac{\partial a_p}{\partial x_3}
\end{aligned}
$$

$$0 = p_1 \frac{\partial f_1}{\partial \alpha} + p_2 \frac{\partial f_2}{\partial \alpha} - \mu \frac{\partial a_p}{\partial \alpha} \,. \tag{3.51}$$

The control function is determined from $a_p = B$ and the multiplier μ from (3.51). Expansion and rearrangement of the constraint equation $a_p = B$ gives

$$b^2 - C_{DO}^2 = \sin^3 \alpha \left[c_1 \sin^3 \alpha + c_2 \sin \alpha + c_3 \right], \tag{3.52}$$

where

$$b = \frac{2m B g_o}{S \rho v^2}$$

$$c_1 = C_{DL}^2 - C_{LO}^2$$

$$c_2 = C_{LO}^2$$

$$c_3 = 2 C_{DO} C_{DL} \,.$$

The right-hand side of (3.52) is a function only of the vehicle aerodynamic coefficients (constants) and $\sin \alpha$. It is zero when $\alpha = 0$ or π, and maximum when $\alpha = \frac{\pi}{2}$. From this it follows that b must satisfy

$$C_{DO} \leq b \leq (C_{DL} + C_{DO}) \,. \tag{3.53}$$

The physical interpretation is that if $C_{DO} > b$ at any point of the path, then α has gone to zero in the futile attempt to keep $a_p = B$. The integration is stopped if condition (3.53) is not satisfied.

Newton's method was chosen to extract α from (3.52). The iteration equation is

$$\Delta\alpha = \frac{(b^2 - C_{DO}^2) - \sin^3\alpha \left[c_1 \sin^3\alpha + c_2 \sin\alpha + c_3 \right]}{\sin^2\alpha \cos\alpha \left[6c_1 \sin^3\alpha + 4c_2 \sin\alpha + 3c_3 \right]} \quad . \qquad (3.54)$$

A $\Delta\alpha$ is calculated from (3.54), using an assumed α (usually the last integration step value). This is added to α, and the new α is used to calculate a new $\Delta\alpha$. The process continues until $\Delta\alpha$ is negligible.

In the vicinity of $\alpha = 0, \frac{\pi}{2}$ or π, the denominator of (3.54) is likely to be quite small. To avoid this difficulty, Equation (3.52) was expanded as a series. The results are:

If $\alpha \sim 0$, $\left(\sin\alpha = \alpha - \frac{\alpha^3}{3!}\right)$, then $\alpha = \left(\frac{b^2 - C_{DO}^2}{c_3}\right)^{1/3}$;

if $\alpha \sim \pi$, $\left[\sin\alpha = (\pi - a) - \frac{(\pi - \alpha)^3}{3!}\right]$,

then $\alpha = \pi - \left(\frac{b^2 - C_{DO}^2}{c_3}\right)^{1/3}$;

If $\alpha \sim \frac{\pi}{2}$, $\left(\cos\alpha = \left(\frac{\pi}{2} - \alpha\right) - \frac{1}{3!}\left(\frac{\pi}{2} - \alpha\right)^3\right)$,

then

$$\alpha = \frac{\pi}{2} \pm \left[\frac{(C_{DL} + C_{DO})^2 - b^2}{3C_{DL}(C_{DL} + C_{DO}) - C_{LO}^2} \right]^{1/2} ,$$

where

the + sign is used if $p_2 > 0$, and

the - sign is used if $p_2 < 0$.

If $p_2 = 0$, choose sign so that $\tan\alpha$ is continuous. The choice of signs again comes from the minimum principle.

It is also noted that the determinant R_2 of Equation (A. 23) in Appendix A is

$$R_2 = \left(\frac{\partial a_p}{\partial \alpha}\right)^2 .$$

Since this must never be zero when $a_p = B$, α must never be $0, \frac{\pi}{2}$ or π.

Finally, μ is calculated from Equation (3. 51) in the form

$$\mu = \frac{1}{\left(\frac{\partial a_p}{\partial \alpha}\right)}\left[p_1 \frac{\partial f_1}{\partial \alpha} + p_2 \frac{\partial f_2}{\partial \alpha}\right] . \qquad (3.55)$$

The reduced differential equations of the extremals for the constrained subarc are now the first three equations of (1. 1) and the system (3. 50). The control function ($0 < \alpha < \frac{\pi}{2}$ or $\frac{\pi}{2} < \alpha_1 < \pi$) from either the iterative Equation (3. 54) or the small angle equations, and the multiplier μ (≤ 0) comes from (3. 55).

The Subarc Junction Points (B-4)

It is known that the multipliers p and the Hamiltonian H are continuous at the junction point of constrained and unconstrained subarcs. It is necessary for this problem that the points at which $\alpha = 0, \frac{\pi}{2}$ be ruled out as junction points, since the determinants R_1 and R_2 of

Equations (A. 13) and (A. 23) must be non-singular at such points. For all other values of α , it turns out that the control function must be continuous at junction points. This is readily verified from examination of the Hamiltonian. It is an analytic function of x, p and α. Since x and p are continuous at junction points, and since the Jacobian R_1 is non-singular, it follows that α is continuous at such points. Similarly, since R_2 is non-singular, Equation (3. 55) shows that μ must be continuous at such points. Thus, μ must start and end with the value zero on constrained subarcs. It then follows that the constrained subarc terminal surface is $\mu = 0$, provided $\dot{\mu} \neq 0$ at the junction point.

The Newton-Raphson Equations (B-5)

The form of the equivalent minimization problem considered here is: Minimize the function $J(T, p_o)$ corresponding to the functional (1. 6) in the variables $y' = (T, p_{10}, p_{20}, p_{30})$ subject to the constraint equation

$$\psi_1 = T - K = 0 . \tag{3.56}$$

The function F of Equation (2. 28) is

$$F = J(T, p_o) + e(T - K) , \tag{3.57}$$

which, when differentiated with respect to T, gives

$$\frac{\partial F}{\partial y_1} (T, p_o, e) = 0 = \dot{J} + e + \nabla_{p_o} \dot{J} \, dp_o , \tag{3.58}$$

since the constraint (3. 56) implies $dT \equiv 0$. The constant e of (3. 58) can always be chosen to satisfy the identity. Differentiation of (3. 57) with respect to the other variables, setting the result to zero, and a little rearrangement then gives the Newton-Raphson iterative equation

$$dp_o = - (\nabla^2_{p_o} J)^{-1} \nabla'_{p_o} J . \tag{3.59}$$

The sufficiency condition reduces to showing that the matrix $\nabla^2_{p_o} J$ is positive-definite. This follows since in the quadratic form

$$dy' \nabla^2_y F \, dy \geq 0 \tag{3.60}$$

$dy_1 \equiv 0$ and the other components of dy are arbitrary.

The steepest descent equation,

$$dp_o = \frac{dJ}{\nabla_{p_o} J \; \nabla'_{p_o} J} \nabla'_{p_o} J \; , \tag{3.61}$$

is readily verified using the methods of subsection II(D). The magnitude of dJ is chosen by experience, usually smaller and smaller as the optimum is approached.

Computer Results (B-5)

Some of the computer results are displayed in Figures 3-1 through 3-4. These trajectories were obtained using the method of estimated partial derivatives of subsection II(E).

The terminal times for the optimal trajectories in Figures 3-1 to 3-3 are 200, 440 and 550 seconds, respectively. It is noted that the angle of attack histories are roughly the same, going from small to large values after about 100 seconds of flight. This corresponds to a shift from maximum positive to maximum negative lift. It is further noted that this shift takes place near the bottom of the first pull-out, where the heating rate is at its peak. The vehicle apparently does not possess enough lift to avoid the heating-rate peak for the given initial conditions, nor can it avoid the mild skip shown in the figures.

Figures 3-2 and 3-3 show that for larger terminal times the vehicle dives rather sharply near its terminal points. Evidently the integral of Equation (1.6) is minimized by this dive, in spite of the large rise, of short duration, in the heating rate. It should be remembered that no restrictions, other than fixed terminal time, were placed on the terminal point.

Figure 3-4 is included to illustrate the sensed acceleration constraint. It does not represent an optimal path. The angle-of-attack history is similar to the other results until the constraint, set at 10 g's, becomes an equality constraint. From this point onward, the angle of attack changes such that 10 g's is never exceeded. The magnitude of the additional multiplier μ is shown at the bottom of the figure.

Do the results of Figures 3-1 to 3-3 represent relative or absolute minimums for the given problem ? An attempt to answer this question was made by re-optimizing with very different initial conditions for the multipliers. Computations were carried far enough to show that the same optimal path would have resulted, indicating that the paths probably represent absolute minimums.

The importance of these results is not that they are optimal paths, for they have many practical short-comings, but that they confirm the validity of the automatic optimization scheme. Further improvement of the optimization method was judged to be more significant and important at this stage than the computation of an operationally desirable re-entry path.

The next stage of development was the method for computing the partial derivatives explicitly (see Subsection II(F)). The computer program incorporating this method calculated the first partials directly from Equation (2.94), whereas the second partial derivative matrix, from Equation (2.108), took the form

$$\nabla^2_{p_o} J = -\left[\nabla'_{p_o} \times \nabla_{p_o} p\right]_{sym} . \qquad (3.62)$$

Attempts were made to duplicate the results of Figures 3.1 through 3.3 to see if further improvement in the trajectories could be made. Some reduction in the optimal criteria was obtained, but it, in all cases, the second derivative matrix was so close to singularity that either bad prediction of multiplier changes resulted, or the matrix became indefinite. This behavior indicated that the surface was extremely flat. It was decided to abandon this program in favor of the more realistic, more complex and, hopefully, less sensitive problem considered in the next section.

This program did show that the method of computing partial derivatives was superior to that of estimation. It also ran from three- to five-times faster than the previous program on the computer.

THE LOW LIFT-DRAG RATIO VEHICLE OPTIMIZATION PROBLEM (C)

The Problem Statement and the Euler-Lagrange Equations (C-1)

A re-entry path which minimizes the total stagnation point heating (1.7) for the blunt-nose body for which the aerodynamic coefficients are given by Equations (1.4) is to be found. The vehicle aerodynamic constants are $C_{DO} = 0.88$, $C_{DL} = 0.52$ and $C_{LO} = -0.505$, and the model equations are again the set (1.1) with the exponential atmosphere (3.35). The terminal surface equations are

$$\psi_1 = v(T) - V = 0$$

$$\psi_2 = h(T) - A = 0 \qquad (3.63)$$

$$\psi_3 = \zeta(T) - \bar{R} = 0 ,$$

with the constants $V = 1650$ feet per second, $A = 75,530$ feet, and $\bar{R} = 979$ statute miles. Thus only the final flight path angle and terminal time are left unspecified. Initial conditions are taken as $v_o = 35,000$ feet per second, $\gamma_o = -5.75$ degrees, $h_o = 400,000$ feet, $\zeta_o =$ zero. Inequality constraints imposed are relation (3.38) and a bound on the control function u, given by

$$u_1^2 - u^2 \geq 0 , \qquad (3.64)$$

with u_1 a constant (16 degrees at present). Equation (3.64) was found necessary to produce initial trajectories which neither skipped out of the atmosphere nor dived in too deeply. It is to be sequentially relaxed as the proper region of p_o space is located during the optimization process.

The integrand of criterion (1.7) is taken as the sum of convective and radiative heating rates:

$$\dot{q} = \dot{q}_c + \dot{q}_r , \qquad (3.65)$$

where the convective component is given by Equation (3.39) and the radiative component by

$$q_r = 7.5\, N \left(\frac{\rho}{\rho_o}\right)^{3/2} \left(\frac{v}{10,000}\right)^{12.5} , \qquad (3.66)$$

in which $N = 4$ feet, the vehicle frontal nose radius. Equation (3.65) may again be identified with the integrand f_o of Equation (2.1), and the

function g is omitted. Thus Equation (2.10) becomes

$$F = \dot{q} + p'(f - \dot{x}) + \mu_1(u_1^2 - u^2 - \dot{\sigma}_1^2) + \mu_2(B - a_p - \dot{\sigma}_2^2) ,$$

where the state coordinate x now has four components with $x_4 = \xi$. The Euler-Lagrange equations are

$$\begin{aligned}
-\dot{p}_1 &= \frac{\partial \dot{q}}{\partial x_1} + p_1 \frac{\partial f_1}{\partial x_1} + p_2 \frac{\partial f_2}{\partial x_1} + p_3 \frac{\partial f_3}{\partial x_1} + p_4 \frac{\partial f_4}{\partial x_1} - \mu_2 \frac{\partial a_p}{\partial x_1} \\
-\dot{p}_2 &= p_1 \frac{\partial f_1}{\partial x_2} + p_2 \frac{\partial f_2}{\partial x_2} + p_3 \frac{\partial f_3}{\partial x_2} + p_4 \frac{\partial f_4}{\partial x_2} \\
-\dot{p}_3 &= \frac{\partial q}{\partial x_3} + p_1 \frac{\partial f_1}{\partial x_3} + p_2 \frac{\partial f_2}{\partial x_3} + p_4 \frac{\partial f_4}{\partial x_3} - \mu_2 \frac{\partial a_p}{\partial x_3} \\
-\dot{p}_4 &= 0 , \quad (p_4 = p_{4o})
\end{aligned} \tag{3.67}$$

$$0 = p_1 \frac{\partial f_1}{\partial u} + p_2 \frac{\partial f_2}{\partial u} - 2\mu_1 u - u_2 \frac{\partial a_p}{\partial u} . \tag{3.68}$$

The Unconstrained Subarc (C-2)

Both the multipliers μ_1 and μ_2 are zero here, as noted in Subsection II(B). Then, when the substitutions from Equations (1.1) and (1.4) have been made, Equation (3.68) becomes

$$\tan u = \frac{-C_{LO} p_2}{C_{DL} p_1 v} , \tag{3.69}$$

where u is centered about zero by the constraint (3.64), i.e.,

$$-u_1 \leq u \leq u_1 \ . \tag{3.70}$$

The minimum principle equation is

$$-p_1 v C_{DL} \cos u + p_2 C_{LO} \sin u \leq -p_1 v C_{DL} \cos U + p_2 C_{LO} \sin U, \tag{3.71}$$

where U is any admissible value in the range (3.70).

The left hand side of (3.71) may be considered as a dot product and the choice of a unit vector (cos u, sin u) which has minimum dot product with the vector $(-p_1 v C_{DL}, p_2 C_{LO})$ is

$$\cos u = \frac{C_{DL} p_1 v}{\sqrt{(C_{LO} p_2)^2 + (C_{DL} p_1 v)^2}}$$

$$\sin u = \frac{-C_{LO} p_2}{\sqrt{(C_{LO} p_2)^2 + (C_{DL} p_1 v)^2}} \ , \tag{3.72}$$

which is parallel but in the opposite direction.

Then from the signs of p_1 and p_2, assuming C_{LO} negative, it follows that:

If

$p_2 = 0$	and $p_1 > 0$,	then	$u = 0$
$p_2 > 0$	$p_1 > 0$		$0 < u < \frac{\pi}{2}$
$p_2 > 0$	$p_1 = 0$		$u = \frac{\pi}{2}$
$p_2 > 0$	$p_1 < 0$		$\frac{\pi}{2} < u < \pi$
$p_2 = 0$	$p_1 < 0$		$u = \pm\pi$ (bang condition if $u_1 = \pi$)
$p_2 < 0$	$p_1 > 0$		$-\frac{\pi}{2} < u < 0$
$p_2 < 0$	$p_1 = 0$		$u = -\frac{\pi}{2}$
$p_2 < 0$	$p_1 < 0$		$-\pi < u < \frac{\pi}{2}$

(3.73)

There are no singular points if p_1 and p_2 are never simultaneously zero. This is verified by computing the determinant R_1 of Equation (A.13). The subarc ends either with (3.38) or (3.64) becomes zero.

The Constrained Subarc $u = \pm u_1$ (C-3)

Let φ be the angle defined by Equations (3.72) and the sign conventions given by (3.73). Then substitution into the minimum principle Equation (3.71) gives

$$\cos(\varphi - u) \geqq \cos(\varphi - U), \tag{3.74}$$

which is satisfied if u and $\varphi < \pm\pi$, have the same sign. The condition $\varphi = \pi$ indicates a bang. Furthermore, substitution into (3.68) (with $\mu_2 = 0$), gives

$$\mu_1 = -\left[\frac{S\rho v}{2m}\sqrt{(C_{LO}p_2)^2 + (C_{DL}p_1 v)^2}\ \frac{\sin(\varphi - u)}{u}\right]. \tag{3.75}$$

Since u and $\sin(\varphi - u)$ have the same sign, $u_1 \leqq 0$, as required by Equation (2.14).

There are no singular points; this is easily shown by computing the determinant R_2 of Equation (A.23). It is also easily shown that the control function is continuous at the junction between constrained and unconstrained subarcs. Thus μ_1, from (3.75), must start and end with value zero, since at such points $u = \varphi$. Then the terminal surface is $\mu_1 = 0$, provided $\dot{\mu}_1 \neq 0$.

The Constrained Subarc $a_p = B$ (C-4)

The control function is determined from $a_p = B$ and the multiplier μ_2 from Equation (3.55). Expansion and rearrangement of the constraint gives

$$a \cos^2 u + 2b \cos u + c = 0 \tag{3.76}$$

where

$$a = C_{DL}^2 - C_{LO}^2$$

$$b = C_{DO} C_{DL}$$

$$c = C_{DO}^2 + C_{LO}^2 - \left(\frac{2m g_o B}{S \rho v^2} \right)^2 .$$

It follows by substituting $u = 0, \pm\pi$ into (3.76) that the inequality

$$(C_{DO} + C_{DL}) \geq \frac{2m g_o B}{S \rho v^2} \geq (C_{DO} - C_{DL}) > 0 \tag{3.77}$$

must hold. Furthermore, the determinant R_2 of Equation (A.23) is singular at these points.

Solution of (3.76) for u gives

$$\cos u = \frac{b}{a} \left[-1 + \sqrt{1 - \frac{ac}{b^2}} \right], \tag{3.78}$$

where the omitted root falls outside the range $|\cos u| \leq 1$. It is easily shown that the term under the square root in (3.78) is positive by substituting the upper limit of (3.77) into the expression and evaluating.

The minimum principle again takes the form (3.74), except that this time

$$-u < \varphi < u. \tag{3.79}$$

Otherwise, φ and u would be identical. Then, once again, $\varphi \neq 0$ and u must have the same sign, and $\varphi = 0$ is the bang condition. It can further be shown that the multiplier μ_2 becomes, when all the substitutions have been made,

$$\mu_2 = -\frac{g_o}{v}\sqrt{\frac{\left[C_L^2 + C_D^2\right]\left[(C_{LO}p_2)^2 + (C_{pL}p_1 v)^2\right]}{b^2 - ac}}\ \frac{\sin(u - \varphi)}{\sin u}$$

Since $\sin(u - \varphi)$ and $\sin u$ have the same signs, $\mu_2 \leq 0$ as required. Again, u is continuous at junction points, so μ_2 must start and end at zero; and $\dot{\mu}_2 = 0$ with $\mu_2 \neq 0$, describes the subarc terminal surface.

The Modified Newton-Raphson Equations (C-5)

The terminal conditions for this problem are of the form (2.47) which means the iterative Equation (2.54) applies with $p_2(T) = 0$, the single multiplier constraint. Let η_{ij} and ζ_{ij}, $i, j = 1, \ldots 4$, be the elements of $\nabla_{p_o} x(T)$ and $\nabla_{p_o} p(T)$, respectively. Then the matrix (2.55) may be written

$$\Lambda(y_o) = \begin{bmatrix} v(T) & \eta_{11} & \eta_{12} & \eta_{13} & \eta_{14} \\ \xi(T) & \eta_{31} & \eta_{32} & \eta_{33} & \eta_{34} \\ \zeta(T) & \eta_{41} & \eta_{42} & \eta_{43} & \eta_{44} \\ 0 & f_1(o) & f_2(o) & f_3(o) & f_4(o) \\ p_2(T) & \zeta_{21} & \zeta_{22} & \zeta_{23} & \zeta_{24} \end{bmatrix}. \tag{3.81}$$

The last vector of Equation (2.54) assumes the form

$$\begin{bmatrix} 0 \\ \xi(y_o) - A/R \\ \zeta(y_o) - \bar{R} \\ H(y_o) \\ p_2(y_o) \end{bmatrix},$$

where the first component $v(y_o) - V = 0$ is the stopping condition on the integrations and, hence, is satisfied by every trajectory.

The matrix of second partial derivatives in Equation (2.105) is the five-by five matrix

$$\nabla_y^2 J(y_o) = \begin{bmatrix} -\dot{p}'(T)\, x(T) & -\dot{p}'(T)\, \nabla_{p_o} x(T) \\ -\nabla'_{p_o} x(T)\, \dot{p}'(T) & -\left[\nabla'_{p_o} x(T)\, \nabla_{p_o} p(T)\right] \end{bmatrix}_{\text{sym.}} \tag{3.82}$$

Both methods of Subsection II(C) were used to reduce this to a two-by-two matrix to be tested for positive-definiteness. For the determination using inequality (2.36), the equations

$$\begin{aligned} \gamma(y_o) &= \gamma(T) + Z_1 \\ y_1 &= T + Z_2 \end{aligned} \tag{3.83}$$

were added to the set (3.63). Then, Equation (2.35) reads

$$\nabla_x \psi_2 \Delta_y = \begin{bmatrix} \dot{v}(T) & \eta_{11} & \eta_{12} & \eta_{13} & \eta_{14} \\ \dot{\xi}(T) & \eta_{31} & \eta_{32} & \eta_{33} & \eta_{34} \\ \dot{\zeta}(T) & \eta_{41} & \eta_{42} & \eta_{43} & \eta_{44} \\ \dot{\gamma}(T) & \eta_{21} & \eta_{22} & \eta_{23} & \eta_{24} \\ 1 & 0 & 0 & 0 & 0 \end{bmatrix} \begin{bmatrix} dT \\ dp_{1_o} \\ dp_{2_o} \\ dp_{3_o} \\ dp_{4_o} \end{bmatrix} = \begin{bmatrix} 0 \\ 0 \\ 0 \\ \Delta Z_1 \\ \Delta Z_2 \end{bmatrix}, \qquad (3.84)$$

and the lower two-by-two matrix of the product

$$(\nabla'_x \psi_2)^{-1} \nabla^2_y J (\nabla_x \psi_2)^{-1} \qquad (3.85)$$

is the desired matrix A_4. In the other method, the first three equations of (3.84) were solved in the form

$$\begin{bmatrix} dT \\ dp_{1_o} \\ dp_{2_o} \end{bmatrix} = - \begin{bmatrix} v(T) & \eta_{11} & \eta_{12} \\ \xi(T) & \eta_{31} & \eta_{32} \\ \zeta(T) & \eta_{41} & \eta_{42} \end{bmatrix}^{-1} \begin{bmatrix} \eta_{13} & \eta_{14} \\ \eta_{33} & \eta_{34} \\ \eta_{43} & \eta_{44} \end{bmatrix} \begin{bmatrix} dp_{3_o} \\ dp_{4_o} \end{bmatrix}. \qquad (3.86)$$

Let D be the matrix of (3.85), and A_1, A_2 and A_3 be, respectively, the upper left hand (3 x 3), upper right-hand (3 x 2) and lower right-hand (2 x 2) submatrices of (3.82). Then the desired matrix is

$$D' A_1 D + D' A_2 + (D' A_2)' + A_3 . \qquad (3.87)$$

Computer Results (C-6)

Figures 3-5 through 3-8 represent one trajectory obtained using the modified Newton-Raphson method and explicitly completed partial derivatives. (Compare these with the extremal of Figures 4-37 through 4-39, which was used as the initial guess at the optimum.) The control function (Figure 3-6) starts on the -16-degree bound (maximum lift condition) and stays there for about 65 seconds. This is reasonable, since the radiative heating rate, proportional to $v^{12.5}$, could become quite large if the density term $\rho^{3/2}$ were not kept small by the control maneuver. As velocity begins to decrease and the path becomes shallower (Figure 3-5), dissipation of energy becomes important; therefore, the control moves toward zero degrees, the maximum drag condition. After the peak heating rate (Figure 3-7), a little more lift is called for, for ranging purposes. Then the control goes to the +16-degree bound, following the rule of thumb that the convective heating load is lighter, the faster the re-entry is accomplished. The peak acceleration is 9.5 g's compared to the 10.3 g's of the original extremal, and comparison of the heating-rate curves of Figures 3-7 and 4-39 shows that the major difference is near the peaks of the radiative curves (peak value is 188 BTU for Figure 4-39 and 182 BTU for Figure 3-7). The value of the optimal criterion was about 27,500 BTU for the extremal, which was reduced to 27,334 BTU by the optimization method. This points out the flatness of the $J(y)$ surface for this problem.

Figure 3-8 is included to show the angle φ of Subsection C-3. It can be interpreted as the unconstrained value of the control function, and, over the unconstrained subarc, u and φ are identical. At the terminal time, φ goes to π because of the necessary condition $p_2(T) = 0$.

There is some doubt that the trajectory of Figures 3-5 through 3-8 is a relative minimum, although, most likely it is. Both test matrices of Subsection C-5 are indefinite, but numerical problems could be the cause of this. The determinant of the matrix in (3.84) is very small (on the order

of 10^{-5}), so its inverse, used in (3.85), cannot be known very accurately. In the matrix (3.87) the middle two terms buck the outer terms, causing loss of from two to four significant digits. This is very severe, considering the accuracy of the original elements and the number of matrix multiplications required to arrive at the result. The primary cause of the trouble appears to be the flatness of the J(y) surface for this problem.

Some workers in the field feel that the initial value method of solving the optimization problem is too sensitive to use (for an example, see Ref. 29). They argue that the Euler-Lagrange equations are the adjoint system to the original system, and that one of these gives unstable solutions. This may well be true for some problems, but no such instabilities were found for this application. The method worked well, and was strongly convergent to the solution. Adequate prediction for all variables was obtained; in fact, the desired terminal altitude and range were achieved to at least eight significant digits. The terminal value of p_2 fared somewhat worse, 7×10^{-3} compared with its original value of 10^6. The Hamiltonian, a crude measure of the integration accuracy, changed from -3×10^{-7} to 10^{-2} at the end of the path, an acceptable value, according to past experience. Other evidence supporting the numerical accuracy may be found in Table 3-1.

Table 3-1. A Comparison of Partial Derivatives Computed in Various Ways

	$\frac{\partial J}{\partial p_{1_o}}$	$\frac{\partial J}{\partial p_{2_o}}$	$\frac{\partial J}{\partial p_{3_o}}$	$\frac{\partial J}{\partial p_{4_o}}$
Estimated	-0.14988×10^{5}	-0.217×10^{-1}	0.184×10^{-3}	0.118×10^{7}
Computed directly	$-0.15057908 \times 10^{5}$	$0.14247518 \times 10^{-1}$	$0.17744375 \times 10^{-2}$	0.12049032×10^{7}
$-p'(T)\nabla_{p_o} x(T)$	-0.150811×10^{5}	$+0.142588 \times 10^{-1}$	$+0.177867 \times 10^{-2}$	$+0.12067 \times 10^{7}$

These results were obtained for the extremal of Figures 4-37 through 4-39. The estimated values were computed for program checkout purposes, and the inaccuracy of the second result comes from differencing solutions which are the same to seven significant digits out of a possible eight. Solutions were the same to six significant digits for the last two results, but to only three for the first. The last row was hand-computed from computer results truncated to eight significant digits.

Table 3-2 is included to illustrate the convergence of the modified Newton-Raphson method for this problem. The criterion J(T) rose in this final series of iterations because the trajectory range had to be lengthened, and ranging always increases total heat.

Table 3-2. Convergence to the Solution

Iteration number	Method Constant	Hamiltonian H(o)	Criterion J(T)	Multiplier $p_2(T)$	h(T)-A feet	$\xi-\bar{R}$ feet
1		13.8	26,774	1.8×10^{4}	0.77	-234,691
2	0.2	11.0	26,887	1.5×10^{4}	0.559	-187,674
3	0.28	7.9	27,019	1×10^{4}	1.121	-132,679
4	0.46	4.3	27,170	5.4×10^{3}	2.313	-69,331
5	0.96	0.15	27,334	-28.0	3.077	-632
6	1.0	-0.2×10^{-5}	27,333	27.0	-0.228	-239
7	1.0	0.84×10^{-8}	27,334	0.88×10^{-1}	zero	-0.1
8	1.0	-0.65×10^{-8}	27,334	0.94×10^{-2}	zero	zero
9	1.0	-0.27×10^{-8}	27,334	0.74×10^{-2}	zero	zero

SECTION IV
LINEAR CONTROL SYNTHESIS AND SIMULATION

DISCUSSION (A)

It is well known that a quadratic integral criterion when applied to linear control systems specifies a linear control law with, in general, time dependent gains. Because of the simplicity of analyzing and mechanizing such systems, linear control in the vicinity of a predetermined reference trajectory is studied.

If the equations of motion for state x under control u are represented by

$$\dot{x} = f(x, u) \tag{4.1}$$

and a control $u(t)$ which transfers the state from given initial conditions x_o at $t = a$ to a final state x_f at a time T has been found, the equation for the correction δx from the reference path $x(t)$ to a disturbed trajectory is

$$\delta \dot{x} = f(x + \delta x, \; u + \Delta u) - f(x, u), \quad \delta x(a) = \Delta x_o, \tag{4.2}$$

where a new control function is represented as $u + \Delta u$. Equation (4.2) is the exact variational equation. In the neighborhood of the reference, the linear approximation to Equation (4.2) will predict a correction Δx which should reasonably approximate δx. The "first variational equation" is

$$\Delta \dot{x} = \nabla_x f \cdot \Delta x + \nabla_u f \cdot \Delta u, \quad \Delta x(a) = \Delta x_o, \tag{4.3}$$

where the matrices of partial derivatives $\nabla_x f$ and $\nabla_u f$ are evaluated along the reference. The problem is to find a correction to the control Δu

so certain final conditions for the reference are also satisfied by the perturbed trajectory. The simplest, though perhaps not the most natural, condition is to require particular components of the state to agree at the end-point. Thus, say

$$\Delta x_i(T) = 0 ; \quad i = q+1, \ldots, n ; \quad 0 \leq q \leq n-1 . \tag{4.4}$$

Then Δu will be completely specified as a function of time if it is chosen so

$$\int_a^T (\Delta u)^2 \, dt \tag{4.5}$$

is a minimum. Conditions (4.4) and criterion (4.5) can be greatly generalized, and the derivation of the control law may be made using many theories: Pontryagin's maximum principle, calculus of variations, dynamic programming, etc. The simplest approach for the case at hand will be used here, since general discussions can be found in the literature (Ref. 27 , for example).

The region of validity for the linear approximation is found by experimentation. It may be necessary that several reference trajectories be used to provide linear control over the entire corridor. This depends on further consideration of navigational accuracy and model fidelity. In a subsequent subsection, some results affecting these problems are discussed, and some preliminary navigation and control systems are evaluated by simulation.

If the control law found by the optimization process is represented by

$$\Delta u = E(t) \, \Delta x , \tag{4.6}$$

Equation (4.3) for the linear prediction becomes the homogeneous equation

$$\Delta \dot{x} = \left[\nabla_x f + \nabla_u f \cdot E \right] \Delta x . \tag{4.7}$$

If all state components must agree at the end-point ($q = 0$), that point must be a singular point of the differential equation, since there are other solutions than the trivial $\Delta x(t) \equiv 0$. As would be expected, this case is difficult to control. For the case studied, range and altitude of the trajectories are required to agree, and velocity and flight-path angle are free. This demands less of the control, but the end-point is still singular, since the solutions begin as a four-parameter family and end as a two-parameter family. This implies that some of the gains, the components of E, must tend to infinity at the end-point, which will lead to difficulties in simulation and mechanizations. Various expedients were tried, and these are discussed in subsequent subsections. A change of the mode of control near the end is probably indicated, since, in any case, the region of validity for the linear approximation is exceeded near the final point.

DERIVATION OF THE CONTROL LAW (B)

Let the row vector λ_i' be the solution of the adjoint homogeneous equation

$$\dot{\lambda}_i' = -\lambda_i' \cdot \nabla_x f \,, \tag{4.8}$$

which has all components zero at $t = T$ except for the ith component, which is unity. By direct calculation, using (4.8) and (4.3), it is found that

$$\frac{d}{dt}(\lambda_i' \cdot \Delta x) = \lambda_i' \nabla_u f \cdot \Delta u \,; \tag{4.9}$$

and, integrating and applying the end conditions (4.4), the equations

$$\lambda_i'(a) \cdot \Delta x(a) + \int_a^T \lambda_i' \cdot \nabla_u f \cdot \Delta u \, dt = 0 \tag{4.10}$$

for $i = q + 1, \ldots, n$ result.

The control must minimize integral (4.5) subject to these conditions. This simple problem can be considered using constant Lagrange multipliers p_i and completing the square on the auxiliary functional

$$\int_a^T (\Delta u)^2 \, dt + \sum_{i=q+1}^{n} p_i \lambda_i^{!}(t_o) \, \Delta x(t_o)$$

$$+ \sum_{i=q+1}^{n} p_i \int_a^T \lambda_i^{!} \cdot \nabla_u f \cdot \Delta u \, dt \qquad (4.11)$$

to get

$$\int_a^T \left[\Delta u + \frac{1}{2} \sum_{i=q+1}^{n} p_i \lambda_i^{!} \cdot \nabla_u f \right]^2 dt$$

$$+ \left\{ \text{terms not containing } \Delta u \right\} \qquad (4.12)$$

The terms which do not contain Δu cannot be influenced. Hence, the minimum occurs for

$$\Delta u = -\frac{1}{2} \sum_{i=q+1}^{n} p_i \lambda_i^{!} \cdot \nabla_u f \, , \qquad (4.13)$$

if there are no further constraints on Δu. The p_i can be determined from Equations (4.10). Substituting this Δu and doing a bit of manipulation yields

$$\sum_{i=q+1}^{n} y_{ij}(T, a_o)\, p_j = 2\,\lambda_i'(a_o) \cdot \Delta x(a_o), \qquad (4.14)$$

when the abbreviation

$$y_{ij}(T, a) = \int_a^T (\lambda_i' \cdot \nabla_u f)(\lambda_j' \cdot \nabla_u f)\, dt \qquad (4.15)$$

is used. All this may be condensed with the following matrix notation: Let

$$\Lambda' = \begin{pmatrix} \lambda'_{q+1} \\ \lambda'_{q+2} \\ \vdots \\ \lambda'_n \end{pmatrix}, \qquad (n \times (n-q))$$

$$Y(T, a) = (y_{ij}(T, a)), \qquad (n-q) \times (n-q)$$

$$p = \begin{pmatrix} p_{q+1} \\ p_{q+2} \\ \vdots \\ p_n \end{pmatrix}.$$

Then Equation (4. 13) reads

$$\Delta u = -\frac{1}{2}\, p'\, \Lambda'\, \nabla_u f \ , \tag{4. 16}$$

and (4. 14) and (4. 15) become

$$Y(T, a)\, p = 2\, \Lambda'(a)\, \Delta x(a) \tag{4. 17}$$

$$Y(T, a) = \int_a^T \Lambda'\, \nabla_u f\, (\Lambda' \cdot \nabla_u f)'\, dt \ . \tag{4. 18}$$

The matrix $Y(T, a)$ is assumed to be nonsingular for $a < T$. This property is related to the controllability of the system. Thus, the control law becomes

$$\Delta u(t) = -[\nabla_u f(t)]'\, \Lambda(t)\, Y^{-1}(T, a)\, \Lambda'(a)\, \Delta x(a), \tag{4. 19}$$

when the transpose of Equation (4. 16) is used. This holds for $a \leq t \leq T$ and may be considered as an open-loop control. Identifying a with t gives the closed-loop operation, and the control law is

$$\Delta u(t) = E(t)\, \Delta x(t) \ , \tag{4. 20}$$

with

$$E(t) = -[\nabla_u f(t)]'\, \Lambda(t)\, Y^{-1}(T, t)\, \Lambda'(t) \ . \tag{4. 21}$$

SIMULATION OF THE LOW-LIFT VEHICLE WITH ROLL MODULATION AND ad hoc REFERENCE TRAJECTORY (C)

The Model (C-1)

The motion of an Apollo-type capsule is assumed to be governed by the two-dimensional Equations (1.1), and control for flights at a fixed angle of attack is to be effected by changing the roll angle φ. It is assumed that the essential characteristics of the motion are preserved when the lateral motion and forces of the more realistic three-dimensional flight are neglected. Hence, the lift and drag coefficients are taken in the form (1.5). The atmosphere is generally considered to be exponential with equation

$$\rho = \rho_o C^{-\beta R \xi}, \qquad (4.22)$$

but the 1959 ARDC atmosphere is also used in places to assess variation in density effects.

The constants in the equations are:

Aerodynamic reference area:	$S = 129$ square feet
Weight:	$W = 8125$ pounds
Drag Coefficient:	$C_{DO} = 1.02$

(The drag coefficient is constant for Mach numbers greater than four; it was found that allowing it to change with Mach number had little effect on the trajectory. Hence, it is taken as constant throughout the analysis.)

Lift coefficient:	$C_{LO} = 0.51 \quad (C_{LO}/C_{DO} = 0.5)$
Ballistic coefficient:	$W/C_{DO} S = 61.7$ lb/sq. ft

Sea level density:	ρ_o	= 0.0023769
Atmosphere coefficient:	β	= 1/123500
Sea level gravity:	g_o	= 32.2 ft/sec^2
Radius of earth:	R	= 20,903,520 ft.

The initial conditions for the trajectories are chosen as:

Velocity:	v_o	= 36,080 ft/sec
Flight path angle:	γ_o	= -6.4 degrees (for standard reference trajectory)
Altitude:	h_o	= 400,000 ft.
Range:	ζ_o	= 0

The terminal conditions expected are:

Altitude:	h_T	= 100,000 ft.
Range:	ζ	= 2100 statute miles

The time of flight is chosen experimentally. This is discussed in the next paragraph.

The rate of roll $\dot{\varphi}$ is limited to 20 degrees/second in the reference trajectories. While no limit is placed on the closed-loop rate $\dot{\varphi} + \Delta\dot{\varphi}$, practical considerations require that this limit not be greatly exceeded. This condition is satisfied on the flight paths studied. The control command variable $\Delta\varphi$ is restricted by the condition that $\varphi + \Delta\varphi$ must fall in the same half-circle, either (o, π) or $(\pi, 2\pi)$, as φ in order that an artificial control reversal does not occur because of the nonlinear manner in which the control enters the equations through the cosine function. An indirect restriction is that the pilot's acceleration, given by

$$a_p = \frac{S \rho v^2}{2m g_o} \sqrt{C_D^2 + C_L^2} \qquad (4.23)$$

not exceed 10 g.

The ad hoc Reference Trajectory (C-2)

To begin the study and map out the re-entry corridor, trajectories were found experimentally by guessing forms of control programs $\varphi(t)$. Trajectories were then computed, beginning at a height of 400,000 feet with a 36,080-feet per second initial velocity and various initial flight-path angles γ_o. It was determined that the safe re-entry corridor was limited to trajectories beginning with γ_o between -5.4 and -7.4 degrees, since, for γ_o greater than -5.4 degrees, there was not sufficient lift to avoid a skip-out, and, if γ_o was less than -7.4 degrees, the 10-g survival deacceleration limit was exceeded.

The form of the roll program adopted is as follows: The roll angle φ is set at zero for maximum positive lift until the tangential acceleration a_t reaches 0.6 g; for purposes of the reference program, time is re-set to zero at this instant. The roll is held at zero for 15 seconds past the re-set time and then is increased linearly with time for 25 seconds until a certain maximum, φ_{max}, is achieved. This maximum is held for the next 80 seconds, after which the roll is decreased linearly for 80 seconds until an angle of 22 degrees is reached. It is kept at this level for the remainder of the flight, which is terminated when the altitude decreases to 100,000 feet. The value of φ_{max} is chosen so that the flight has a range of 2100 miles. A plot of γ_o against the value of φ_{max}, which gives the 2100-mile range, is shown in Figure 4-1. It is observed from this

graph that a constant-range controller, using the -6.4 degree case as a base, can control most of the re-entry corridor (-7.4 to -5.9) with a maximum $\Delta\varphi$ correction of less than 15 degrees.

The roll program, for the trajectory beginning with $\gamma_o = -6.4$ degrees is shown in Figure 4-2; this is taken as the standard control program. Its analytical representation is

$$\begin{aligned}
\varphi(t) &= 0, \quad 0 \leq t \leq 15; \\
\varphi(t) &= \varphi_{max} \frac{t - 15}{25}, \quad 15 \leq t \leq 40; \\
\varphi(t) &= \varphi_{max}, \quad 40 \leq t \leq 120; \\
\varphi(t) &= \varphi_{max} + (22 - \varphi_{max}) \frac{t - 120}{80}, \quad 120 \leq t \leq 200; \\
\varphi(t) &= 22, \quad 200 \leq t.
\end{aligned} \tag{4.24}$$

The quantity φ_{max} for this trajectory is 90.97 degrees. The pilot's acceleration for three trajectories with roll programs of this type is shown in Figure 4-3. These trajectories cover the entire re-entry corridor for this family of roll programs. The re-set time is plotted against initial angle in Figure 4-4.

Characteristics of the standard reference trajectory ($\gamma_o = 6.4$ degrees) are given in Figures 4-5, 4-6, 4-7, 4-8. These are plots at height, velocity and re-entry angle against range, and range against time after re-set. The closed-loop flights described later use this as a reference.

Sensitivity of the standard trajectory to various types of errors is illustrated in Figures 4-9 through 4-16. Range effects from shifting the roll timing ±2 seconds indicate that roll timing is critical (Figure 4-9). Roll magnitude variations of ±2 degrees are shown in Figure 4-10, and the effect of a change of ±0.5 degrees of initial re-entry angle on range is given in Figure 4-11.

Figure 4-12 shows the effect on range when the initial height on the standard reference is changed by either +20,000 feet or - 50,000 feet. Skip-out occurs with an altitude error much above 20,000 feet in an open-loop run.

Initial velocity changes of ±1000 feet per second, ballistic coefficient variations of ±10 per cent and change in density by a factor of

$$1.0 \pm 0.5 \frac{h - 110,000}{290,000} , \qquad (4.25)$$

are plotted in Figures 4-13 through 4-15. Finally, Figure 4-16 shows the range effects of varying the time that φ_{max} is held in the standard roll program (Figure 4-2) by ±20 seconds. By comparing this result with the runs in which the complete roll timing program was changed by ±2 seconds (Figure 4-9), it can be seen that the range effects are about three times as great as those in Figure 4-16, even though the timing change in Figure 4-16 is 10 times larger. Roll changes applied at a later time have less effect on ranging than the same roll changes applied earlier.

Some of the considerations leading to this choice of roll programs are given in the following discussion:

The roll φ must be set equal to zero to obtain maximum positive lift during the initial re-entry phase, at least until the first acceleration peak is passed, to prevent the vehicle diving into the atmosphere and causing an increase in magnitude of the peak. The first acceleration peak for the - 7.4-degree trajectory is equal to the - 10-g acceleration limit.

After the first acceleration peak is passed, the vehicle would soon skip out of the atmosphere if the roll angle were left zero. Within the bound of the Apollo roll-rate limit of 20 degrees per second, it was necessary to apply rapidly a roll sufficient to prevent skip-out.

When the vehicle slows enough that a skip-out can no longer occur, the roll must be decreased to a small value, such as 45 or 22 degrees, to prevent the trajectory from going too deeply into the atmosphere and exceeding the acceleration limit. The high negative lift needed to prevent a skip-out in the case in which γ_o equal -5.4 degrees cannot be left in effect too long, or too much acceleration will occur. The final value of roll used is not critical, because most of the ranging is done by the maximum roll value. It is best not to use a final roll of zero degrees, because no additional lift is then available for control about the reference.

By basing the roll control on the interval after a_t = 0.6 g, the large variability between initial time and the time when the vehicle is experiencing significant aerodynamic effects is eliminated from roll control timing. With the standard roll control timing, which can be used over the whole corridor to get a constant range, the reference is less sensitive to perturbations and, also, requires smaller $\Delta\varphi$ corrections.

This roll control was satisfactory for the whole corridor if timing errors are held to within a few seconds. A better timing would start the roll 22 seconds after the a_t = 0.4 point. This would delay the roll application in the -5.4-degree case and prevent the slight increase in the acceleration peak of the a_t = 0.6 g time reset. The alternate timing is set to leave the -5.4-degree case unchanged, because any delay in this timing of more than a few seconds would cause a skip-out. Roll timing based on initial time is unsatisfactory because different initial conditions would require initiation of the roll program to occur over a range of 40 seconds.

The roll angle magnitude which will maintain a constant-altitude flight at the turnover point ($\gamma = 0$) is an important quantity. Increasing this value more than seven degrees will cause the vehicle to dive into the atmosphere so deeply that the 10-g limit will be exceeded; decreasing this value more than seven degrees will result in a skip-out. Ranges between 2000 and 5000 miles are possible for all initial conditions by using different values of roll within seven degrees of turnover roll. Ranging possibilities rapidly decrease after the turnover point, especially in the - 7.4-degree case. It is, therefore, necessary that the correct roll magnitude be closely approximated in the vicinity of the turnover point in order to get the desired range.

The Linear Perturbation Controller (C-3)

The closed-loop system is diagrammed in Figure 4-17. For now, it is assumed that the navigation system produces an accurate estimate $x^m(t)$ of the state $x(t)$. (The effect of errors in navigation is discussed under Subheading C-6.) The state estimate is differenced with the state of the reference trajectory, and this result is used to provide a correction $\Delta\varphi$ to the reference roll command. The inner-loop controller causes the vehicle to assume this roll angle; this controller is assumed perfect and is not studied here. The related equations are

$$\begin{aligned} x^m(t) &= x(t) \\ \Delta\varphi(t) &= E(t)\left[x^m(t) - x^r(t)\right] \\ \varphi(t) &= \varphi^c(t) = \varphi^r(t) + \Delta\varphi(t) \\ \frac{dx}{dt} &= f(x, \varphi(t)) \end{aligned} \qquad (4.26)$$

where $x^r(t)$ and $\varphi^r(t)$ are the reference trajectory state and corresponding control, as developed in the previous section. The feedback gains, represented by matrix $E(t)$, are computed according to the theory outlined under Subsection B.

The equations of linear prediction (4.3) for the particular model represented in Equations (1.1) are

$$\dot{\Delta v} = -\frac{S\rho v}{m} C_{DO}\,\Delta v - \frac{g_o \cos\gamma}{(1+\xi)^2}\,\Delta\gamma$$

$$+\left[-\frac{Sv^2}{2m} C_{DO}\,\frac{\partial\rho}{\partial\xi} + \frac{2 g_o \sin\gamma}{(1+\xi)^3}\right]\Delta\xi$$

$$\dot{\Delta\gamma} = \left\{\frac{\cos\gamma}{1+\xi}\left[\frac{1}{R} + \frac{g_o}{v^2(1+\xi)}\right] + \frac{S\rho}{2m} C_{LO}\cos\varphi\right\}\Delta v$$

$$-\frac{\sin\gamma}{1+\xi}\left[\frac{v}{R} - \frac{g_o}{v(1+\xi)}\right]\Delta\gamma - \frac{S\rho v C_{LO}}{2m}\,\Delta\varphi\,\sin\varphi$$

$$+\left\{-\frac{\cos\gamma}{(1+\xi)^2}\left[\frac{v}{R} + \frac{2 g_o}{v(1+\xi)}\right] + \frac{S v C_{LO}\cos\varphi}{2m}\,\frac{\partial\rho}{\partial\xi}\right\}\Delta\xi$$

$$\dot{\Delta\xi} = \frac{\sin\gamma}{R}\,\Delta v + \frac{v\cos\gamma}{R}\,\Delta\gamma$$

$$\dot{\Delta\zeta} = \frac{\cos\gamma}{1+\xi}\,\Delta v - \frac{v\sin\gamma}{1+\xi}\,\Delta\gamma - \frac{v\cos\gamma}{(1+\xi)^2}\,\Delta\xi\,.$$

(4.27)

(The quantities ρ, v, γ, ξ, ζ are, of course, those of the reference; the superscript r has been dropped for convenience.) The guidance sensitivity matrix E(t) is calculated according to formulas (4.18) and (4.21) from solutions of the equations adjoint to (4.27). These components are plotted in Figures 4-18 and 4-19.

The elements of E(t), from the theory and as demonstrated in the graphs, become infinite at the end-point, and it is necessary to introduce some modification to take care of this singularity. A transformation,

$$\Delta\varphi_c = \arctan \Delta\varphi, \tag{4.28}$$

was used for this purpose. Experiments indicate that this transformation actually increases the region of controllability. The additional restriction discussed under C-1 now reads: $\varphi + \Delta\varphi_c$ is limited to $(0, \pi)$ or $(\pi, 2\pi)$. The full $\Delta\varphi$ control can be used during the time φ_{max} is being applied because φ_{max} is close to 90 degrees, and the ±90 degree range of $\Delta\varphi_c$ will not cause a crossing of either the zero-or 180-degree limits on the roll angle.

Closed-Loop Results, Precise Navigation Assumed (C-4)

Satisfactory performance was obtained over almost the entire corridor. Typical terminal errors are summarized in Table 4-1.

Table 4-1. Terminal Errors Caused by Various Errors in the Model

Model Variation	Resulting Terminal Error		
	$\Delta v(T)$ feet/second	$\Delta h(T)$ feet	$\Delta \zeta$ miles
1. φ bias - 1 degree	15	-21	0
2. $\bar{\rho} = \rho\left(1 + 0.5\ \frac{h - 110,000}{290,000}\right)$	173	1791	0.1
3. $\bar{\rho} = \rho\left(1 - 0.5\ \frac{h - 110,000}{290,000}\right)$	-169	-2584	-0.1
4. γ_o = - 6.9 degrees	86	- 462	0
5. γ_o = - 7.4 degrees	180	1282	-0.1
6. v_o + 1000 feet/second	-23	- 53	-0.0
7. v_o - 1000 feet/second	31	- 49	0
8. 1.1 $W/C_D S$*	-286	-10,510	-0.2
9. 0.9 $W/C_D S$*	137	4845	-0.5

*The constraint on $\Delta \varphi^c$ would have reduced these errors

The particular case in which the initial re-entry angle is - 5.9 degrees (compared to - 6.4 for the reference path) and in which the exponential atmosphere model is replaced by the ARDC '59 form was chosen to illustrate the results. The roll correction $\Delta\varphi_c$ for this flight is shown in Figure 4-20; note the maximum positive lift condition of - 22 degrees correction after 370 seconds. The final state errors are increased

several times if this limit is not imposed. Figures 4-21 through 4-25 plot the deviations from the reference for range, flight-path angle, altitude, velocity and tangential acceleration. This case will subsequently be referred to as the standard perturbed trajectory.

A flight beginning with angle - 6.9 degrees is graphed in Figure 4-26 and 4-27. Note that the roll corrections are more in the linear range than in the previous case because this perturbation is toward the acceleration limit boundary, and the other is toward the skip-out limit.

Figure 4-28 is a plot of $\Delta\zeta$, the range deviation, against time for two closed-loop trajectories with the same conditions as the reference, except h_o is changed by ±50,000 feet. Since, in the open-loop case with Δh_o = 25,000 feet, skip-out occurs, this run shows that the linear control scheme can control large perturbations.

Other perturbations were investigated. The results are summarized in Tables 4-2, 4-3.

Table 4-2. Perturbation Study Results (1)

Case	ΔV(T)	Δh(T)	Δζ
1	126	688	- 1.5
2	-197	-2648	0.1
3	-330	-6295	- 4.0
4	-529	-17885	- 2.0

Case 1 is the standard perturbed reference. Cases 2, 3 and 4 have the same initial conditions as Case 1, γ_o = - 5.9 degrees, except that they all use the exponential atmosphere instead of the ARDC '59 atmosphere. Cases 1 and 2 indicate that the effects of using the exponential atmosphere are not large. In Cases 1 and 2, a roll correction greater in magnitude than - 22 degrees is called for after the time the reference roll φ is set to its final value of 22 degrees. $\Delta\varphi_c$ is then set equal to - 22 degrees, so that $\varphi(t) + \Delta\varphi_c(t) = 0$, the maximum lift condition. In Case 4, $\Delta\varphi_c$ is allowed to cross the zero point, and, in Case 3, $\Delta\varphi_c$ is set zero. Because Case 2 has final errors several times smaller than Cases 3 and 4, it is concluded that the best choice is to hold $\Delta\varphi_c$ at - 22 degrees.

Table 4-3. Perturbation Study Results (2)

Case	ΔV(T)	Δh(T)	ΔRange
5	- 891	-20,508	- 26
6	255	- 455	0.2
7	-1634	-63,055	- 65

Cases 5 and 6 have the standard reference conditions, except the initial height is perturbed 50,000 feet in Case 5 and - 50,000 feet in Case 6. Case 5 shows the effect of a large perturbation towards the skip-out boundary, and Case 6 a larger perturbation toward the acceleration boundary. Without the transformation (4.28), it was found, in other runs, that too much acceleration for survival occurs (Case 5) or a skip-out occurs (Case 6). Both Case 5 and Case 7 have the same initial conditions, initial Δh = 50,000 feet, but Case 7 uses the unlimited $\Delta\varphi_c$. In Case 4, the use of the unlimited $\Delta\varphi$ results in a several-fold increase in final errors, but, in Case 7, the same several-fold increase of the already large final errors of Case 5 may affect survival.

A Perturbational Navigation System (C-5)

The navigation calculation may be incorporated into the control scheme as diagrammed in Figure 4-29. The estimate of the perturbation of the state is calculated by subtracting the reference trajectory acceleration from that which is measured and then carrying out navigation computations. The set of equations to estimate the state perturbation is the same as system (4, 27) when the $\Delta\varphi$ -term in the second equation of that set is omitted. Since the aerodynamic force terms are determined with accelerometers, a more convenient form for the first two of these equations is

$$\Delta\dot{v} = -\Delta a_t + \frac{g_o}{(1+\xi)^2}\left[-\Delta\gamma\cos\gamma + \frac{2\sin\gamma}{1+\xi}\Delta\xi\right]$$

$$\Delta\dot{\gamma} = \frac{\Delta a_n}{v} + \frac{g_o}{v(1+\xi)^2}\left[\Delta\gamma\sin\gamma + \frac{2\cos\gamma}{1+\xi}\Delta\xi\right] \qquad (4.29)$$

$$+\frac{g_o\cos\gamma}{v^2(1+\xi)^2}\Delta v - \frac{v\sin\gamma}{R(1+\xi)}\Delta\gamma$$

$$+\frac{\cos\gamma}{1+\xi}\left[\frac{\Delta v}{R} - \frac{v}{R(1+\xi)}\Delta\xi\right]$$

A mechanization could be achieved using these equations. A diagram of such a system is given in Figure 4-30. However, not all terms are of

equal importance. It was found that the equations could be simplified to the form

$$\Delta\dot{v} = -\Delta a_t$$

$$\Delta\dot{\gamma} = \frac{1}{v}\left[\Delta a_n - (a_n + \Delta a_n)\frac{\Delta v}{v}\right] + \frac{1}{1+\xi}\left[\frac{1}{R} + \frac{g_o}{v^2(1+\xi)}\right]\Delta v \qquad (4.30)$$

$$\Delta\dot{\xi} = (v + \Delta v)(\gamma + \Delta\gamma)\frac{1}{R}$$

$$\Delta\dot{\zeta} = \frac{1}{1+\xi}\Delta v .$$

Note that some second-order terms are retained, while certain first-order terms are dropped. A mechanization for these equations is shown in Figure 4-31.

Using the approximate scheme, an exponential atmosphere and the standard perturbed reference trajectory, the following terminal errors were found:

Range = 6 miles
Altitude = 13,025 feet
Velocity = 525 feet per second.

A further analysis shows that γ_o must be known to about 0.2 degrees. Since γ_o cannot be inferred adequately from inertial measurements alone, external information is required.

The accuracy required in measuring acceleration is indicated by inserting an 0.05-g bias into Δa_t and Δa_n. The results are given in Table 4-4.

Table 4-4. Terminal Errors Caused by Accelerometer Bias for Standard Perturbed Trajectory

Error Source	Terminal Errors					
	Actual			System		
	Range	Altitude	Velocity	Range	Altitude	Velocity
Standard perturbed trajectory	6.0 miles	-13,025 feet	-525 ft/second			
$\Delta a_n = \Delta a_t = 0.05\ g$	54.5	1000	44	-1.0 miles	-6000 feet	-920 ft/second
$\Delta a_n = \Delta a_t = -0.05\ g$	-40.0	-20,000	-850	8.6	-35,000	-205

A control system which uses only measurements of normal and tangential acceleration components plus a roll angle determination was developed and simulated. It was found that it could control only about one-fifth of the re-entry corridor and, so, was unsatisfactory.

Effect of State-Measurement Errors (C-6)

The initial conditions for the flight path may be obtained on board the vehicle from several sources:

Propagation of known mid-course errors

Information telemetered from a ground fix near the onset of re-entry

Instruments in the vehicle.

The accuracy and availability of the first two sources for estimating the initial state are not known, and it is doubtful that the last one can provide the flight path angle to the accuracy required for successful re-entry, since simple

flight path indicators generally have errors of about one degree. The simulations reported here indicate that this information must be known to ± 0.2 degrees or the linear control scheme may fail. Initial conditions on the state other than the flight path angle are not critical. Velocity will be known to 100 feet per second from energy considerations. The range of a perturbed trajectory at re-set may be estimated closely by multiplying the range of the reference path by the ratio of perturbed time to re-set to the reference time of reset (re-set time is the instant the tangential acceleration reaches 0.6 g). From this experience, the following procedure was adopted:

For the control calculations, assume initial range to be the reference range and velocity and altitude at re-set time to be that of the reference trajectory at the corresponding instant. The range at re-set is estimated as outlined above.

This procedure causes errors in altitude of about 5,000 to 10,000 feet because the perturbed ρ is based on the ARDC '59 atmosphere, and the reference ρ comes from the exponential atmosphere. Since the ARDC '59 atmosphere gives a -35 per cent to 20 per cent density variation from the exponential atmosphere, a realistic test was made on the effect of density variations on the controller.

It was not possible to handle the flight path angle in this manner.

At one stage of the investigation, it was hoped to estimate the perturbed γ when $a_t = 0.6$ g by using the time it takes a_t to go from 0.2 g to 0.6 g. This time is called the rise time. The rise times for a series of initial re-entry angles were determined with computer runs. Then, by an inverse interpolation, γ could be estimated to within 0.15 degree when using the exponential atmosphere, even with perturbations such as:

Changes in the ballistic coefficient of ± 10 per cent

Accelerometer bias less than 0.02 g

Density changes by a factor of $1 \pm 0.5 \frac{h - 110,000}{290,000}$

If the exponential atmosphere is replaced by the ARDC '59 atmosphere, an error of -1.35 degrees occurs in the γ estimation. Also, it was noticed that the ARDC '62 atmosphere gives a -0.7 degree error. The γ estimation errors between the different atmospheres are caused by changes of the derivative of the density with respect to height. Because the change of density with respect to height is almost inversely proportional to molecular temperature, and this temperature fluctuates a great deal daily, the rise time of a_t is not a satisfactory estimator of γ. When the atmosphere is changed by a factor as above, the height at which $a_t \doteq 0.6$ g changes by ±7000 feet; but a similar change in the height occurs at the point at which $a_t = 0.2$ g, so the difference in altitudes is still within 800 feet of the 26,000-foot difference of the standard reference. Using the ARDC '59 atmosphere, the height difference is 19,000 feet, which is less than with the exponential atmosphere. The shorter rise time is interpreted as a steeper flight path.

Many closed-loop trajectories were calculated to determine the effect of errors in the state on the $\Delta\phi(t)$ calculation. The standard perturbed closed-loop trajectory conditions were used in these runs. Table 4-5 gives some of this data.

Table 4-5. Effect of Errors in the State on the $\Delta\phi(t)$ Calculation

	Actual Errors			Estimated Errors		
Case	$\Delta v(T)$	$\Delta h(T)$	$\Delta\zeta$	$\Delta v(T)$	$\Delta h(T)$	$\Delta\zeta$
1	126	678	-1.5			
17	-525	-13025	5.7	-702	-20922	2.1
18	44	-1077	54.6	-920	-6235	-1.4
19	-851	-19672	-40.3	-206	-35306	8.3
20	-289	-7982	54.8	-1072	-32421	8.5
21	-420	-8902	-42.1	132	-2939	-0.4
22	25	-1037	-9.4	3	6603	-11.6
23	-702	-16048	14.8	-939	-39975	10.3

Case 1 is the standard perturbed case, which uses the exact state in calculating $\Delta\phi(t)$; it is given so comparisons may be made with Cases 17 through 23, which are under the same conditions except the approximate state error is used. The integration of Equation (4-2) on board the vehicle gives an inexact state error rather than the exact state error because both the initial state error is unknown and the output of imperfect accelerometers must be used in calculating the derivatives.

Cases 17, 22, and 23 show the effects of integrating Equation (4-2) when perfect accelerometers are used but the initial conditions are the inexact values. In Case 17, the value of γ (0) is assumed to have no error; in Cases 22 and 23, the error in the γ (0) estimation is assumed to be 0.1 and -0.1 degrees, respectively. In Cases 18 and 19, the a_t and a_n accelerometers have a steady-state bias of 0.05 g and -0.05 g, respectively. In Cases 20 and 21, the accelerometers have 2 per cent and -2 per cent error, respectively. The initial state errors in Cases 18 through 21 are estimated in the same way as in Case 17. The reset times in the last cases are slightly different than in Case 17 because an imperfect accelerometer is being used to determine the point at which a_t = 0.6 g.

Integration with an accelerometer bias of 0.05 g for 600 seconds gives rise to about a 900-foot-per-second velocity error and a 50-mile range error, which explains the 50-mile final difference in $\Delta\zeta$ and Δv in Cases 18 and 19. The controller based on the estimated initial state does a good job of reducing the final value of estimated $\Delta\zeta$ to around five miles, but it is off about 50 miles from the real range error.

Table 4.6. Perturbation Study Results (4)

Case	$\Delta v(T)$	$\Delta h(T)$	$\Delta\zeta$
24	-549	-11890	66.5
25	-733	-15623	-78.1

Cases 24 and 25 correspond to the standard perturbed Case 1, except that, when computing the control $\Delta\phi$ in Case 24, $\Delta\gamma$ was omitted, and, in Case 25, Δh was omitted. In the above cases, the exact state is known but not completely used. When both $\Delta\gamma$ and Δh are ignored, control is lost, and the trajectory hits the ground at 440 seconds with a 350-mile range error, showing the necessity of estimating the complete state error. If the perturbation errors get too large, for instance integrating from a poor path angle estimate, the controller fails.

Figures 4-32 to 4-36 present the different state errors in Cases 1 and 20. These are plots of $\Delta\phi$, $\Delta\zeta$, $\Delta\alpha$, Δh and Δv with time. The quantities marked with the tilda are the errors computed with the inexact initial conditions.

The difference between the exact and inexact error, shown by Figures 4-34 and 4-35, is small for about the first 100 seconds, so the trajectory is controlled correctly during this critical time. After this, the approximate state estimate deteriorates, but bad control $\Delta\phi$ (t) at this time has little effect, and a good re-entry is still accomplished. When the initial $\Delta\gamma$ estimate is in too-great error, ± 0.4 degree, the altitude estimate rapidly deteriorates, and erroneous control signals are given during the early critical part of the re-entry. This sometimes causes the trajectory either to exceed the acceleration limit of 10 g's or to skip a thousand miles or more.

STUDY OF A LOW-LIFT VEHICLE WITH ANGLE OF ATTACK MODULATION AND EXTREMAL REFERENCE TRAJECTORY (D)

The Model and the Controller (D-1)

The re-entry body considered in this subsection is the capsule studied in Section III (C). The equations of motion are assumed to be the system (1.1), and control is produced by changing angle of attack to vary lift and drag coefficents according to Equations (1.4). The numerical values for the coefficients

in these equations are

$$C_{DO} = 0.88, \quad C_{DL} = 0.52, \quad C_{LO} = -0.505, \quad e = 2.4.$$

The atmosphere is again assumed to be represented by the exponential low.

A linear controller is studied, the theory of which is found in subsection B. It is the same type of linear, closed-loop controller used in the previous simulation. The control attempts to drive altitude and range errors to zero, but velocity and flight path angle are left free. Again, because of the singularity at the end-point, special procedures are employed to limit the control command in that neighborhood. Two methods are compared: One limits the control correction predicted by $\Delta u = E(t)\Delta x$ by ± 15 degrees; the other bounds the Δu near the end of the trajectory by 1 1/2-times the maximum correction used in the beginning of the flight. (The maximum usually occurs at the first turn-over after about 90 seconds of flight). The second technique, which allows smaller variations, was generally found to give better end-point results when the disturbances were small; but with large perturbations, the results are inconclusive.

The Extremal Reference Trajectory (D-2)

The linear controller is intended to operate about the optimal reference path which was computed in Section III. That calculation had not been completed when this controller study was begun, so an extremal trajectory was chosen as the reference for an intermediate analysis.

An extremal was defined in Section II as a path which satisfies the Euler-Lagrange equations and the Weierstrass-Clebsch conditions, but not necessarily the required boundary conditions. Here, this may be interpreted as a path satisfying the equations of motion with the control required by the

minimum principle. As in Section III, the control command was limited to excursions between ± 16 degrees (in future work this bound is to be extended).

The control for the reference is plotted in Figure 4-37 along with the pilot's acceleration. Figure 4-38 shows the state variables v, α, h as functions of time, and the heating characteristics for a re-entry along this path are recorded in Figure 4-39. Note the similarity of these graphs to those for the optimal trajectory (Figures 3-5 to 3-7).

The reference was computed by beginning with the conditions

$$v_o = 35,000 \text{ feet per second}$$
$$\gamma_o = -5.75 \text{ degrees}$$
$$h_o = 400,000 \text{ feet}$$
$$\zeta_o = \text{zero},$$

and a particular choice of the adjoint variables, in this case

$$b_{10} = 3.6565$$
$$b_{20} = 230$$
$$b_{30} = 67931.9$$
$$b_{40} = -2565.54,$$

and terminating when the second adjoint variable became zero. The range of initial guesses on the adjoints which gives reasonable re-entry paths was found by trial and error.

The control sensitivity along the reference path was studied by applying a constant correction to the angle of attack ($\Delta u = e\Delta\alpha = 2.4\ \Delta\alpha$) and integrating the first variational Equations (4.3) backward in time from the end

of the trajectory. Typical trends are shown in Figures 4-40 and 4-41 for a one-degree change in angle of attack. These curves may be interpreted as the errors in Δv, Δh, and $\Delta \zeta$, which will be nulled by a one-degree correction in control applied at the time indicated by the abscissa and held to the end. Note that not much control may be exercised near the end, and the controllability diminishes rapidly after the first 90 seconds of flight.

Open- and Closed-Loop Results (D-3)

The controller was tested by calculating a series of trajectories in which a single perturbation was made in an initial condition, or in one of the parameters of the vehicle. Each quantity was varied by small positive and negative increments and by large changes which were chosen to be 2 1/2-times the small variations. The open-loop paths, which use the reference program for angle of attack with no added control correction, were computed for comparison.

A typical case is illustrated by Figures 4-42 to 4-44; the initial flight path angle was increased by 0.05 degree in this example. The control correction, plotted as a function of time in Figure 4-44, saturates at about 220 seconds, and was limited to -15 degrees, as shown by the dashed line, or taken as -3.91 degrees, drawn in a solid curve. This last bound is 1 1/2-times the control correction peak value which occurred at 87 seconds flight time. The final altitude error, shown in Figure 4-42, was reduced from 568 feet to 25 feet, and the final range error, Figure 4-43, was changed from 0.096 mile to 0.006 mile, when the smaller bound was used. These numbers are compared to an altitude error of 2784 feet and a range error of 22.7 miles for the open-loop trajectory, also illustrated in the figures.

Terminal errors resulting from perturbations of the initial state are listed in Table 4-7. For each change two closed-loop runs with the different final control bounds and the open-loop run are given. Note that the controller allows altitude errors less than 100 feet and range errors less than 0.01 mile, usually, with small perturbations. The large changes are controlled within a few thousand feet in altitude and a half-mile in range.

Table 4-7. Initial-State Error Cases

Type of Perturbation	Maximum Δu Correction in Degrees	Final Perturbed-State Differences from Reference					
		ΔV ft/sec.	$\Delta \gamma$ degrees	Δh feet	$\Delta \zeta$ miles	Δ_{q_c} BTU's	Δ_{q_r} BTU's
None	0.33	0.015	-0.003	0.018	0.0000	0.01	0.002
	15	-0.765	0.299	1.595	0.0004	0.01	0.002
	zero	-0.036	0.002	-1.205	-0.0048	-0.05	0.005
ΔV = 200 ft/sec	3.23	-11	0.008	47	0.008	197	442
	15	-11	2	485	0.081	197	442
	zero	90	4	2602	19.892	535	392
ΔV = -200 ft/sec	3.21	4	8	-4	-0.001	-193	-417
	15	zero	2	60	0.012	-193	0.147
	zero	-67	-4	-2254	-18.455	-509	-377
ΔV = 500 ft/sec	8.12	-56	-0.2	-1051	-0.112	499	1156
	15	-57	2.2	- 606	-0.033	499	1156
	zero	295	12.0	7378	53.011	1394	1007
ΔV = -500 ft/sec	8.00	8	2	-14	-0.002	-474	-997
	15	6	3	21	0.006	-474	-997
	zero	-142	-9	-5124	-43.864	-1229	-916

Table 4-7. Initial-State Error Cases (Continued)

Type of Perturbation	Maximum Δu Correction in Degrees	Final Perturbed-State Differences from Reference					
		ΔV ft/sec	$\Delta \gamma$ degrees	Δh feet	$\Delta \zeta$ miles	Δ_{q_c} BTU's	Δ_{q_r} BTU's
Δh = 2000 ft	2.46	- 9	- 0.2	- 20	0.003	- 69	- 40
	15	- 6	- 0.5	28	0.005	- 69	- 40
	zero	41	2.2	1249	13.059	163	- 76
Δh = - 2000 ft	2.35	4	0.7	- 10	-0.002	65	43
	15	0	2.3	60	0.012	65	43
	zero	- 36	- 2.0	-1161	-12.793	-161	74
Δh = 5000 ft	6.37	- 44	- 0.1	- 697	- 0.077	-179	- 95
	15	- 46	2.9	- 137	0.020	-179	- 96
	zero	117	5.7	3320	33.234	411	- 192
Δh = - 5000 ft	5.67	- 16	1.2	- 956	-0.130	157	110
	15	6	2.9	19	0.006	157	110
	zero	- 81	- 4.9	-2763	-31.563	- 401	183
$\Delta \gamma$ = -0.05 deg	3.65	5	1	- 14	- 0.002	29	103
	15	1	3	60	0.013	29	103
	zero	- 70	- 4	-2337	-20.952	- 344	156

Table 4-7. Initial-State Error Cases (Continued)

Type of Perturbation	Maximum Δu Correction in Degrees	Final Perturbed-State Differences from Reference					
		ΔV ft/sec	$\Delta\gamma$ degrees	Δh feet	$\Delta\zeta$ miles	Δ_{q_c} BTU's	Δ_{q_r} BTU's
$\Delta\gamma$ = 0.05 deg	3.91	- 18	1	25	0.006	- 35	- 99
	15	- 17	3	568	0.096	- 35	- 99
	zero	97	5	2784	22.715	355	-156
$\Delta\gamma$ = 0.15 deg	10.27	- 40	1	-2173	-0.168	72	319
	15	- 6	3	- 781	-0.115	73	319
	zero	455	16	10337	75.112	1151	-485
$\Delta\gamma$ =-0.15 deg	12.63	-100	- 2	-3013	-0.318	-121	-277
	15	-102	- 1	-3001	-0.304	-121	-277
	zero	-163	-11	-6043	-58.716	-954	437
$\Delta\zeta$ = 10 miles	2.40	- 24	- 0.4	- 316	-0.039	-193	35
	15	- 28	3.9	483	0.090	-193	35
	zero	zero	zero	zero	10	zero	zero
$\Delta\zeta$ = - 10 miles	-2.40	- 6	0.7	- 413	-0.049	200	- 33
	15	1	2.5	54	0.011	200	- 33
	zero	zero	zero	zero	-10	zero	zero

Table 4-7. Initial-State Error Cases (Continued)

Type of Perturbation	Maximum Δu Correction in Degrees	Final Perturbed-State Differences from Reference					
		ΔV ft/sec	$\Delta\gamma$ degrees	Δh feet	$\Delta\zeta$ miles	Δ_{q_c} BTU's	Δ_{q_r} BTU's
$\Delta\zeta$ = 25 miles	5.98	-118	-5.5	-4167	-0.448	-468	88
	15	-131	-3.5	-4481	-0.459	-468	88
	zero	zero	zero	zero	zero	zero	zero
$\Delta\zeta$ = - 25 miles	6.16	- 21	1.4	-1338	0.476	515	-81
	15	17	1.0	39	0.007	513	-81
	zero	zero	zero	zero	-25	zero	zero

The first three cases of Table 4-7 are a check on the accuracy of numerical integration, since the reference trajectory and control are computed by a backwards integration from terminal time, which differs from the forward calculation by small amounts. This gives rise to a control correction in the closed-loop case.

Errors produced by vehicle parameter changes are summarized in Table 4-8. The controller does not cope as well with these perturbations, as with initial condition errors, because the control correction gains E(t) were based on the vehicle parameters of the reference. The final-state errors are usually less than 5,000 ft. in attitude and 1 1/2 - miles in range.

Table 4-8. Vehicle Parameter Change Cases

Type of Perturbation	Maximum Δ Correction in Degrees	Final Perturbed-State Differences					
		ΔV ft/sec	$\Delta\gamma$ degrees	Δh feet	$\Delta\zeta$ miles	Δ_{q_c} BTU	Δ_{q_r} BTU
4 per cent S	3.87	0.111	3.9	4480	0.48	- 505	- 495
	15	132	0.6	3845	0.45	- 505	- 495
	zero	- 17	- 0.9	382	- 5.96	- 464	- 391
-4 per cent S	3.70	- 96	- 4.2	- 4716	- 0.26	528	539
	15	- 130	- 2.9	- 6059	- 0.47	528	539
	zero	19	1.0	- 378	6.26	494	429
10 per cent S	7.43	165	3.2	5506	0.61	- -965	- 929
	15	140	- 1.6	3246	0.28	- 964	- 929
	zero	- 39	- 2.2	959	- 14.38	- 1108	- 914
-10 per cent S	7.05	- 173	- 8.2	- 9268	- 0.16	1109	1161
	15	- 204	- 8.0	-10819	- 0.46	1110	1161
	zero	52	2.7	- 931	16.29	1300	1158
4 per cent C_{LO}	2.04	7	- 0.8	18	- 0.002	- 2	- 12
	15	0	1.3	- 4	0.003	- 2	- 12
	zero	4	zero	- 41	4.046	73	- 17
-4 per cent C_{LO}	2.19	- 8	0.7	- 46	0.002	3	13
	15	- 6	3.3	629	0.105	3	13
	zero	- 3	zero	58	- 3.972	- 72	17

Table 4-8. Vehicle Parameter Change Cases (Continued)

Type of Perturbation	Maximum Δu Correction in Degrees	Final Perturbed-State Differences					
		ΔV ft/sec	$\Delta \gamma$ degrees	Δh feet	$\Delta \zeta$ miles	Δ_{q_c} BTU	Δ_{q_r} BTU
10 per cent C_{LO}	4.21	17	- 1.7	60	- 0.002	- 4	- 30
	15	9	- 0.3	- 155	- 0.024	- 4	- 30
	zero	11	zero	- 67	10.260	183	- 41
-10 per cent C_{LO}	5.35	- 21	1.5	- 253	- 0.020	8	34
	15	- 24	4.6	321	0.073	8	34
	zero	- 7	0.1	175	- 9.798	- 179	41
4 per cent C_{DO}	1.05	49	2.3	2222	0.205	- 256	- 246
	15	76	- 1.4	1722	0.202	- 256	- 246
	zero	- 13	- 0.6	275	- 6.292	- 342	- 247
-4 per cent C_{DO}	1.06	- 46	- 2.3	- 2267	- 0.144	266	261
	15	- 78	0.2	- 3160	- 0.265	266	261
	zero	14	0.6	- 280	6.542	358	256
10 per cent C_{DO}	2.48	182	4.9	5361	0.246	- 624	- 590
	15	141	1.8	4419	0.511	- 624	- 590
	zero	- 31	- 1.5	678	-15.298	- 828	- 580
-10 per cent C_{DO}	2.51	- 107	- 5.7	- 5595	- 0.210	683	685
	15	- 152	- 4.7	- 7511	- 0.554	684	685
	zero	38	1.6	- 709	16.867	926	668

Table 4-8. Vehicle Parameter Change Cases (Continued)

Type of Perturbation	Maximum Δu Correction in Degrees	Final Perturbed-State Differences					
		ΔV ft/sec	Δγ degrees	Δh feet	Δζ miles	Δ_{q_c} BTU	Δ_{q_r} BTU
4 per cent C_{DL}	0.71	28	1.3	1293	0.114	- 148	- 144
	15	53	- 2.8	613	0.076	- 148	- 144
	zero	- 8	- 4	151	- 3.649	- 198	- 141
-4 per cent C_{DL}	0.64	- 27	- 1.3	- 1297	- 0.093	151	149
	15	- 51	2.0	- 1629	- 0.120	151	149
	zero	8	0.4	- 152	3.732	203	146
10 per cent C_{DL}	1.41	70	3.2	3095	0.298	- 354	- 351
	15	101	- 0.1	3703	0.328	- 364	- 351
	zero	- 19	- 0.9	376	- 8.974	- 486	- 345
-10 per cent C_{DL}	1.48	- 64	- 3.3	- 3208	- 0.182	384	384
	15	- 99	- 1.2	- 4377	- 0.369	385	384
	zero	21	0.9	- 384	9.492	519	374
Δu = 1 deg	1.52	10	0.4	173	0.028	- 22	20
	15	3	1.6	35	0.007	- 22	20
	zero	- 118	- 7.4	- 4383	-16.496	- 239	32
Δu = 1 deg	1.53	- 13	0.0	- 150	- 0.019	22	- 20
	15	- 11	2.8	610	0.102	20	- 20
	zero	170	8.0	4991	17.755	254	- 32
Δu = 2.5 deg	3.77	21	2.0	470	0.108	- 55	51
	15	- 6	4.4	- 46	0.022	- 55	51
	zero	- 237	- 16.8	- 9996	-39.107	- 572	82
Δu = -2.5 deg	3.77	- 40	- 0.5	- 815	- 0.097	57	- 48
	15	- 43	3.5	- 30	0.032	57	- 48
	zero	596	20.4	13850	46.955	669	- 80

Comparison of Studies in Subsections C and D (D-4)

The studies of a control for modulating angle of attack in this subsection differ in several aspects from those for roll angle control reported in Subsection C. The object of that work was to find a control for the whole re-entry corridor, assuming only a crude navigational system. Very large perturbations could be controlled--50,000 feet initial altitude error, for example--with a navigation calculation from biased acceleration data. The reference path was chosen so the system would be very controllable.

The extremal path, on the other hand, was found to yield a much less controllable system, and the perturbations had to be strongly restricted.

MISCELLANEOUS IDEAS FOR CONTROL (E)

The linear control scheme presented appears to provide a reasonable engineering solution for the re-entry problem considered. There are, however, a number of questions which must be answered to round out this research effort. For example, what is the justification in using the linear Equations (4.3) for prediction so feedback gains may be found when, in fact, this equation holds for the closed-loop system only in a very narrow neighborhood of the reference and not in the whole controllable corridor? Why is improvement noted when the control is modified by transformations like (4.28), or bounds imposed when these modifications were not considered in the basic derivation of the control law? What relations are implied when the reference trajectory is found by using one criterion and the feedback control found by using another? A more difficult area of study, considered a little in Subsection C, is to find the minimum information of the state, number of variables and accuracy, which will allow a successful design.

Some of the answers lie in a more careful study of the effects of the essential nonlinearities of the system. A step along these lines is to investigate a controller based on a prediction from error equations linearized in the state variables,

but in which the nonlinear aspects of the control authority is retained. The control criterion must also be changed to retain the nonlinear character of this detail of the system. Or, the nonlinearities may be avoided by adding more reference trajectories and error equations. If two paths were employed as reference, an auxiliary calculation to choose the reference can be based on the construction of a plane midway between the reference states and perpendicular to the plane formed by them.

Another approach is to make the system explicit, calculating a new optimal trajectory at each point along the motion. This may be done by simplifying the Newton-Raphson method of Section II, by dropping more unessential terms using schemes based on the second variation, or, by using a Newton-Kantorovich-type of iteration to predict an optimal path. Or, the equations of motion may be solved approximately by Galerkin's technique, and a suboptimal path found by the Rayleigh-Ritz procedure. This would require relatively elementary calculations.

SECTION V
CONCLUSIONS AND RECOMMENDATIONS

ACCOMPLISHMENTS

A computational procedure is developed which yields the control program and the corresponding re-entry flight path to minimize a given criterion. In the particular case studied, this criterion is the total heat to the vehicle. The calculation is automatic, in that the calculation will run on a large digital computer, iterating as need be, until an optimal trajectory is found, without intervention by the operator. The basis of the calculation is the theory of the calculus of variations. It is demonstrated that, when suitably modified, this theory provides the flexibility and a generality to encompass a large class of control synthesis problems.

The chief numerical method employed is a modified Newton-Raphson technique. The method is superior to both the gradient approach and standard Newton-Raphson methods, which were tried, in terms of rapidity of convergence, ease of automation and auxiliary computations. The scheme is insensitive to round-off errors, and it exhibits no tendencies toward instability because of adjoint solutions. It was found to be better, for accuracy and computer usage, to compute the necessary partial derivatives from explicit formulas derived from the second variations, rather than calculate them from finite differences.

The success in computing optimal trajectories is due, in part, to the simple device of limiting the control authority so that a reasonable guess, close to a ballistic trajectory and in the region of convergence for the method, may be made and subsequently relaxing this limit as the re-entry corridor is studied.

It is demonstrated that a linear perturbational control could be designed to provide control within a substantial re-entry corridor about a carefully chosen reference path. The accuracy requirements for system mechanization are not

severe. A system with accelerometers and an attitude reference of reasonable accuracy would assure safe re-entries. It will control vehicles with errors in parameters and changes in atmosphere density profile. Modification of the linear controller gains at the end-point is examined with care.

Several complicated digital computer programs, which use specially developed integration and interpolation methods, were constructed. These will be invaluable for future investigations.

This study was conducted with a two-dimensional model of the re-entry maneuver.

This research has laid the theoretical foundations requisite for engineering feasibility studies of optimal re-entry control. Further, limited experience with these techniques suggests that an optimal re-entry trajectory has real and significant performance advantages in terms of the chosen optimization criterion. This research has also made it clear that on-board computation of true optimal trajectories is not likely to be feasible in the foreseeable future. However, such trajectories can be pre-computed and stored on board for use in the linear control scheme. Alternatively, there is a good probability that simplifying approximations can be made to the theory which will make feasible the on-board computation of sub-optimal paths. The merits of these simplified schemes can be evaluated by comparison with optimal trajectories computed by the methods developed during this research program.

RECOMMENDATIONS

An original objective of this program was, and still is, to examine the mechanization problems associated with optimal or near-optimal re-entry control systems. The prerequisite theoretical work is now sufficiently complete that these problems may be studied. The program suggested below has, as its principal purposes, the development of a technologically feasible mechanization and the evaluation of the performance degradation which this sub-optimal system exhibits with respect to an optimal system.

Task 1: Optimization

There are still some aspects of the Newton-Raphson optimization scheme which should be pursued. These are minor in nature, but should produce dividends in faster determination of optimal trajectories. They are:

Examine methods for increasing rate of convergence to the optimal trajectory

Examine other differential equation integration algorithms for faster path solution.

Examine other optimization criteria

Task 2: Linear Control

The various linear control schemes now known should be tested against each other to determine their effect upon the optimization criterion. The results of these studies will determine the linear control law to be mechanized. The linear control schemes include:

Minimum deviation of control from reference control

Minimum deviation of state from reference state

Optimal control in the vicinity of the optimal trajectory

Task 3: Approximation Techniques

The most fruitful areas of on-going research will be those of finding suitable simplifying approximations which will permit near-optimum trajectories to be

computed on board the vehicle and of evaluating the performance of the resulting sub-optimal control scheme.

Practical utilization of the theory which has been developed depends on the successful extension of these results toward simplifying approximations which retain as many performance advantages of an optimal system as possible. Some promising approaches are:

Rayleigh-Ritz techniques for optimization and a Galerkin approximation to solve the equations of motion

Optimal solutions of simplified equations of motion

Dynamic programming techniques for on-board computation of a crude approximation to the optimal path

Task 4: Simulation

A re-entry control simulation, designed to evaluate the most promising techniques resulting from Tasks 2 and 3 with respect to engineering feasibility, should be accomplished.

SECTION VI
REFERENCES

1. Eggers, Alfred J., Jr., Allen, H. Julian, and Neice, Stanford E.: "A Comparitive Analysis of the Performance of Long-Range Hypervelocity Vehicles." NACA TN 4046, (1957)

2. Allen, H. Julian, and Eggers, Alfred J., Jr.: "A Study of the Motion and Aerodynamic Heating of Missiles Entering the Earth's Atmosphere at High Supersonic Speeds." NACA TN 4047, (1957)

3. Allen, H. Julian: "Hypersonic Flight and the Re-Entry Problem." 21st Wright Brothers Lecture, Journal of the Aeronautical Sciences Vol. 25 No. 4, p. 217, (1958)

4. Gazley, Carl, Jr.: "Deceleration and Heating of a Body Entering a Planetary Atmosphere from Space." Rand Report P-988, (1958)

5. Lees, Lester, Hartwig, Frederic W., and Cohen, Clarence B: "The Use of Aerodynamic Lift During Entry Into the Earth's Atmosphere." Space Technology Lab. Report GM-TR-0165-00519, (1958)

6. Chapman, Dean R.: "An Approximate Analytical Method for Studying Entry Into Planetary Atmospheres." NASA Report 11, (1959)

7. Chapman, Dean R.: "An Analysis of the Corridor and Guidance Requirements for Supercircular Entry Into Planetary Atmosphere." NASA Report R-55, (1959)

8. Robinson, Alfred C. and Besonis, Algimantas J.: "On the Problems of Re-Entry Into the Earth's Atmosphere." WADC TR-58-408, (1958)

9. Wong, Thomas J. and Slye, Robert E.: "The Effect of Lift on Entry Corridor Depth and Guidance Requirements for the Return Lunar Flight." NASA Report R-80, (1960)

10. Young, John W. and Eggleston, John M.: "The Variations and Control of Range Traveled in the Atmosphere by a High-Drag Variable Lift Entry Vehicle." NASA TN D-230, (1960)

11. Luidens, Roger W.: "Approximate Analysis of Atmospheric Entry Corridors and Angles." NASA TN D-590, (1961)

12. Assadourian, Arthur and Cheatham, Donald: "Longitudinal Range Control During the Atmospheric Phase of a Manned Satellite Re-Entry." NASA TN D-253, (1960)

13. Grant, Frederick C.: "Analysis of Low-Acceleration Lifting Entry From Escape Speed." NASA TN D-249, (1960)

14. Levy, Lionel L.: "An Approximate Analytical Method for Studying Atmosphere Entry of Vehicles with Modulated Aerodynamic Forces." NASA TN D-319, (1960)

15. Levy, Lionel L. : "Atmosphere Entries with Spacecraft Lift-Drag Ratios Modulated to Limit Decelerations." NASA TN D-1427, (1962)

16. General Electric Company: "Flight Control Study of a Manned Re-Entry Vehicle." WADD TR 60-695 Vol. I and Vol. II, (1960)

17. Austin, R. W. and Ryken, V. M. : "Study and Preliminary Design of an Energy Management Computer for Winged Vehicles." ASD TD R-62-51, (June 1962)

18. Loh, W. H. T.: "A Second-Order Theory of Entry Mechanics into a Planetary Atmosphere." Journal Aerospace/Sciences, Vol. 29, No. 10, pp. 1210-1221 (October 1962)

19. Bryson, A. E., Denham, W. F., Carroll, F. J., and Mikamic, K.: "Determination of the Lift or Drag Program that Minimizes Re-Entry Heating with Acceleration or Range Constraints Using a Steepest Descent Computation Procedure." Paper given at the January, 1961 IAS Meeting. This paper with abbreviated title will also be found in the Journal of Aerospace Science, Vol. 29, No. 4, (April 1962) pp. 420-430

20. Bryson, A. E., Denham, W. F.: "Multivariable Terminal Control to Minimize Mean Square Deviation from a Nominal Path." Proceeding of the Symposium on Vehicle Systems Optimization, Inst. Aerospace Sci., (Nov. 1961)

21. Breakwell, J. V., Speyer, J. L., and Bryson, A. E.: "Optimization and Control of Nonlinear Systems Using the Second Variation." SIAM Journal on Control, Vol. 1 No. 2, (June 1963)

22. Bliss, G. A.: "Lectures on the Calculus of Variations." The University of Chicago Press, Chicago, (1946)

23. Valentine, F. A.: "The Problem of Lagrange with Differential Inequalities as Added Side Conditions." Contributions to the Theory of Calculus of Varations, pp. 403-447, (1933-1937), University of Chicago

24. Berkovitz, L. D.: "Variational Methods in Problems of Control and Programming." Journal of Mathematical Analysis and Applications Vol. 3, No. 1, (August 1961), pp. 145-169

25. Breakwell, J. V.: "The Optimization of Trajectories." J. Soc. Industr. Applied Mathematics 7, 215, (1959)

26. Kelley, H. J. : "Gradient Theory of Optimal Flight Paths." Jour. Amer. Rocket Soc., Vol. 30, No. 10, pp. 947-953, (October 1960)

27. Kalman, R. E.: "The Theory of Optimal Control and the Calculus of Variations." RIAS Technical Report 61-3

28. Berkovitz, L. D.: "On Control Problems with Bounded State Variables." Rand Memorandum RM-3207-PR, (July 1962)

29. Dreyfus, S.: "The Numerical Solution of Variational Problems." Jour. of Math. Anal. and Appl., Vol. 5, No. 1, (August, 1962)

30. Troitskii, V. A.: "Variational Problems on the Optimization of Control Processes in Systems with Bounded Coordinates." Prikladnay a Matematika I Makhanika, Vol. 26, No. 3, pp. 431-443, (May-June, 1962), Available as Minneapolis-Honeywell translation No. 385

31. Spang, III, H. A. : "A Review of Minimization Techniques for Nonlinear Functions." SIAM Journal, Vol. 4, No. 4, (October 1962), pp. 343-365

APPENDIX A

THE EXTREMAL DIFFERENTIAL EQUATIONS AND PARAMETERS

An extremal is defined in Section II as a path satisfying the relations (reproduced here for convenience)

$$-p' = \nabla_x f_o + p'\nabla_x f + \mu'\nabla_x G \tag{A.1}$$

$$0 = \nabla_u f_o + p'\nabla_u f + \mu'\nabla_u G \tag{A.2}$$

$$0 = \mu_j G_j, \quad j = 1, \ldots, q \tag{A.3}$$

$$0 \leq \mu \tag{A.4}$$

$$\dot{x} = f, \qquad x(o) = x_o \tag{A.5}$$

$$\dot{\sigma}^2 = G \geq 0 \tag{A.6}$$

$$H(t, x, p, u) \leq H(t, x, p, U) \tag{A.7}$$

$$\pi' \nabla_u^2 (H + \tilde{\mu} G)\, \pi \geq 0 \tag{A.8}$$

$$\nabla_u G\, \pi = 0 \tag{A.9}$$

It is convenient to consider each subarc of the extremal separately. For this purpose, it will be assumed that all the constraints are greater than zero along the first subarc. Then, according to Valentine (Reference 23) the inequality constraints may be neglected over this subarc.

The corresponding Euler-Lagrange Equations (A. 1) and (A. 2) are

$$-\dot{p}' = \nabla_x f_o + p'\nabla_x f = \nabla_x F_1 \tag{A. 10}$$

$$0 = \nabla_u f_o + p'\nabla_u f = \nabla_u F_1. \tag{A. 11}$$

It is well known from implicit function theory that Equations (A. 11) can be solved (at least in principle) in the form

$$u = u(x, p) \tag{A. 12}$$

if the determinant

$$R_1 = \det \nabla_u^2 F_1 = \det \begin{bmatrix} \dfrac{\partial^2 F_1}{\partial u_1^2}, \ldots, & \dfrac{\partial^2 F_1}{\partial u_1 \partial u_m} \\ \dfrac{\partial^2 F_1}{\partial u_m \partial u_1}, \ldots, & \dfrac{\partial^2 F_1}{\partial u_m^2} \end{bmatrix} \tag{A. 13}$$

is different from zero. Equation (A. 13) is the determinant of the Hilbert differentiability condition for this problem. Substitution of (A. 12) into (A. 10) and (A. 5) thus produces a 2n set of differential equations

$$\dot{x} = f_1(x, p), \qquad x(0_o) = x_o \tag{A. 14}$$

$$-\dot{p}' = \nabla_x F_1 (x, p). \tag{A. 15}$$

These will be called the reduced differential equations of the extremals for the first subarc. It is well known from the theory of differential equations that (A. 14) and (A. 15) have a unique solution for a given set of initial conditions.

But half of these, x_o, are given for the problem. The solution is thus a function of the n initial conditions p_o and is said to be imbedded in an n-parameter family of extremals. Over the first subarc, then, the solution has the form

$$x = x(t, x_o, p_o) = x(t, p_o) \tag{A.16}$$

$$p = p(t, x_o, p_o) = p(t, p_o) \tag{A.17}$$

$$u = u(t, x_o, p_o) = u(t, p_o). \tag{A.18}$$

It is further known from the theory of differential equations that Equations (A.16) and (A.17) and, consequently, (A.18), have continuous partial derivatives in the variables t, x_o and p_o of at least second order.

The above results are, of course, obtainable from the general form of the problem of Bolza. It is known that the arc can be imbedded in an (n+m) parameter family of arcs, and that there are 2n + 2m differential equations of the extremals. The 2m differential equations become the m algebraic Equations (A.11) and their time derivatives (which introduce no new information) when initial conditions are imposed. Furthermore, the determinant in the Hilbert differentiability condition reduces to the form (A.13).

Over the second subarc, it is assumed that one of the inequality constraints, say G_1, is equal to zero. The function (2.10) is written, following Valentine (Reference 23), as

$$F_2 = f_o + p'(f - \dot{x}) + \mu_1 G_1 \tag{A.19}$$

and the Euler-Lagrange equations as

$$-\dot{p}' = \nabla_x f_o + p' \nabla_x f + \mu_1 \nabla_x G_1 = \nabla_x F_2 \tag{A.20}$$

$$O = \nabla_u f_o + p' \nabla_u f + \mu_1 \nabla_u G_1 = \nabla_u F_2. \tag{A.21}$$

To this is added the equality constraint

$$0 = G_1. \tag{A.22}$$

If the m+1 Equations (A.21) and (A.22) are to be solved for the m+1 variables u and μ_1, the determinant

$$R_2 = \det \begin{bmatrix} \nabla_u^2 F_2 & \nabla_u' G_1 \\ \nabla_u G_1 & 0 \end{bmatrix} \tag{A.23}$$

must not be zero. Equation (A.23) is the determinant of the Hilbert differentiability condition for this arc. It is then found that

$$u = u(x, p) \tag{A.24}$$

$$\mu_1 = \mu_1 (x, p) \tag{A.25}$$

and, consequently, that

$$\dot{x} = f_2 (x, p) \tag{A.26}$$

$$-\dot{p}' = \nabla_x F_2 (x, p) \tag{A.27}$$

are the reduced differential equations of the extremals for this arc. These equations again have a unique solution for a given set of initial conditions. Furthermore, the solutions possess continuous partial derivatives of at least second order with respect to t and the initial conditions x_1 and p_1. It remains to be shown that the solutions over this arc are continuous functions of the initial conditions p_0 and that partial derivatives of at least second order exist.

The terminal point of the first subarc is defined by the equation

$$G_1\left[x(t_1, p_o),\ p(t_1, p_o)\right] = 0. \tag{A.28}$$

This may be solved for $t_1(p_o)$ if the derivative

$$\dot{G}_1 = \nabla_x G_1 \dot{x} + \nabla_p G_1 \dot{p}$$

is non-zero. Equation (A.28) represents the equation for the terminal surface of the family of extremals which are solutions of Equations (A.14) and (A.15). This terminal surface represents the initial surface for the family of extremals over the second subarc which are solutions of Equations (A.26) and (A.27). For a given set p_o, the terminal values $x(t_1, p_o)$, $p(t_1, p_o)$ are the initial values for the differential Equations (A.26) and (A.27). This follows from the continuity of $x(t)$ and $p(t)$. Then, since the solutions

$$x(t) = x(t, x_1, p_1), \qquad t \geq t_1 \tag{A.29}$$

$$p(t) = p(t, x_1, p_1), \qquad t \geq t_1 \tag{A.30}$$

are continuous functions of x_1 and p_1, and since

$$x_1 = x(t_1, p_o) = x_1(p_o) \tag{A.31}$$

$$p_1 = p(t_1, p_o) = p_1(p_o) \tag{A.32}$$

are continuous functions of p_o alone, it follows that

$$x(t) = x(t, p_o), \qquad t \geq t_1 \tag{A.33}$$

$$p(t) = p(t, p_o), \qquad t \geq t_1 . \tag{A.34}$$

Furthermore, since continuous partial derivatives of at least second order exist for Equations (A. 29) - (A. 32) in the indicated variables, it follows that (A. 33) and (A. 34) possess partial derivatives of at least second order in t, p_o. Since there are no corners, μ_1 is, at least, absolutely continuous.

Further subarcs may now be added, as long as the number of equality constraints does not exceed m, the dimension of the control vector. Each subarc possesses control functions and multipliers of the form (A. 24) and (A. 25) and, furthermore, differential equations similar to (A. 26) and (A. 27). It is readily verified that the solutions are continuous functions of the initial conditions, p_o and t, and that continuous partial derivatives of at least second order exist.

Points where equality constraints change to the "greater-than" state will now be examined. For this purpose it will be assumed that only one of the constraints, say G_1, is zero over the first subarc, and that it is greater than zero over the second. Equations (A. 24) - (A. 27) hold over the first subarc, and (A. 12), (A. 14) and (A. 15) over the second subarc. The Equation (A. 28) for the terminal surface is replaced by the equation

$$\mu_1 \left[x\,(t_1, p_o),\ p(t_1, p_o)\right] = 0, \qquad \text{(A. 35)}$$

since μ_1 is a continuous function and must go to zero before G_1 can be greater than zero. It is then seen that the arguments follow through as before, provided the determinants R_1 and R_2 are different from zero and that the derivative

$$\dot{\mu}_1 = \nabla_x \mu_1 \dot{x} + \nabla_p \mu_1 \dot{p}$$

is non-zero on the terminal surface of the first subarc. On the second subarc, then, the solution is a continuous function of t and p_o, and partial derivatives in these variables of at least second order exist. The result is easily generalized to several equality constraints going to the "greater-than" state over a series of subarcs.

To sum up, a path is composed of a finite number of subarcs, each of which has its own set of differential equations and terminal surfaces. The first subarc has a specified set of initial conditions, x_o, and the last has a specified terminal surface, Equations (2.4). The equations of this terminal surface have continuous partial derivatives of at least second order with respect to the initial conditions p_o, and the terminal value of the independent variable T.

Now introduce the new differential equation

$$\dot{x}_{n+1} = f_o, \qquad x_{n+1}(0_o) = 0, \tag{A.36}$$

where f_o is the integrand of Equation (2.1). The solution to this is easily seen to be of the form

$$x_{n+1} = x_{n+1}(t, p_o) = \int_{0_o}^{t} f_o(x, p)d\tau \tag{A.37}$$

over the path and, on the terminal surface,

$$x_{n+1}(T) = x_{n+1}(T, p_o). \tag{A.38}$$

Furthermore, since g of Equation (2.1) is a functional of continuous functions,

$$J(T) = J(T, p_o) = g\left[T, x(T, p_o)\right] + x_{n+1}(T, p_o). \tag{A.39}$$

The terminal surface Equations (2.4) may be expressed in the form

$$\psi(T) = \psi(T, p_o) = \psi\left[T, x(T, p_o)\right] = 0. \tag{A.40}$$

Thus, the problem reduces to that of minimizing (A.39) subject to the constraint Equations (A.40) in the indicated variables.

APPENDIX B

THE SUFFICIENCY CONDITION FOR THE FIXED END-POINT PROBLEM

When the terminal surface consists of less than (n+1) equations of the form (2.4) it is always possible to use the sufficiency conditions of Section II (C). As shown in Section II (F), the second derivative matrix comes from evaluation of the second variation, using neighboring extremals (the accessory minimum problem) which satisfy the necessary conditions on the problem*. When the end-point is fixed, i.e., r = n+1, it is in general impossible to satisfy both the initial and terminal conditions with this type of neighboring extremal (assuming the problem is normal and that the ∇_{p_o} x matrix is non-singular at the end-point). However, it is still possible to construct neighboring extremals which have discontinuous derivatives at one point and which do satisfy end conditions. The second variation is evaluated with these neighboring extremals to establish the sufficiency condition for a relative minimum for this problem. Bliss' theorem 86.1 establishes the basis for the development.**

The complete fundamental solution matrix of the system (2.80) and (2.81) is

$$\begin{bmatrix} \nabla_{x_o} x & \nabla_{p_o} x \\ \nabla_{x_o} p & \nabla_{p_o} p \end{bmatrix} = \begin{bmatrix} \pi_{11} & \pi_{12} \\ \pi_{21} & \pi_{22} \end{bmatrix} \qquad (B.1)$$

where the π notation is introduced for the convenience of the following development. The initial condition for (B.1) is the 2n x 2n identity matrix. Then any solution $\delta x(t)$ and $\delta p(t)$ which starts with $\delta x(0) = 0$ must be composed of a

---

*See Bliss, reference 22, pp. 226-234, 243-247, and 253-257 for the discussion presented here.

**Ibid, p. 246

linear combination of π_{12} and π_{22}:

$$\delta x(t) = \pi_{12}(t)a, \qquad \delta x(o) = 0 \tag{B.2}$$

$$\delta p(t) = \pi_{22}(t)a, \qquad \delta p(o) = a, \tag{B.3}$$

where a is an arbitrary (nx1) dimensional vector. It is desired to construct similar neighboring extremals which have the property that $\delta x(T) = 0$. This is done by requiring

$$\begin{bmatrix} U(T) \\ V(T) \end{bmatrix} = \begin{bmatrix} \pi_{11}(T) & \pi_{12}(T) \\ \pi_{21}(T) & \pi_{22}(T) \end{bmatrix} \begin{bmatrix} C \\ D \end{bmatrix} = \begin{bmatrix} Z \\ I \end{bmatrix} \tag{B.4}$$

where C and D are (nxn) matrices to be determined, Z is the zero matrix and U and V are matrices such that

$$\delta x(t) = U(t)b, \qquad \delta x(T) = 0 \tag{B.5}$$

$$\delta p(t) = V(t)b, \qquad \delta p(T) = b, \tag{B.6}$$

and b is an arbitrary (nx1) dimensional vector. Now matrix (B.1) is non-singular by definition, so it may be inverted. Call the inverse at t = T the Λ matrix. Then, from (B.4)

$$\begin{bmatrix} C \\ D \end{bmatrix} = \begin{bmatrix} \Lambda_{11} & \Lambda_{12} \\ \Lambda_{21} & \Lambda_{22} \end{bmatrix} \begin{bmatrix} Z \\ I \end{bmatrix} = \begin{bmatrix} \Lambda_{12} \\ \Lambda_{22} \end{bmatrix} \tag{B.7}$$

from which it follows that

$$U(t) = \pi_{11}(t)\,\Lambda_{12} + \pi_{12}(t)\,\Lambda_{22} \tag{B.8}$$

$$V(t) = \pi_{21}(t)\,\Lambda_{12} + \pi_{22}(t)\,\Lambda_{22}. \tag{B.9}$$

Other relationships required in the development are

$$\pi_{21}' \pi_{11} = \pi_{11}' \pi_{21} + C_1 \tag{B.10}$$

$$\pi_{22}' \pi_{12} = \pi_{12}' \pi_{22} + C_2 \tag{B.11}$$

$$\pi_{22}' \pi_{11} = \pi_{12}' \pi_{21} + C_3 \tag{B.12}$$

which hold at any point t. These relationships may be verified by differentiating and substituting Equations (2.80) and (2.81) into the result. It is readily verified that $C_1 = C_2 = Z$ and that $C_3 = I$ for the initial conditions following Equation (B.1). However, if a path consists of more than one subarc, these constants will assume different values because of the discontinuities at the junctions of the subarcs.

The development assumes that the second variation is evaluated at a point t_3 on the last subarc. The assumption of continuity at this point requires that

$$\delta x(t_3) = \pi_{12}(t_3)\, a = U(t_3)\, b \,. \tag{B.13}$$

When the second variation is evaluated at $t = t_3$, it is found that

$$a' \left[\pi_{12}'(t_3)\, V(t_3) - \pi_{22}(t_3)\, V(t_3) \right] b \geq 0 \tag{B.14}$$

for all a, b satisfying (B.13). Assuming that π_{12} has an inverse at $t = t_3$, this is equivalent to stating that the matrix of

$$b' \left[U'V - U' (\pi_{12}^{-1})\, \pi_{22}' U \right]_{t = t_3} b \geq 0 \tag{B.15}$$

must have no negative eigenvalues (although some can be zero). Substitution of (B.8) - (B.12) into (B.15), and subsequent rearrangement, then gives the desired result,

$$b'\, \pi_{12}(T) \left[\pi_{12}^{-1}(t_3)\, \pi_{11}(t_3)\, \Lambda_{12} + \Lambda_{22} \right] b \geq 0 \,, \tag{B.16}$$

at an arbitrarily selected point $t = t_3$ on the last subarc.

Notice that if T is selected as t_3, the matrix of (B. 16) reduces to U(T) = Z. This is reasonable, since the only unbroken extremal between the two end-points is the original extremal, so the value of the second variation is, naturally, zero.

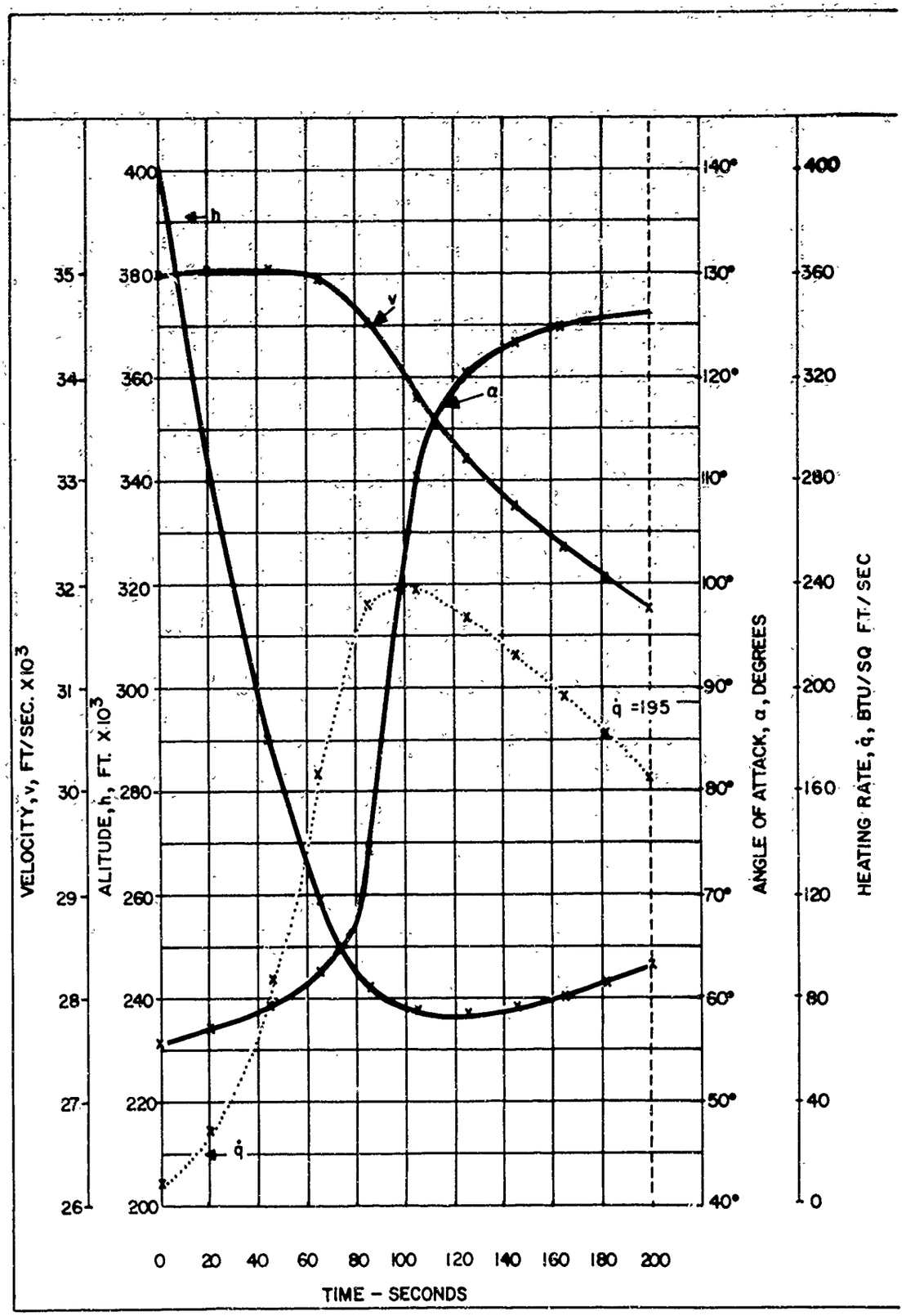

Figure 3-1. Altitude (h); Velocity (v); Heating Rate ($\dot{q}$); Angle of Attack (α) Versus Time for Relative Minimum of $J = \frac{1}{T - t_o}\int_{t_o}^{T} (\dot{Q} - \dot{q})^2 \, d\tau$; where $T = 200$ sec; $t_o = 0$; $\dot{Q} = 195$ BTU/sq ft/sec.

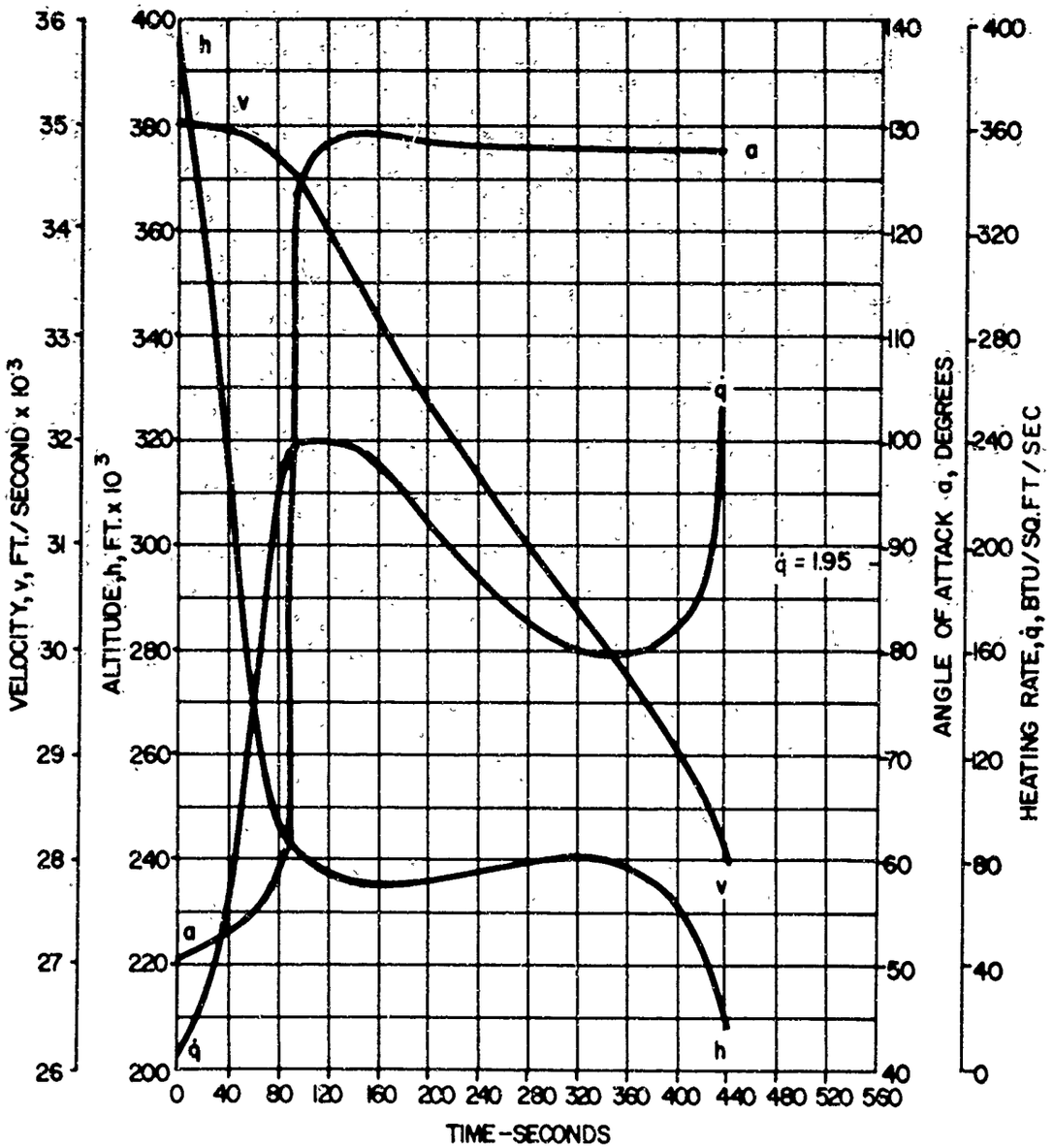

Figure 3-2. Altitude (h); Velocity (v); Heating Rate ($\dot{q}$); and Angle of Attack (α) Versus Time for Relative Minimum of $J = \frac{1}{T - t_o} \int_{t_o}^{T} (\dot{Q} - \dot{q})^2 \, d\tau$; $T = 440$ sec; $\dot{Q} = 195$ BTU/sq ft/sec; $t_o = 0$.

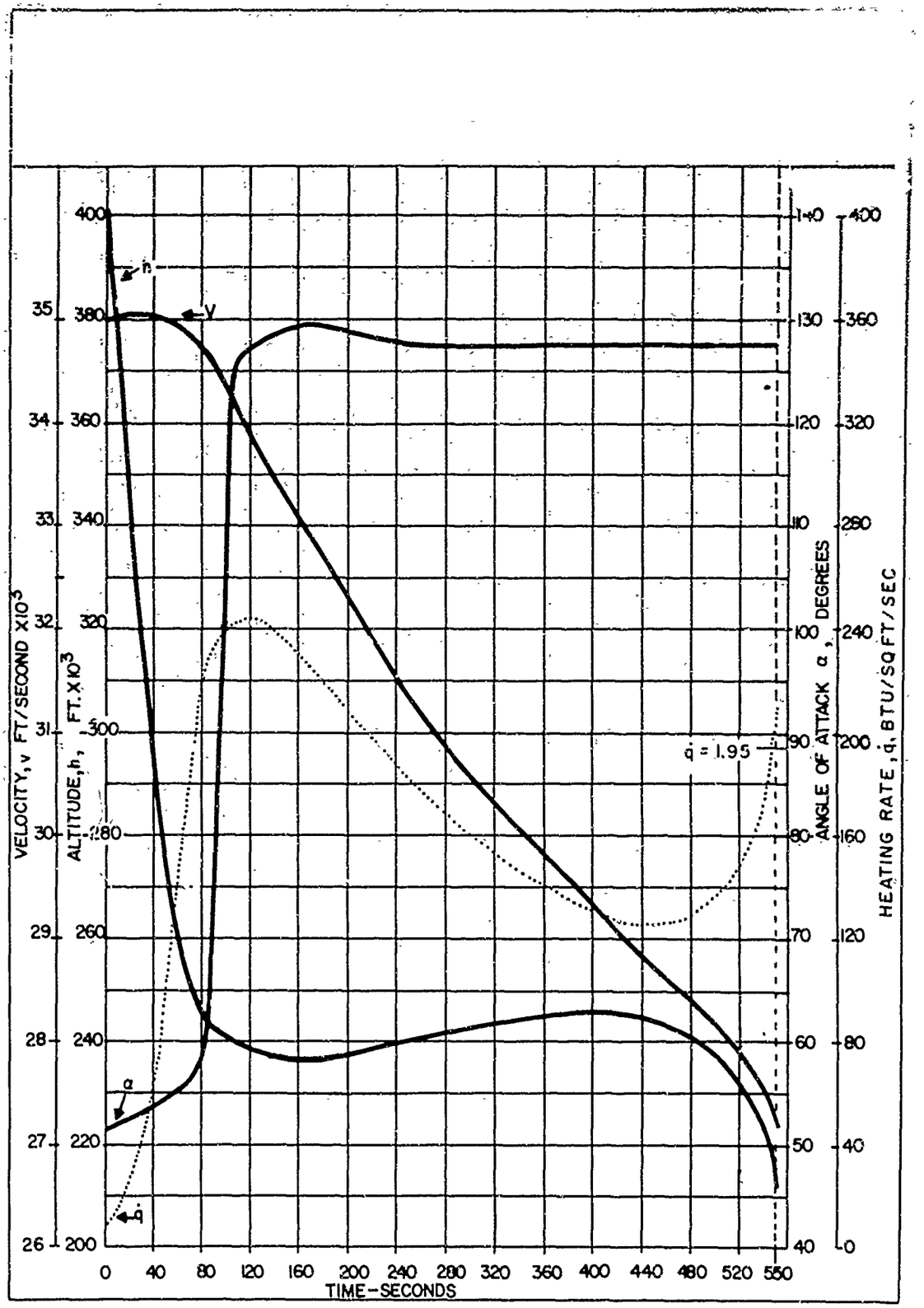

Figure 3-3. Altitude (h); Velocity (v) Heating Rate ($\dot{q}$); and Angle of Attack (α) Versus Time for Relative Minimum of $J = \frac{1}{T - t_o} \int_{t_o}^{T} (\dot{Q} - \dot{q})^2 \, d\tau$; $T = 550$ sec; $t_o = 0$; $\dot{Q} = 195$ BTU/sq ft/sec.

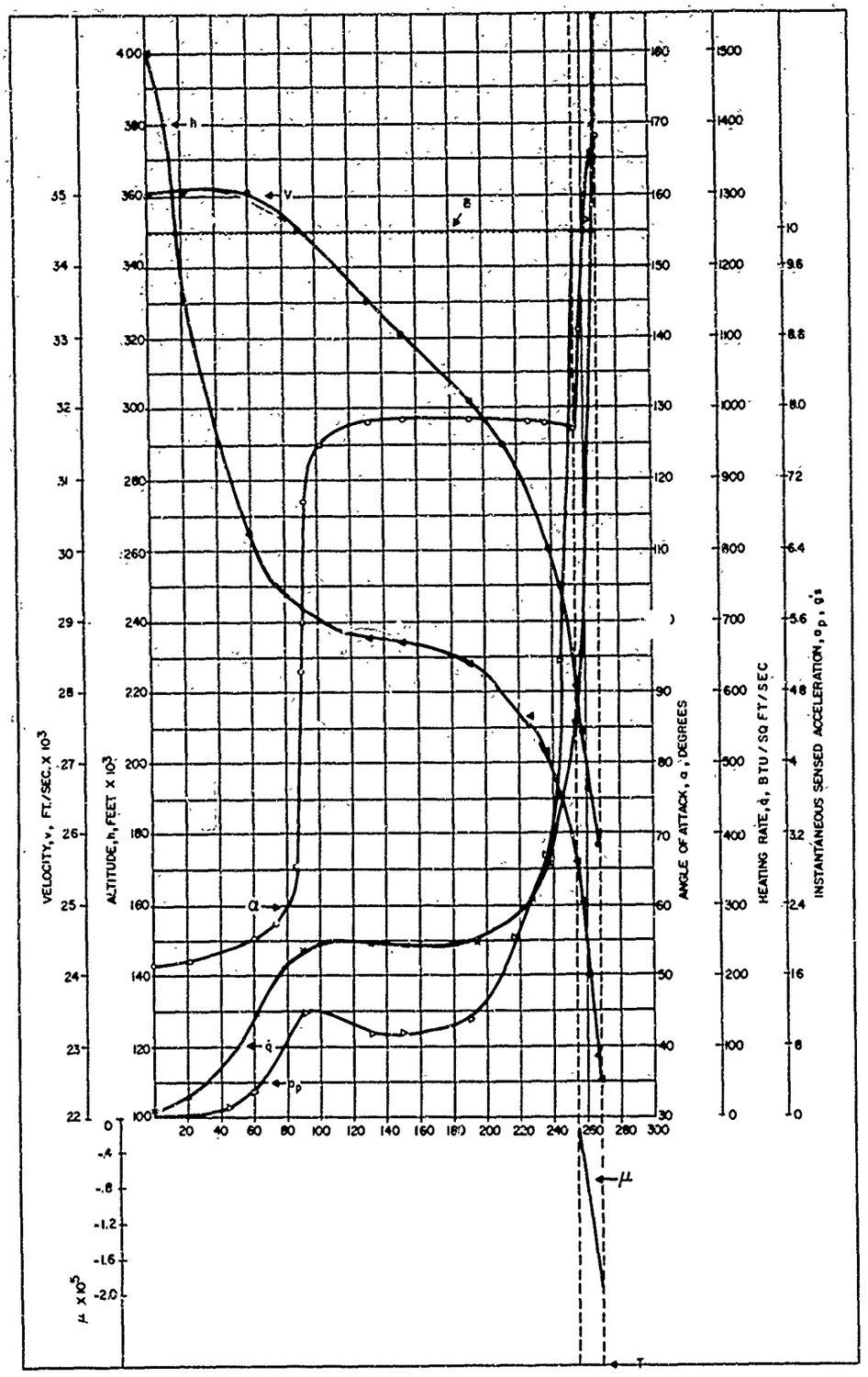

Figure 3-4. Altitude (h); Velocity (v); Heating Rate ($\dot{q}$); Angle of Attack (α); Pilot's Acceleration (a_p); and Additional Multiplier (μ) Versus Time for Non-Optimal Re-entry Trajectory

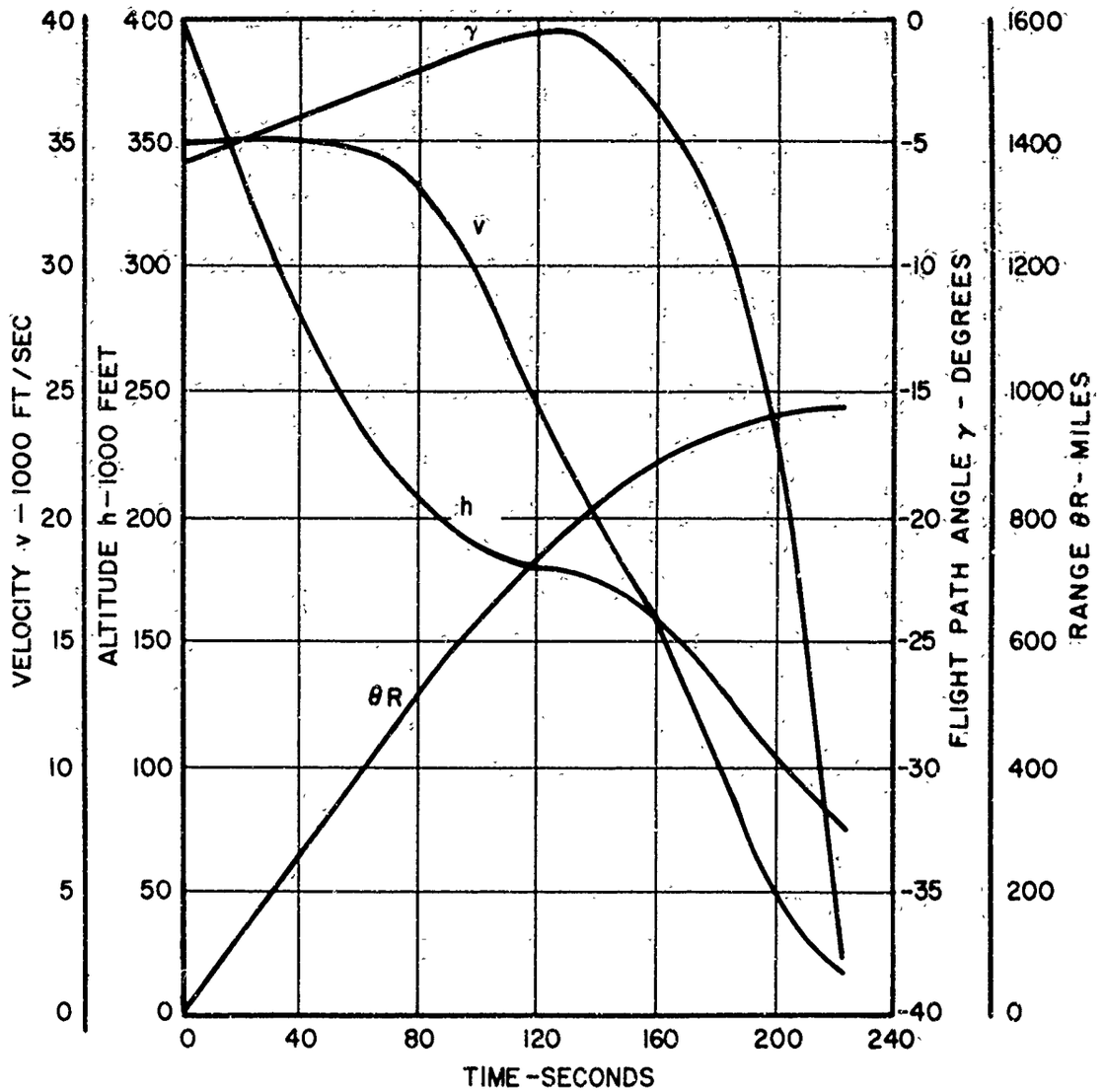

Figure 3-5. Supercircular Re-entry Trajectory Optimized for Minimum Total Heat Absorbed, $-16 \leq u \leq 16$ degrees, (a) Velocity, Altitude, Flight Path Angle and Range versus Time

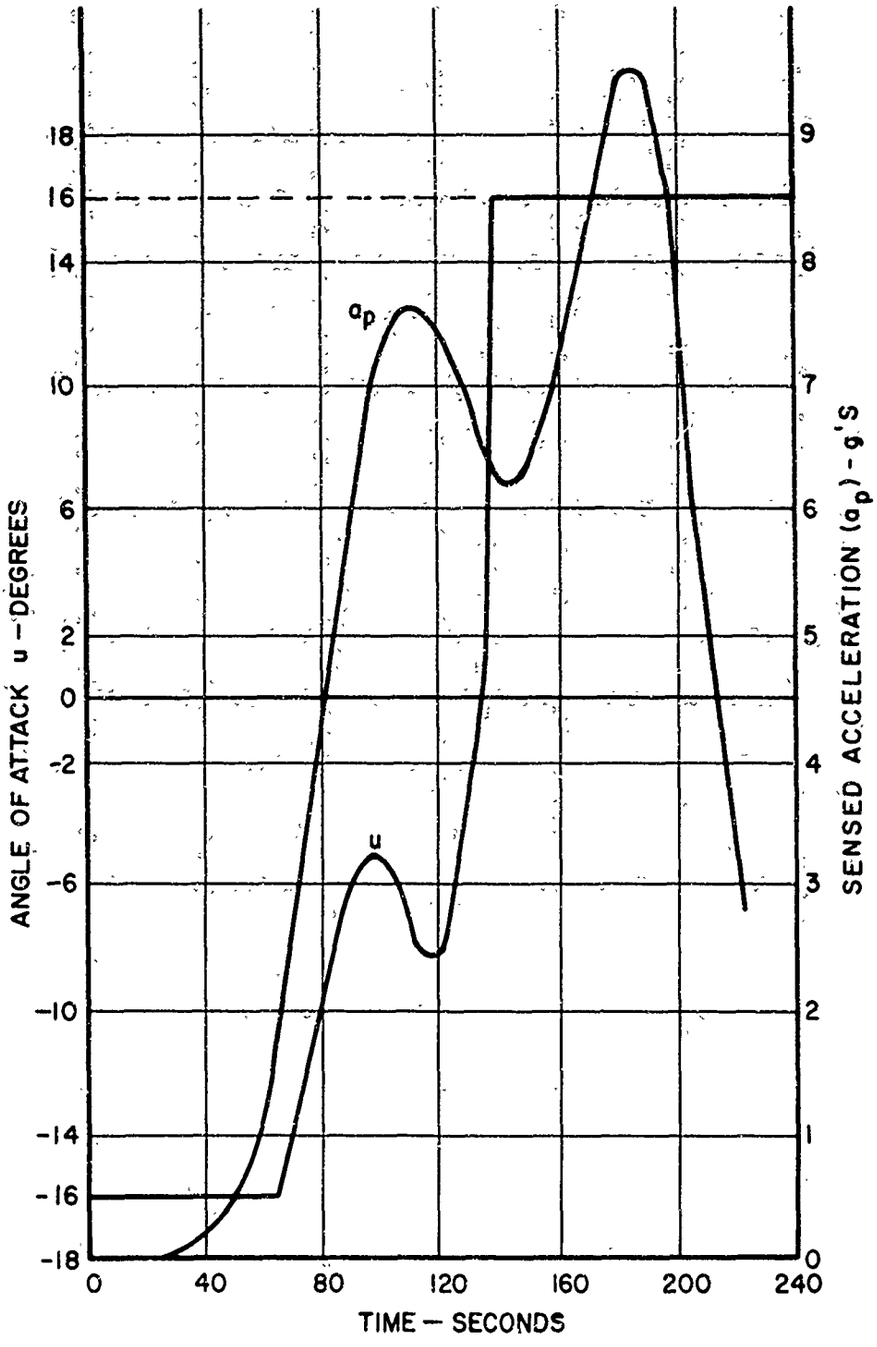

Figure 3-6. Supercircular Re-entry Trajectory Optimized for Minimum Total Heat Absorbed, $-16 \leq u \leq 16$ degrees, (b) Angle of Attack and Sensed Acceleration versus Time

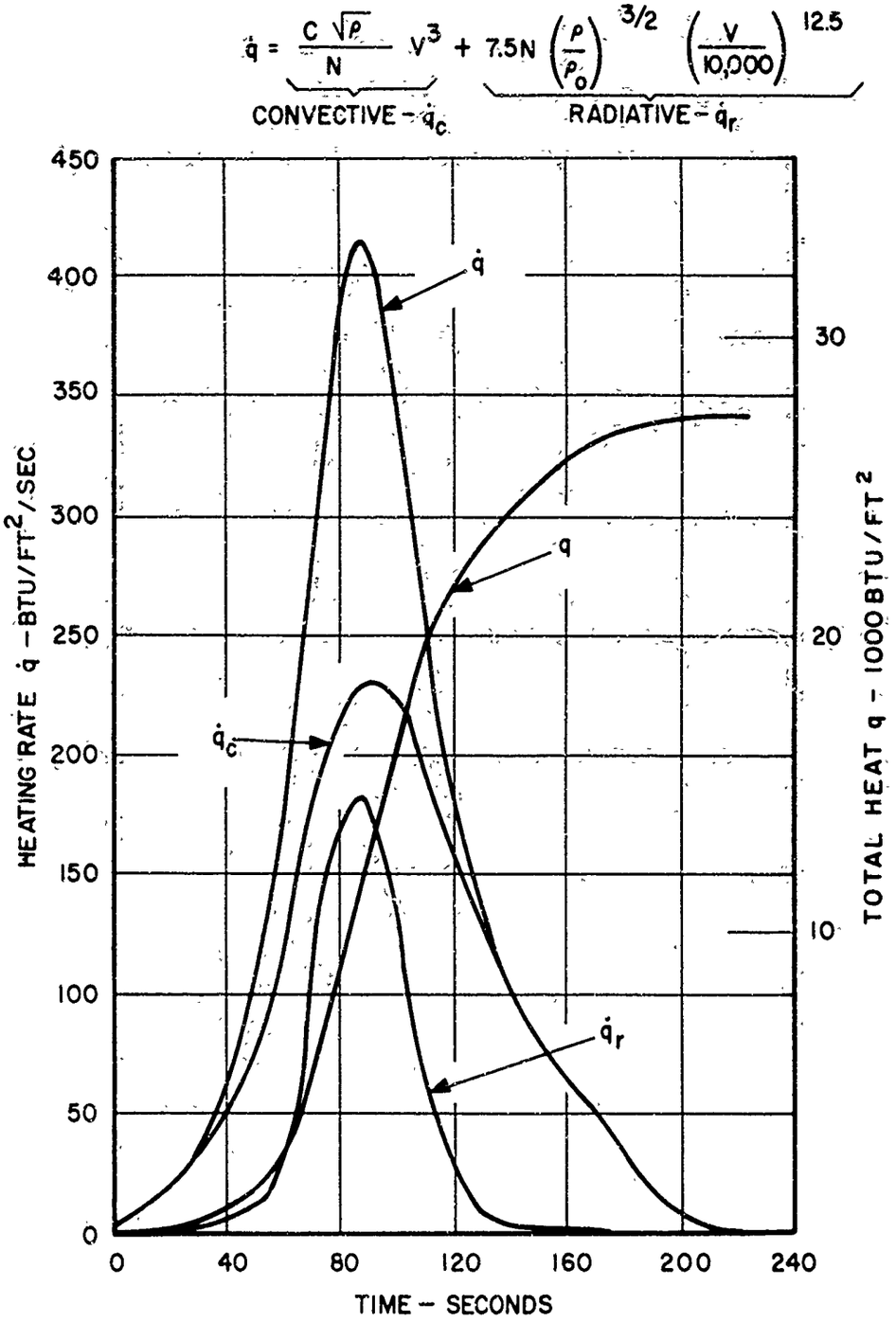

Figure 3-7. Supercircular Re-entry Trajectory Optimized for Minimum Total Heat Absorbed, $-16 \leq u \leq 16$ degrees, (c) Heating Rate and Total Heat versus Time

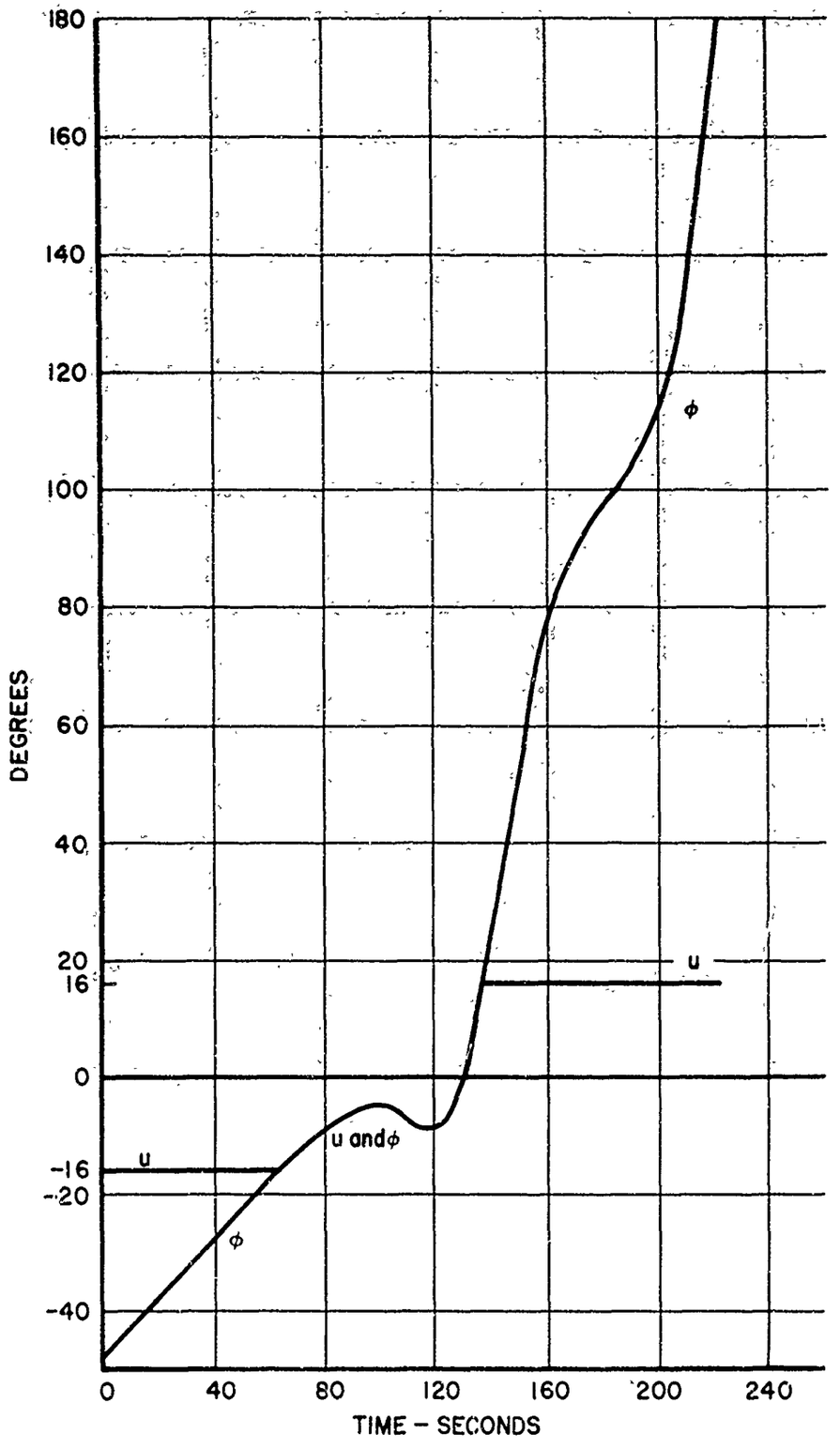

Figure 3-8. Constrained Angle of Attack U and Unconstrained Value ϕ

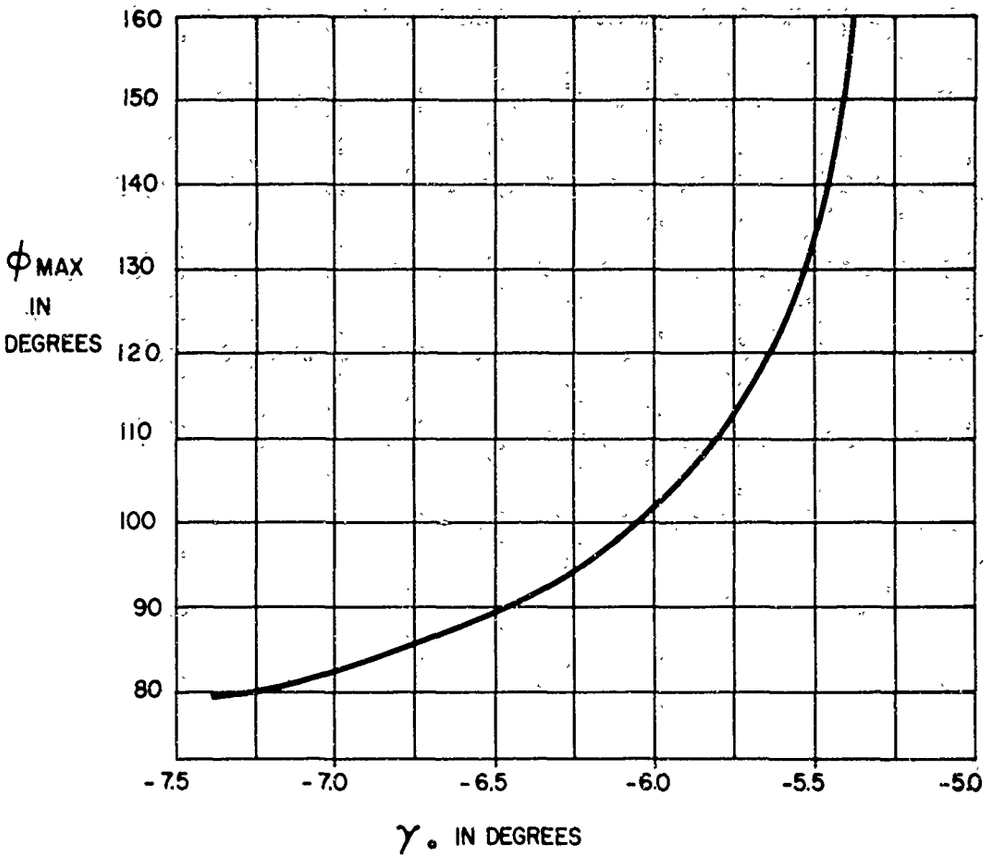

Figure 4-1. Constant Range Relationship of γ_o and ϕ_{max}

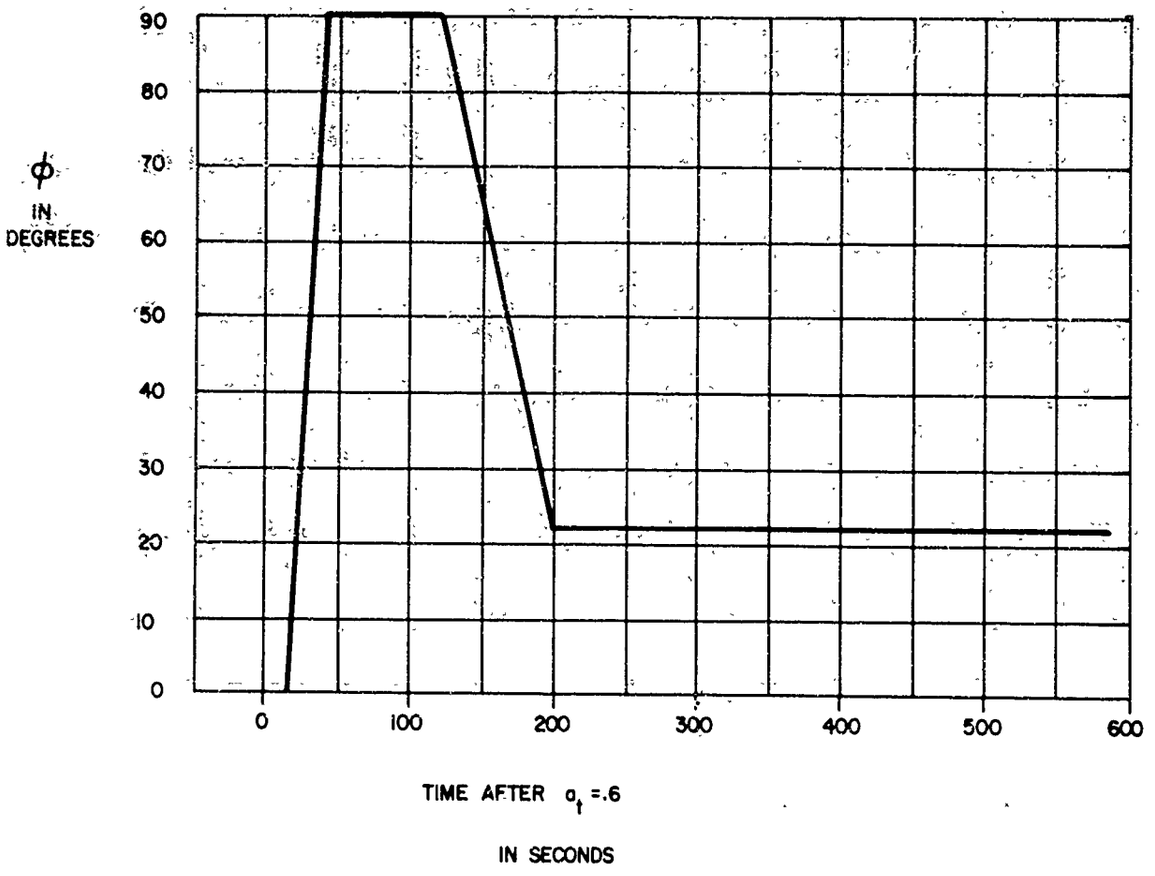

Figure 4-2. Standard Roll Function $\phi(t)$

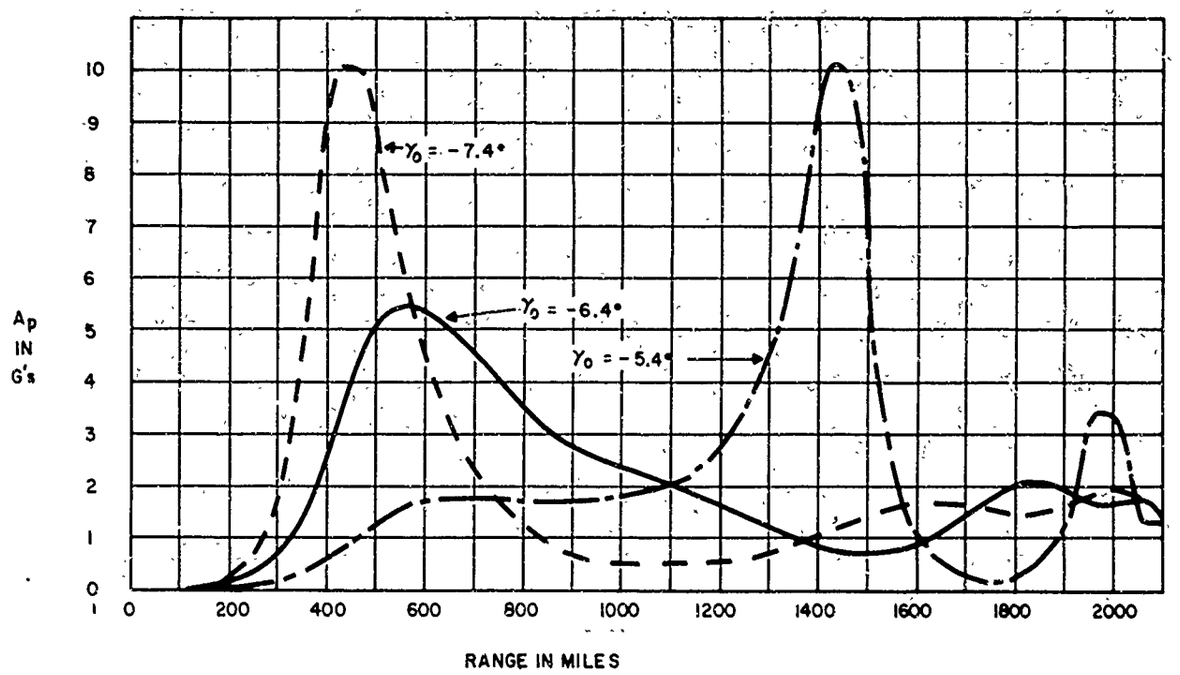

Figure 4-3. Acceleration Trajectories for γ_o = 5.4°, -6.4°, -7.4°

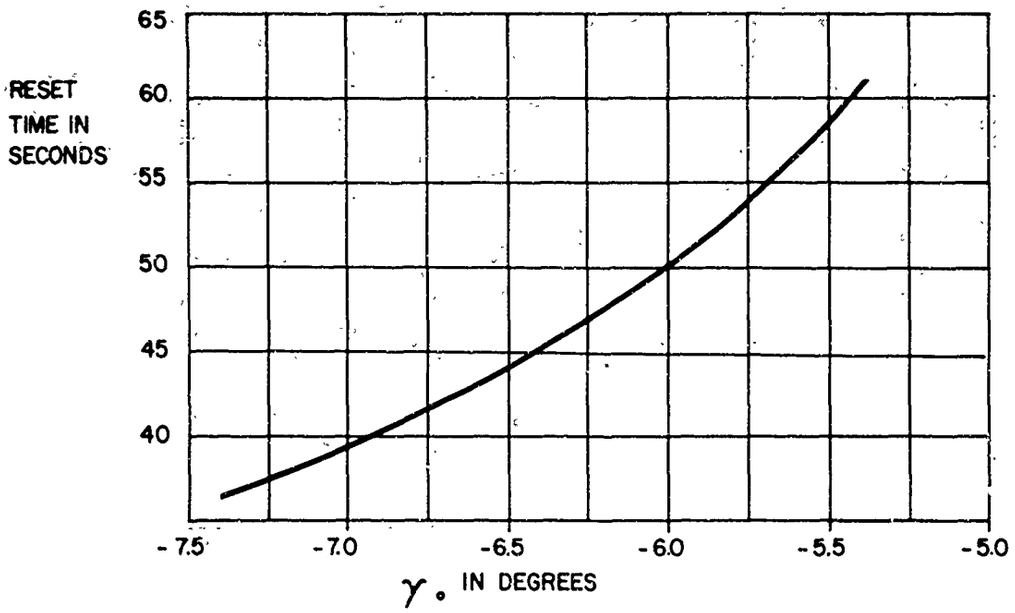

Figure 4-4. Reset Time Variability

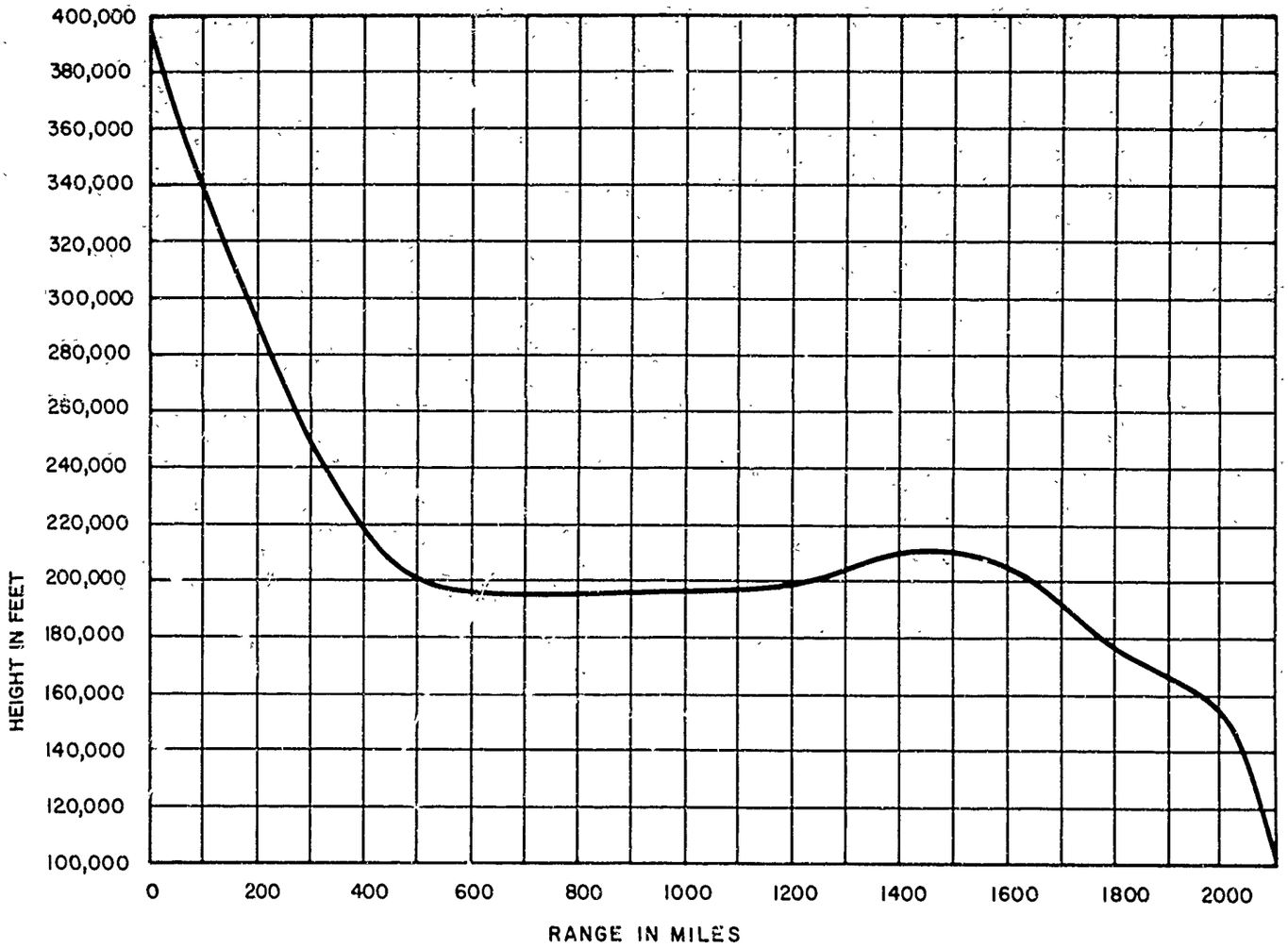

Figure 4-5. Height for Standard Reference γ_o = -6.4°

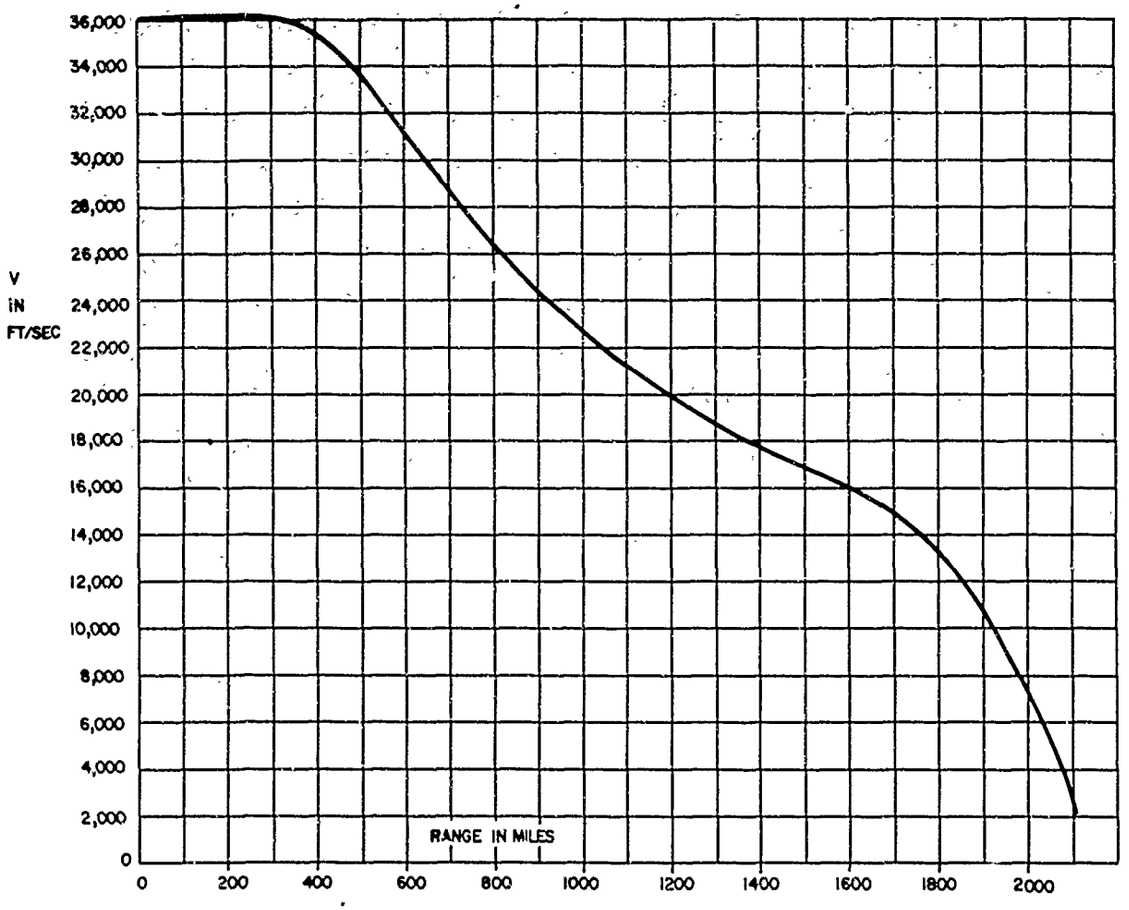

Figure 4-6. Velocity for Standard Reference γ_o = -6.4°

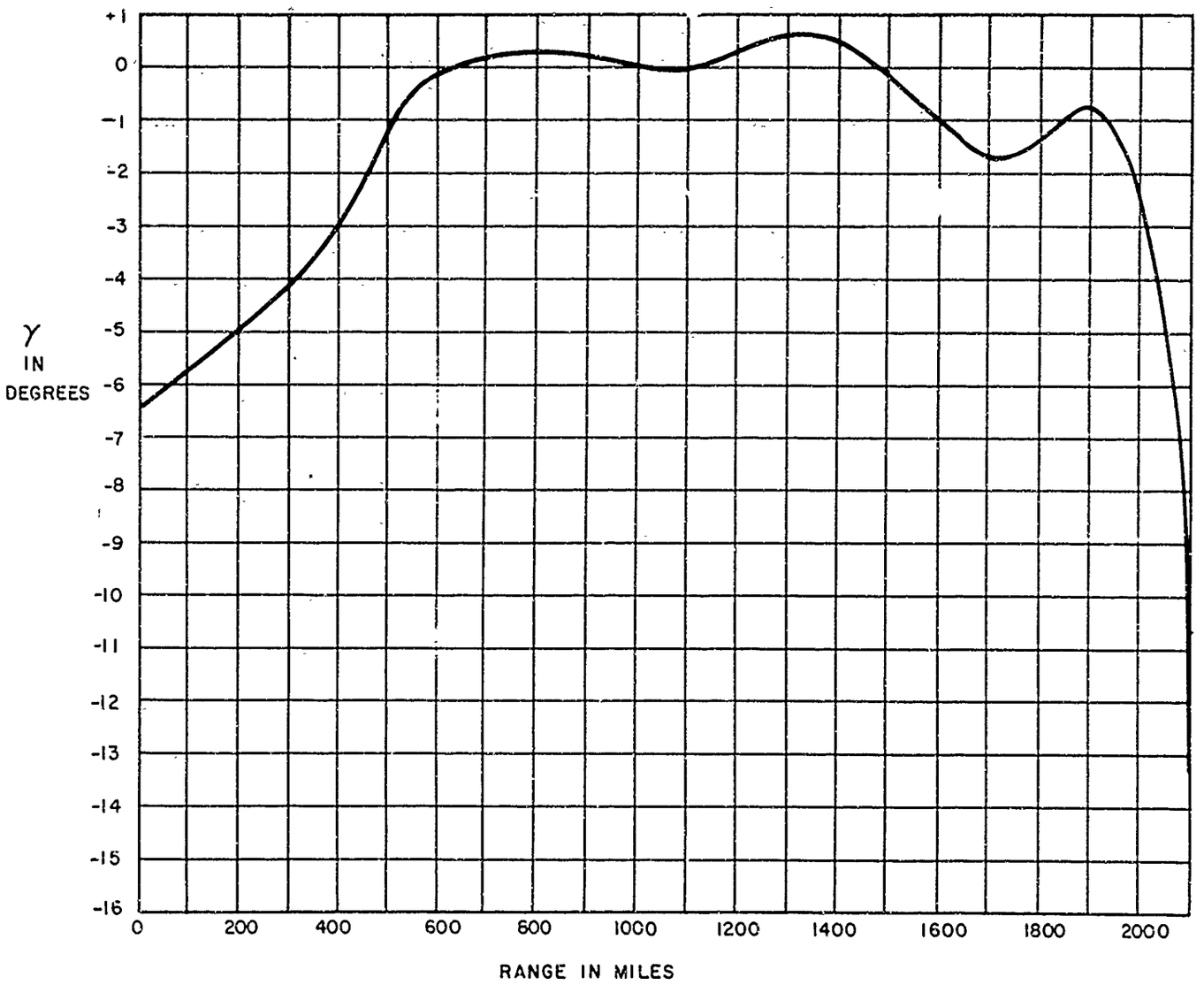

Figure 4-7. Re-entry Angle for Standard Reference

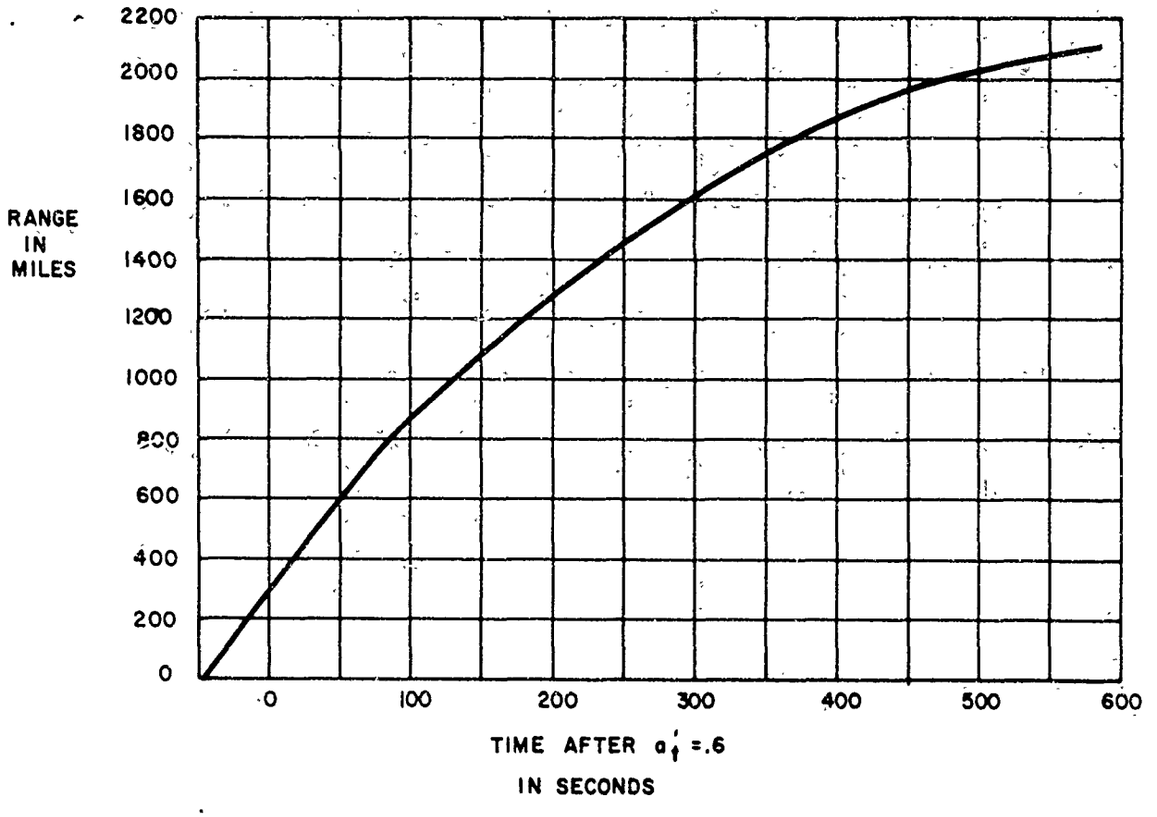

Figure 4-8. Standard Reference Range

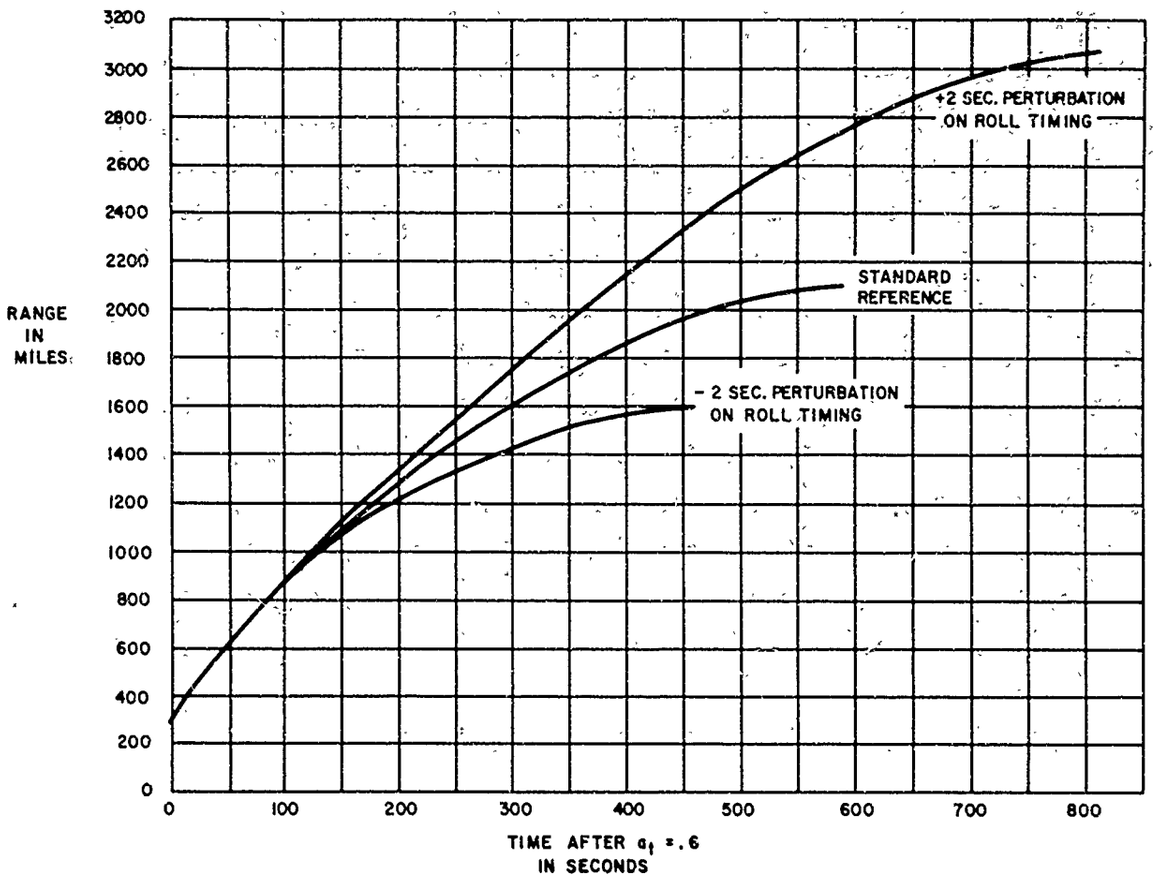

Figure 4-9. Roll Timing Range Effects

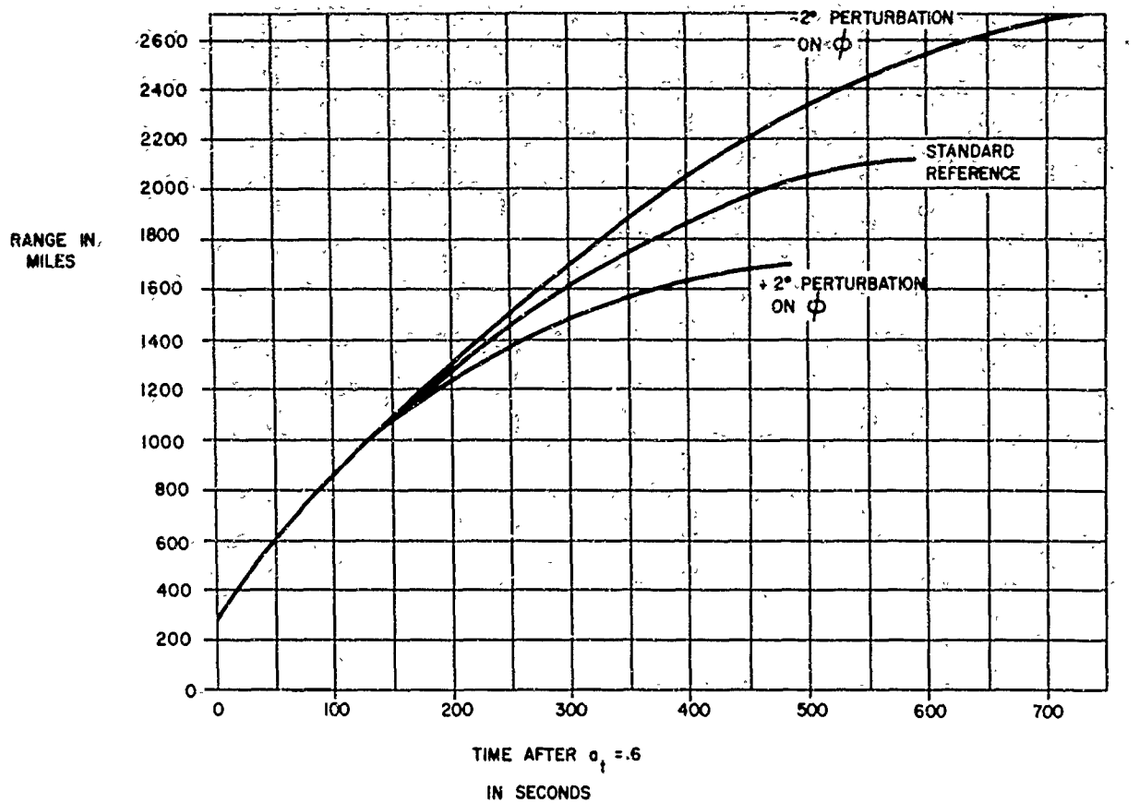

Figure 4-10. Roll Magnitude Range Effects

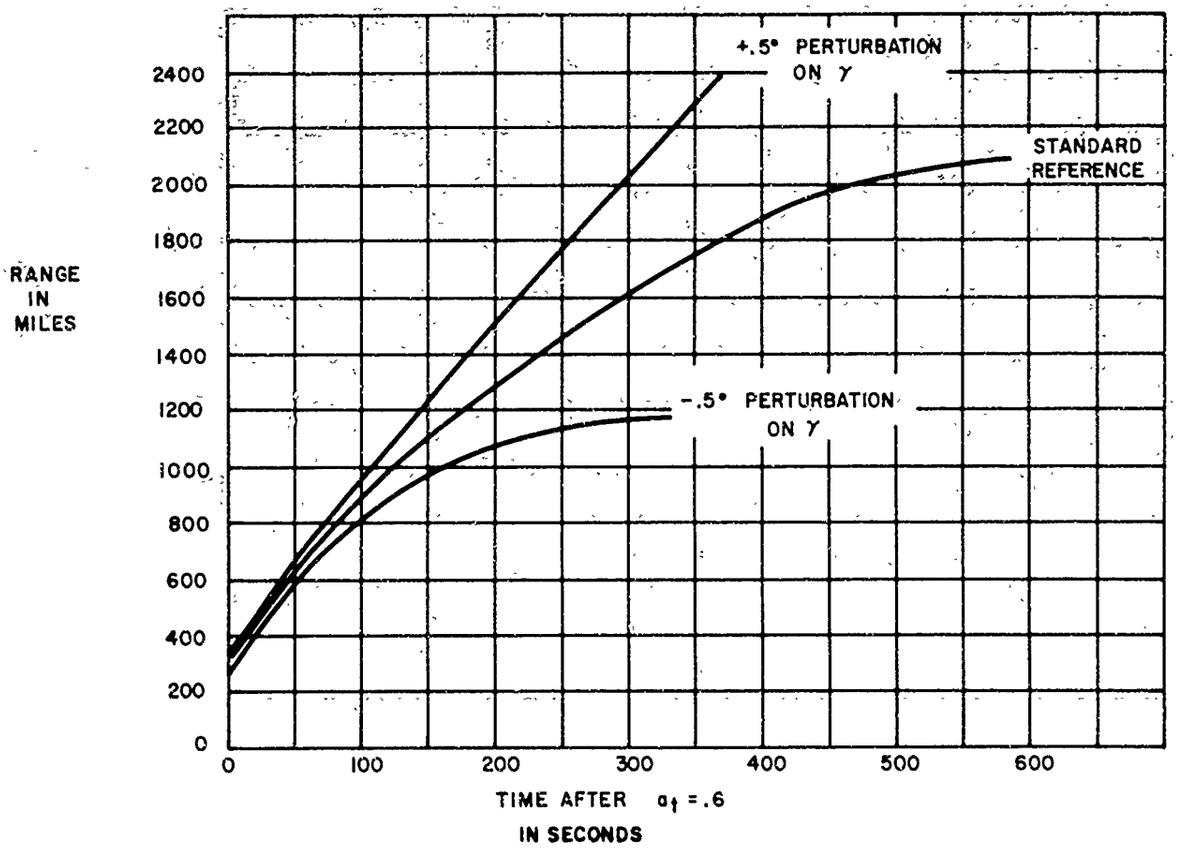

Figure 4-11. Re-entry Angle Range Effects

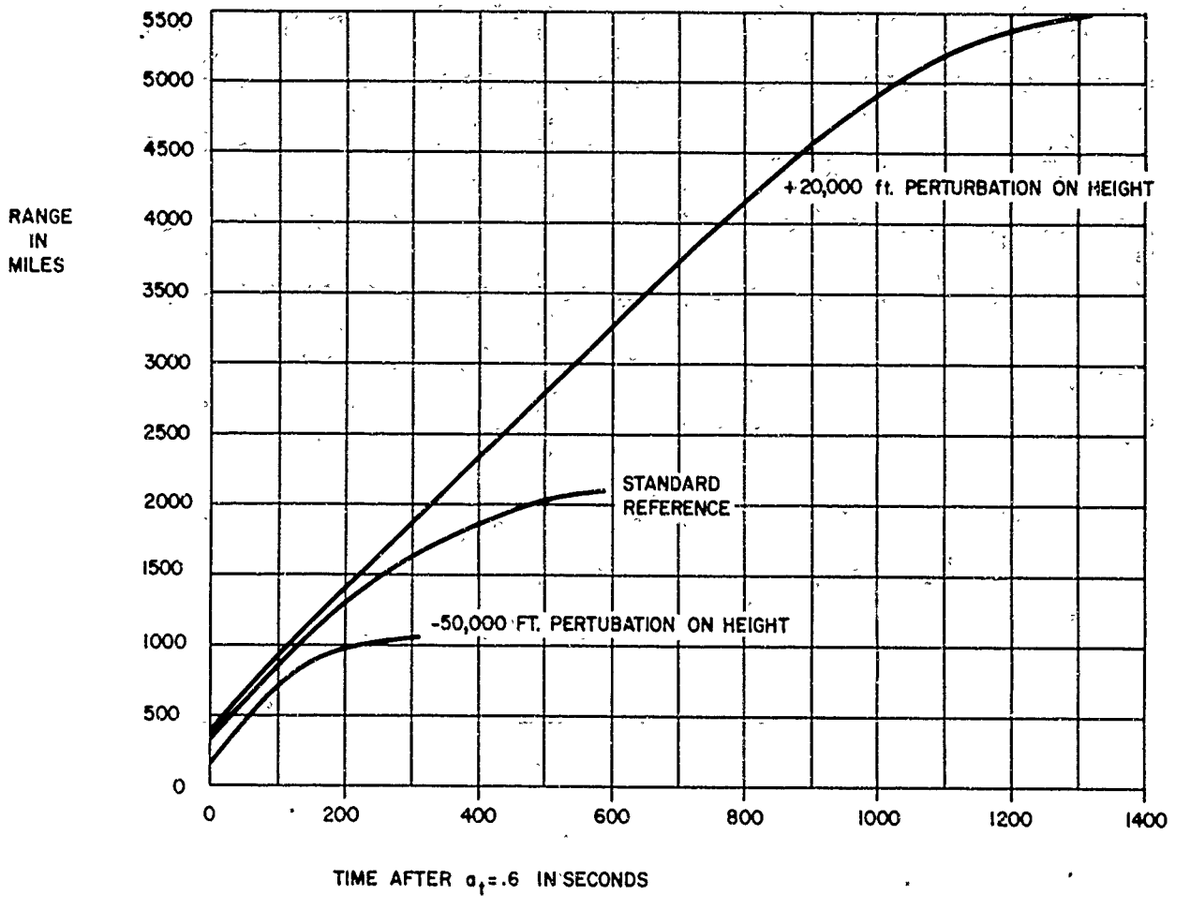

Figure 4-12. Height Range Effects

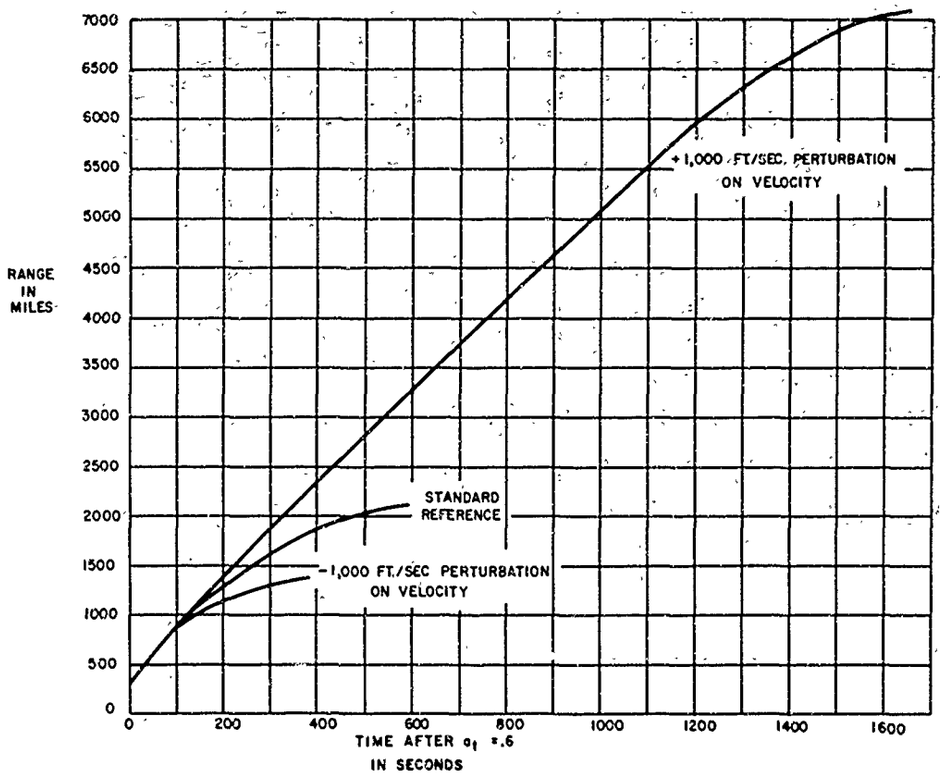

Figure 4-13. Velocity Range Effects

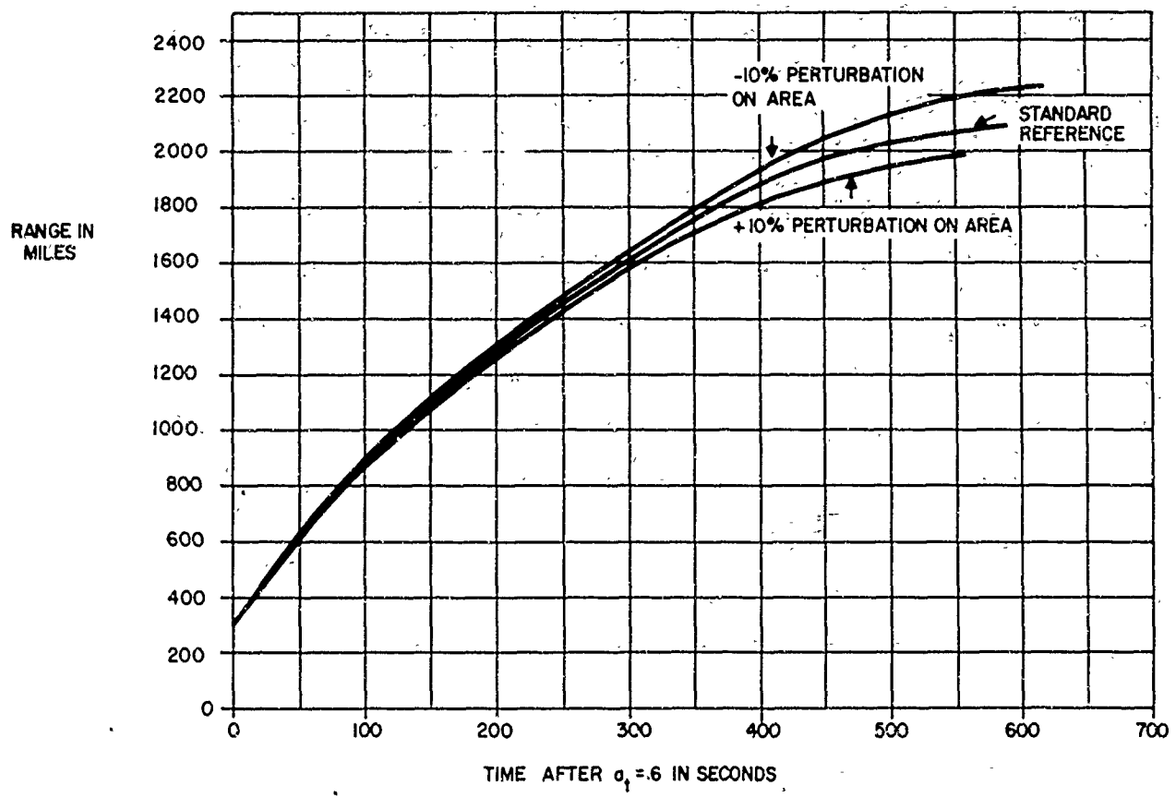

Figure 4-14. Ballistic Coefficient Range Effects

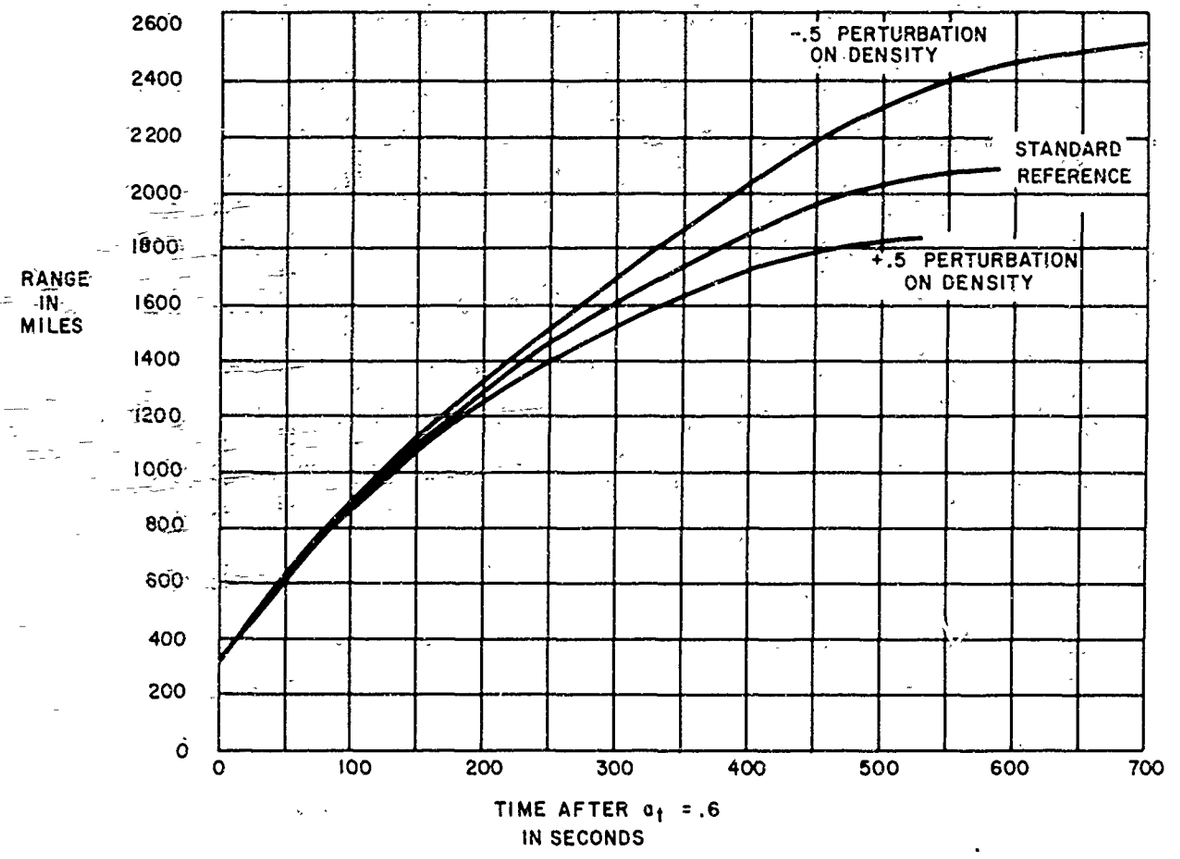

Figure 4-15. Density Change Range Effects

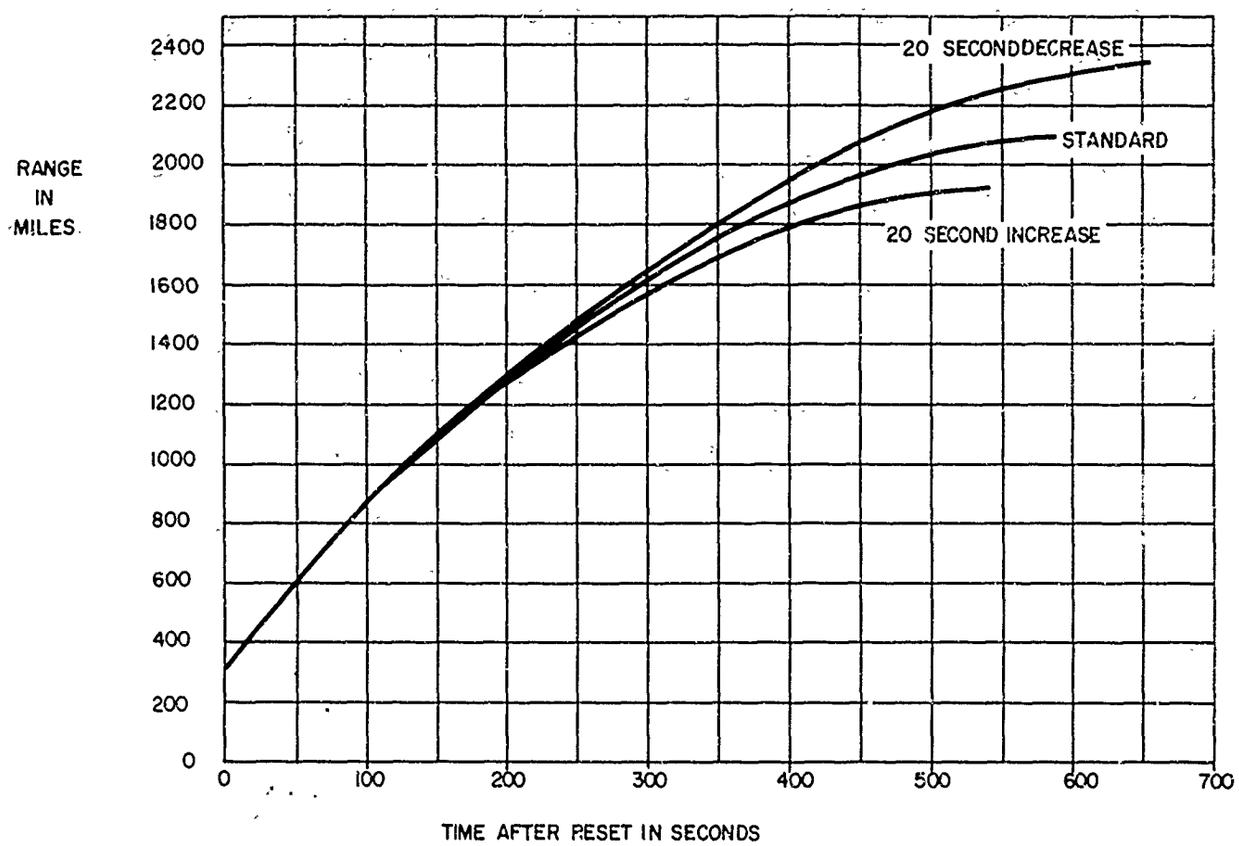

Figure 4-16. ϕ_{max} Hold Time

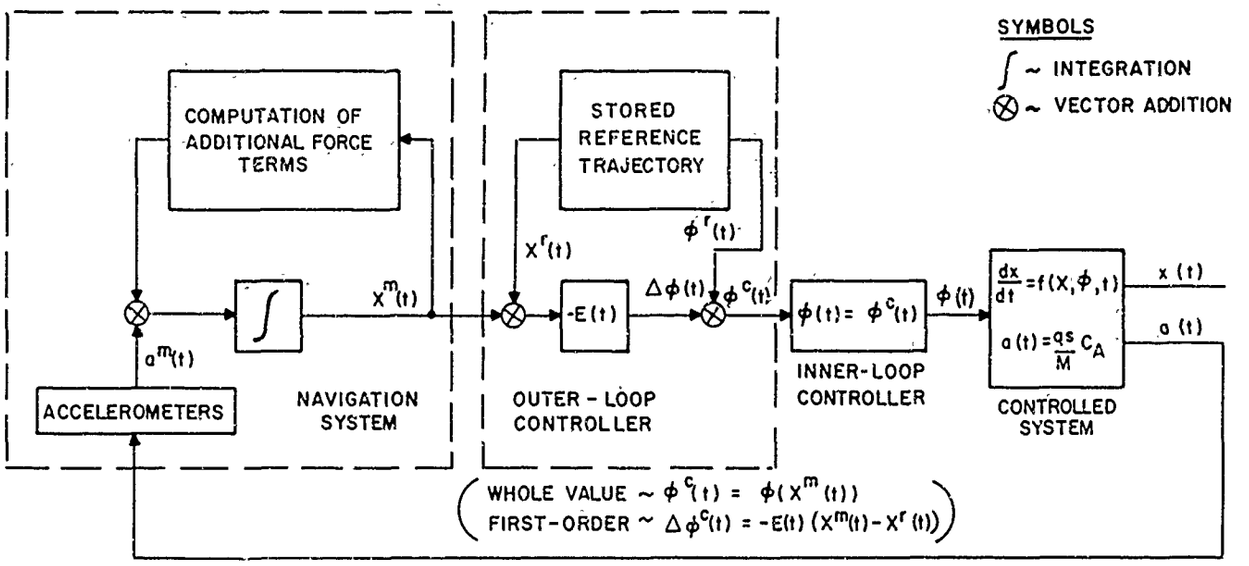

Figure 4-17. Closed-Loop System

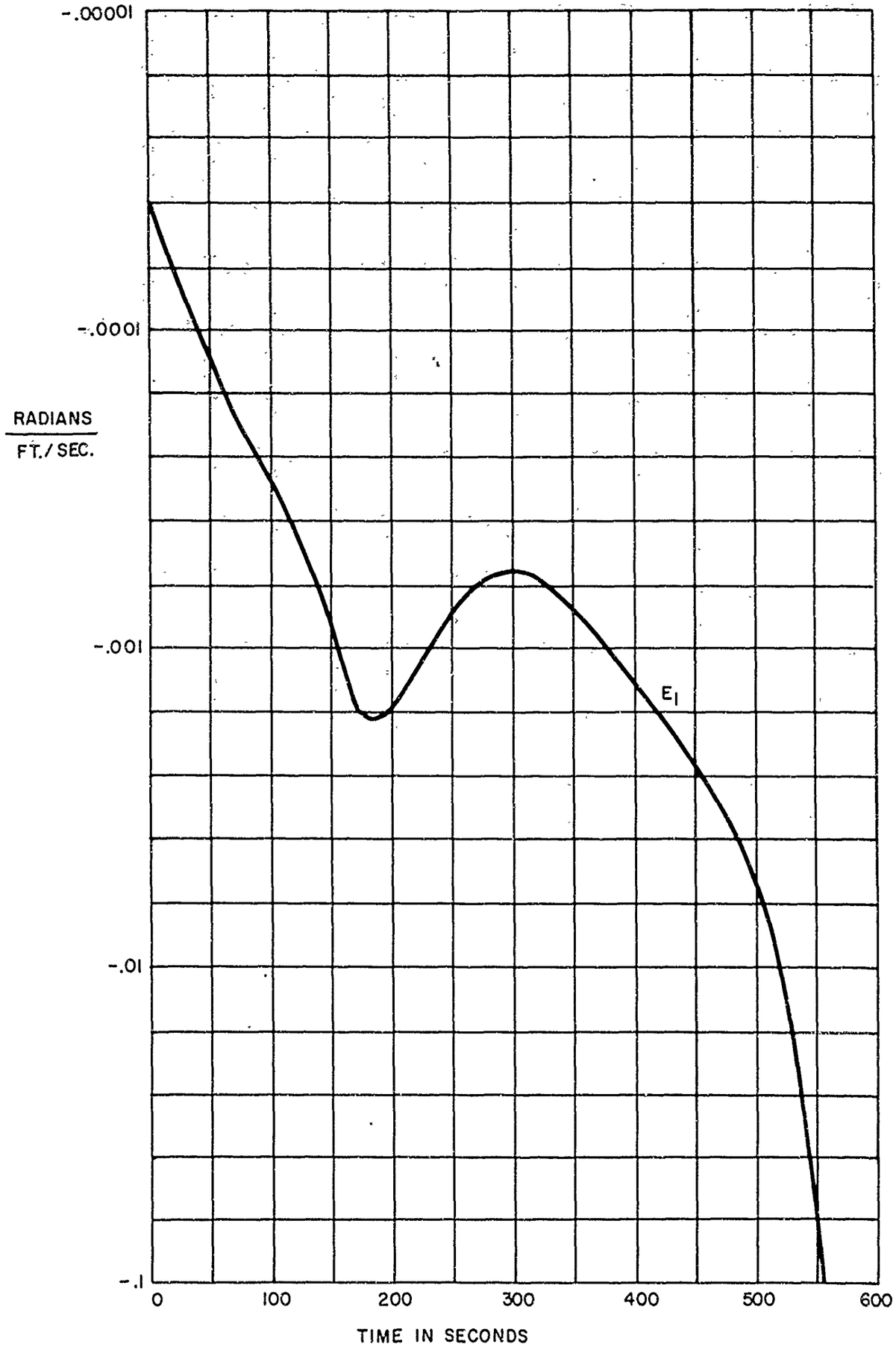

Figure 4-18. $\Delta\phi$ Guidance Sensitivities

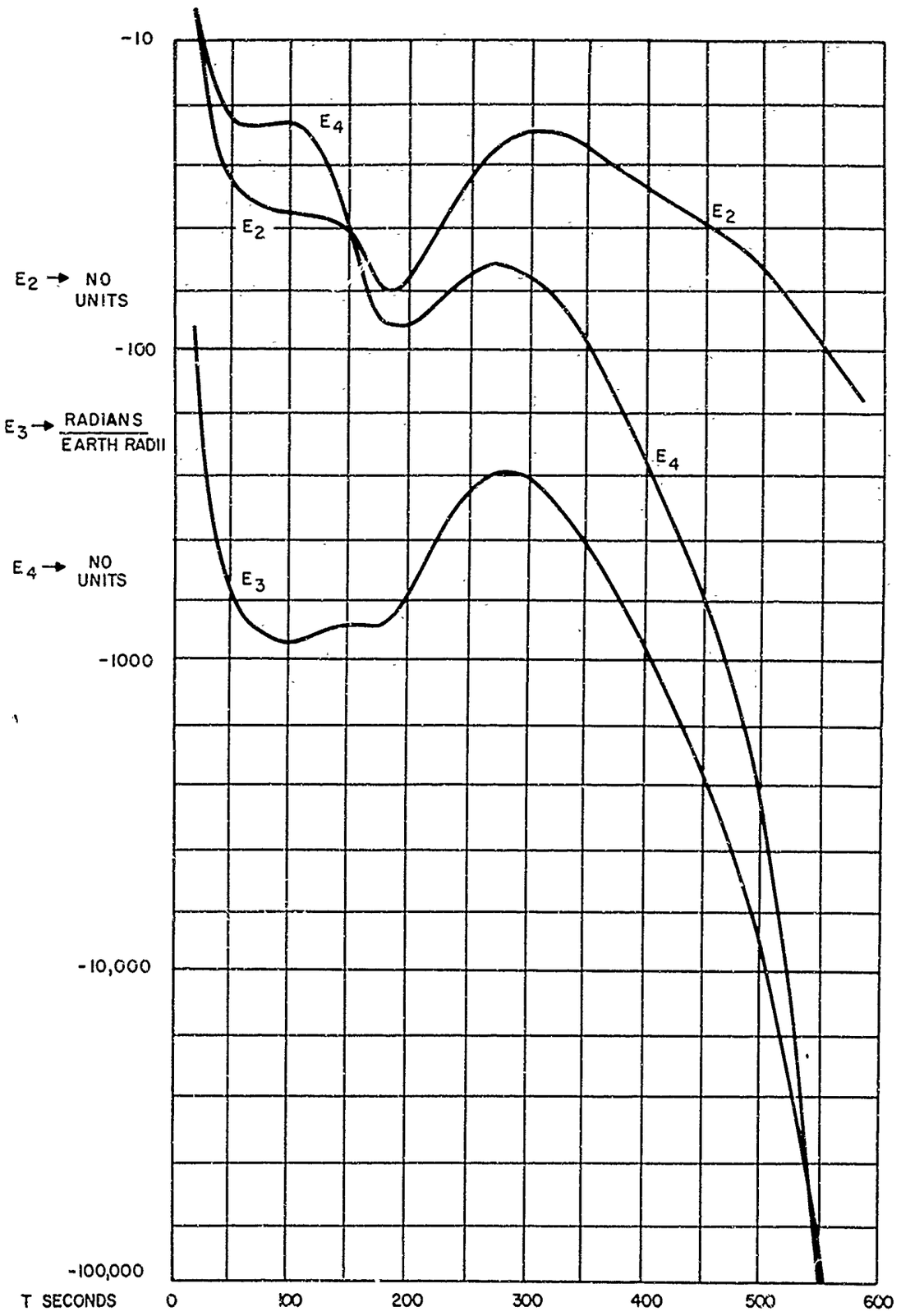

Figure 4-19. $\Delta\phi$ Guidance Sensitivites

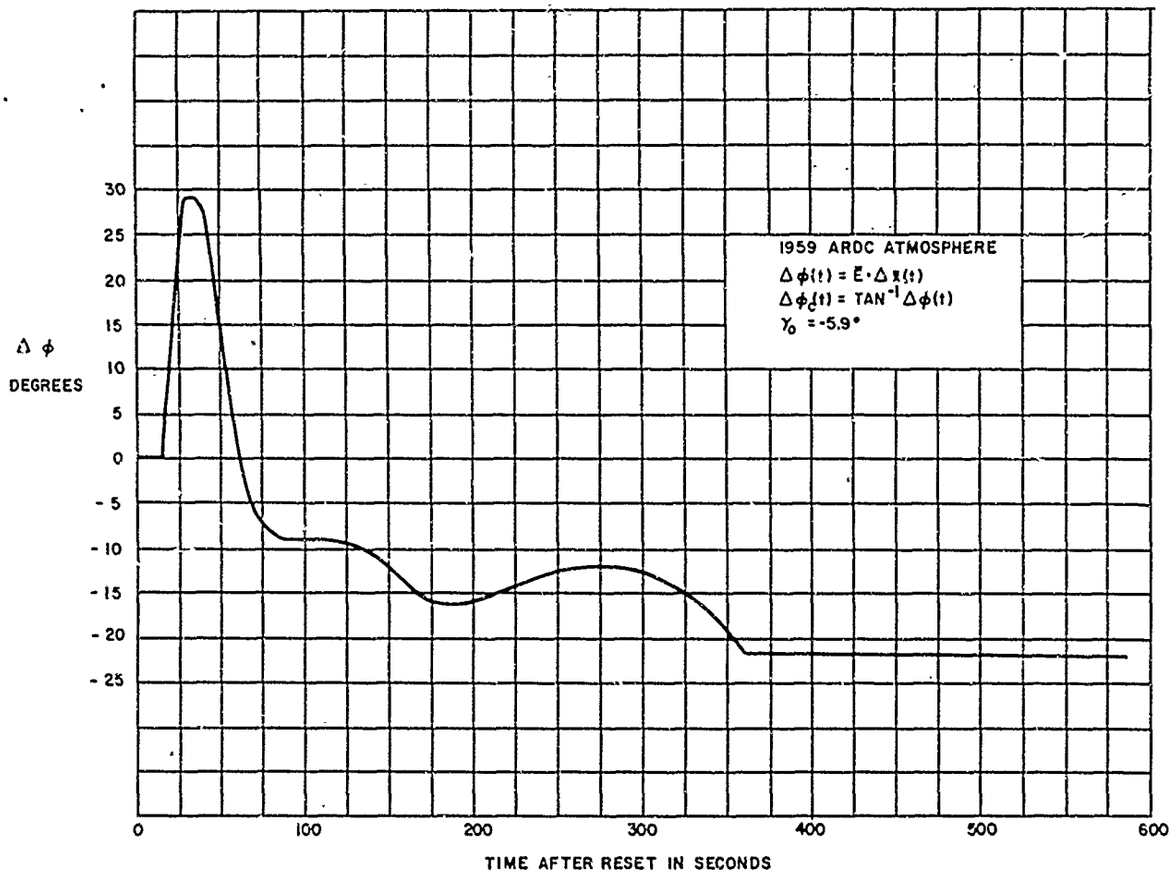

Figure 4-20. Closed-Loop Trajectory

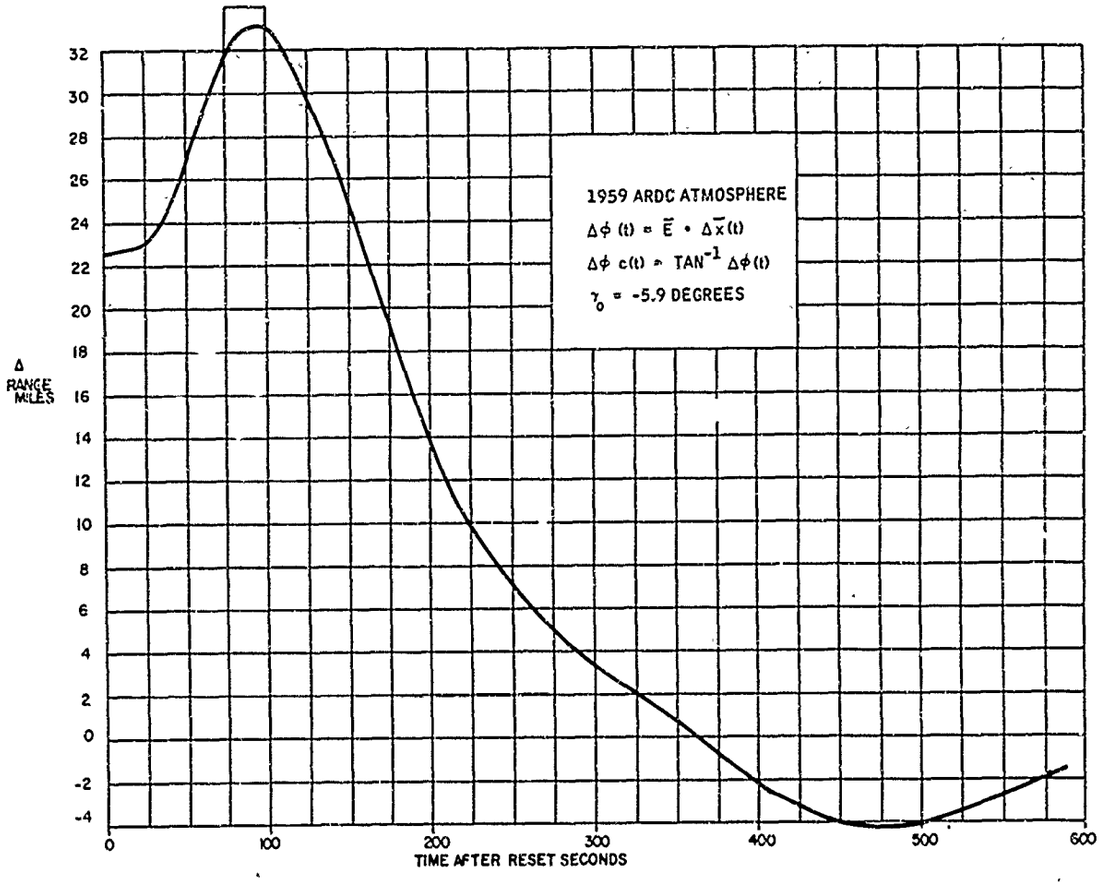

Figure 4-21. Closed-Loop Trajectory

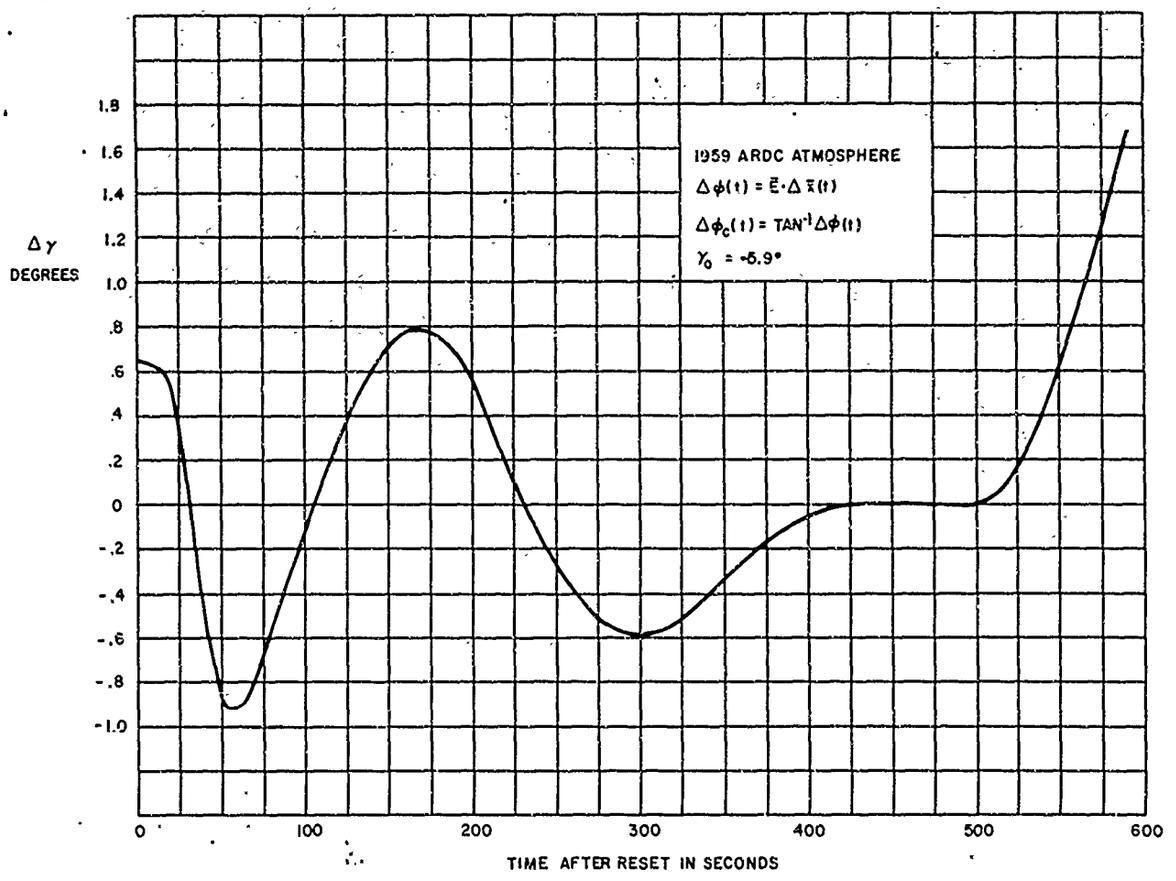

Figure 4-22. Closed-Loop Trajectory

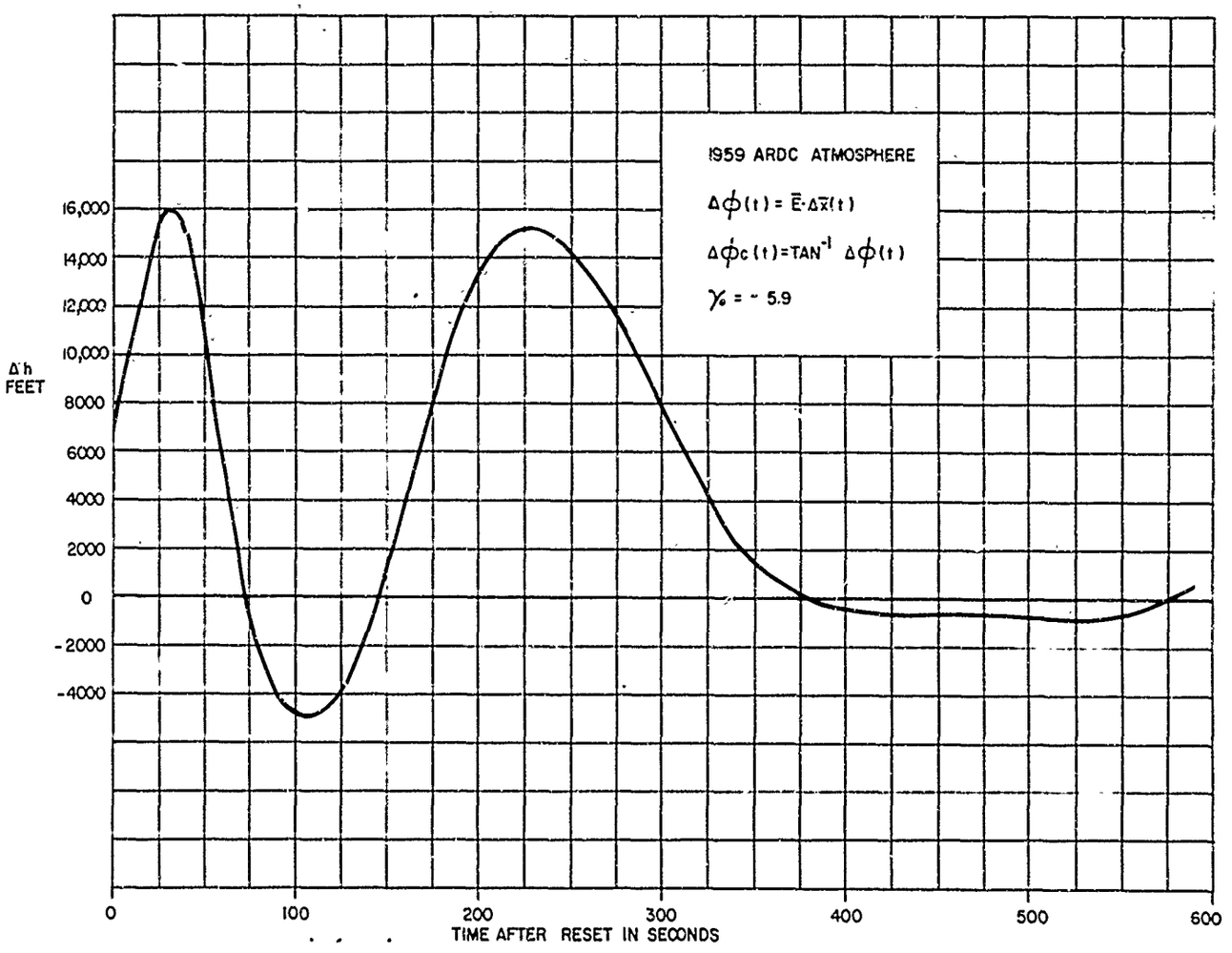

Figure 4-23. Closed-Loop Trajectory

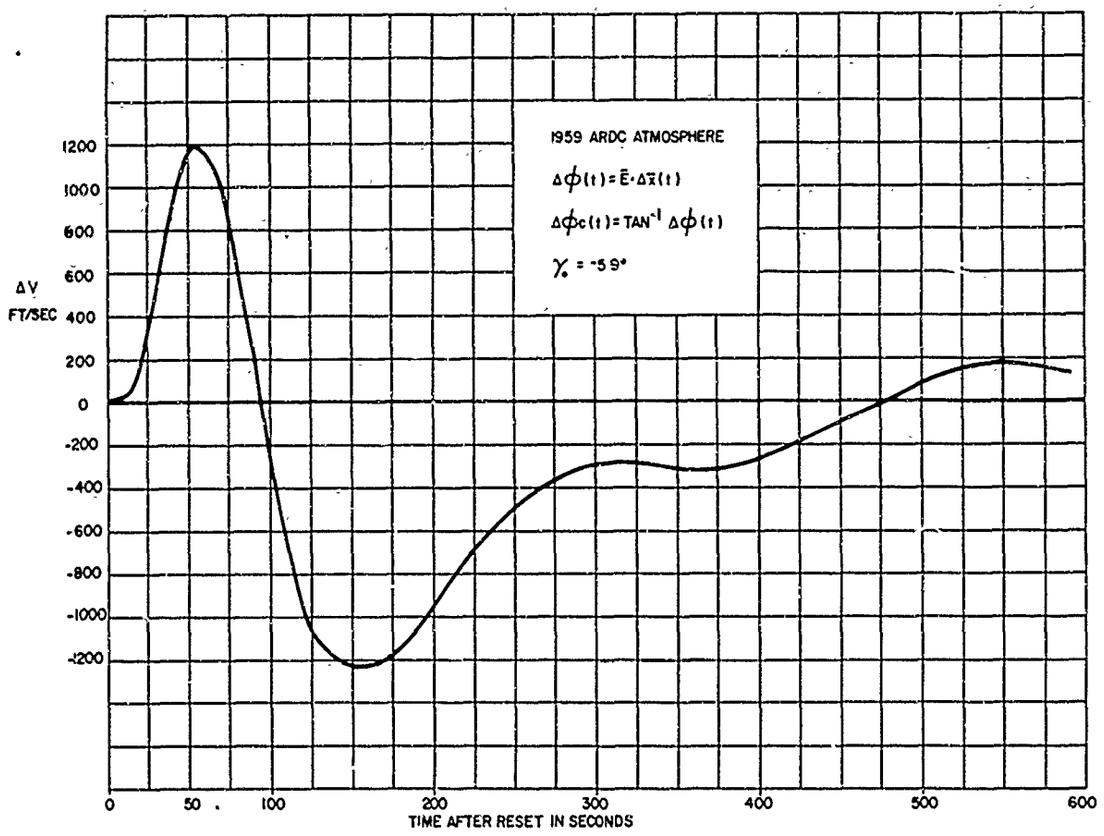

Figure 4-24. Closed-Loop Trajectory

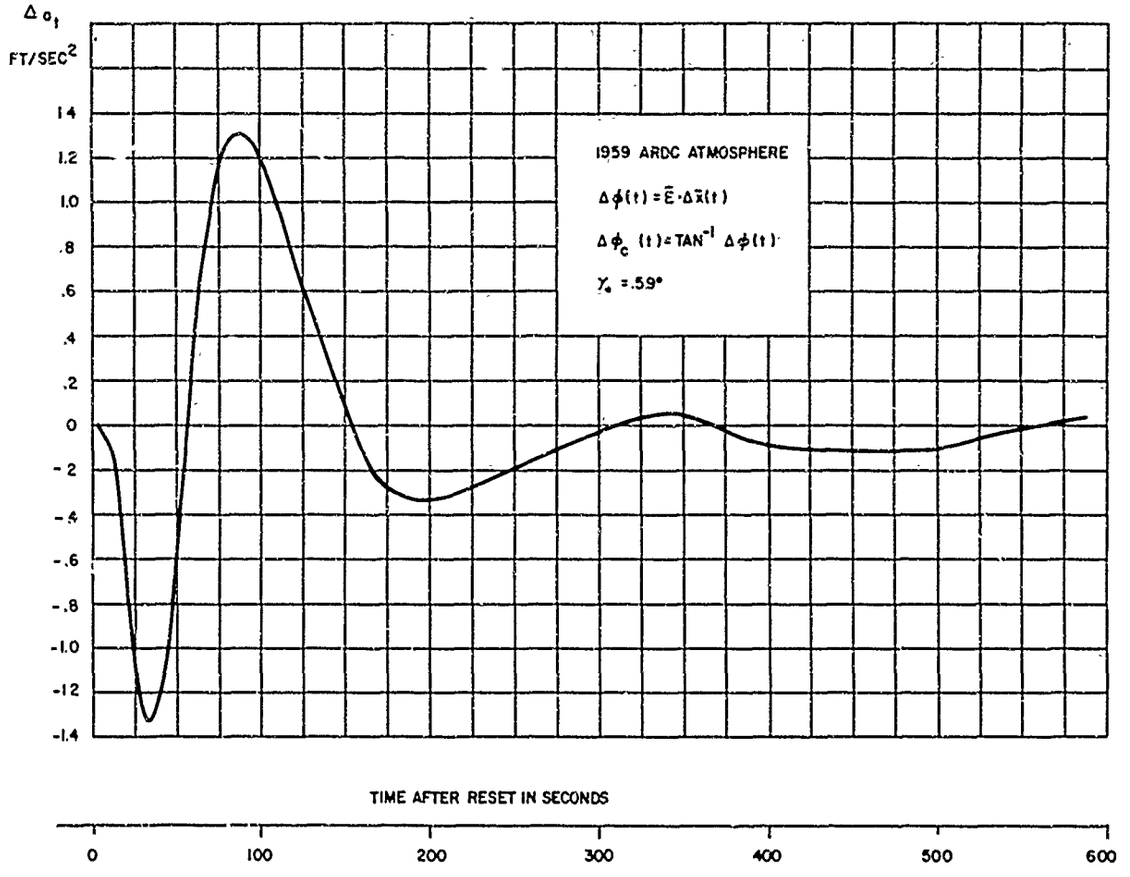

Figure 4-25. Closed-Loop Trajectory

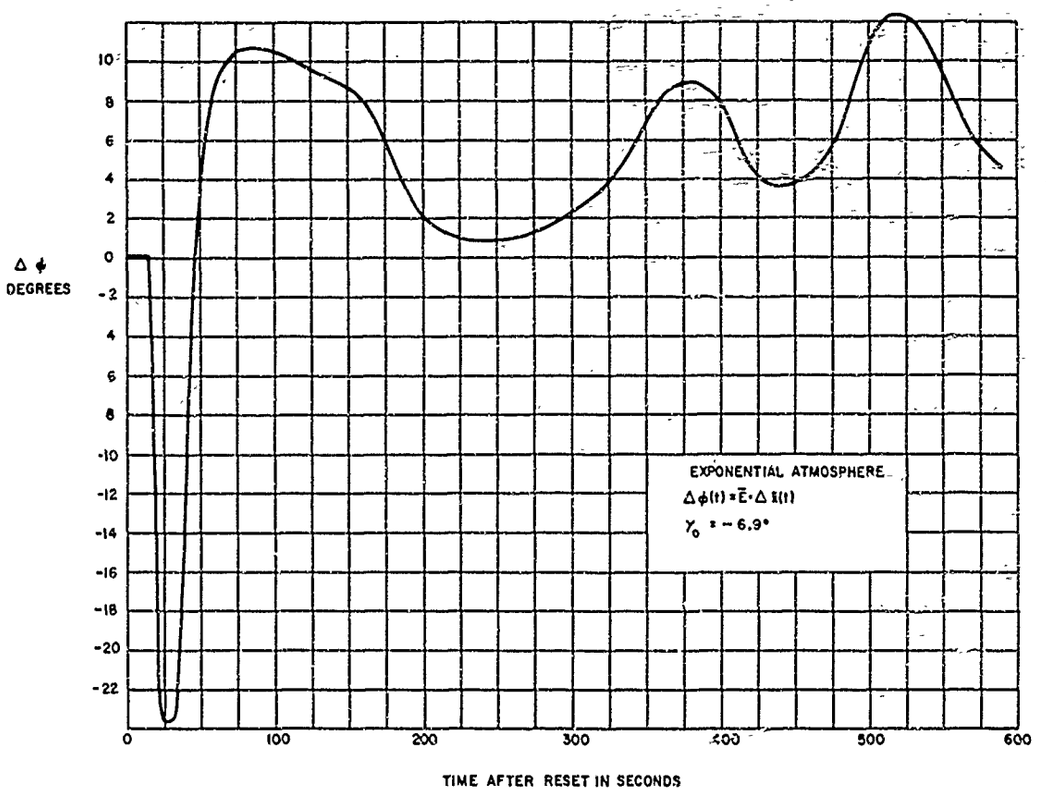

Figure 4-26. Closed-Loop Trajectory

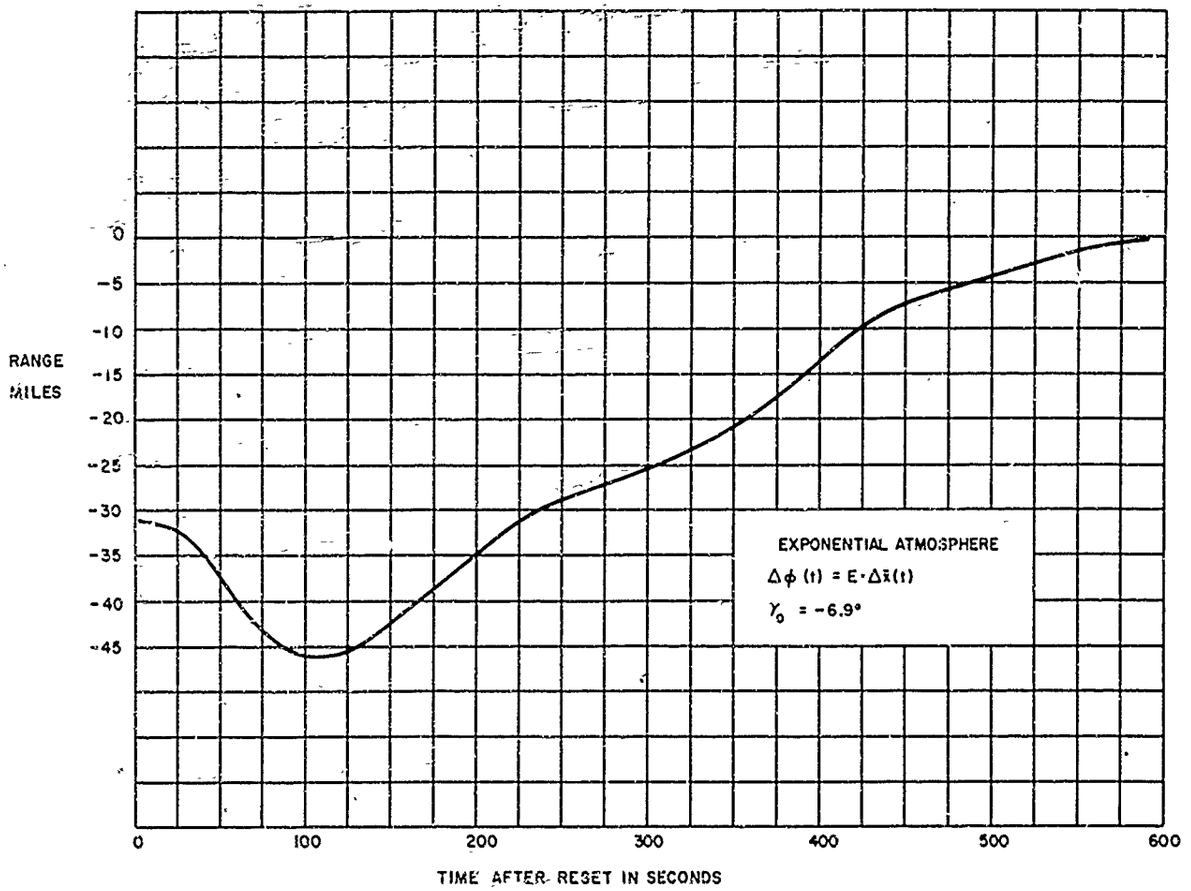

Figure 4-27. Closed-Loop Trajectory

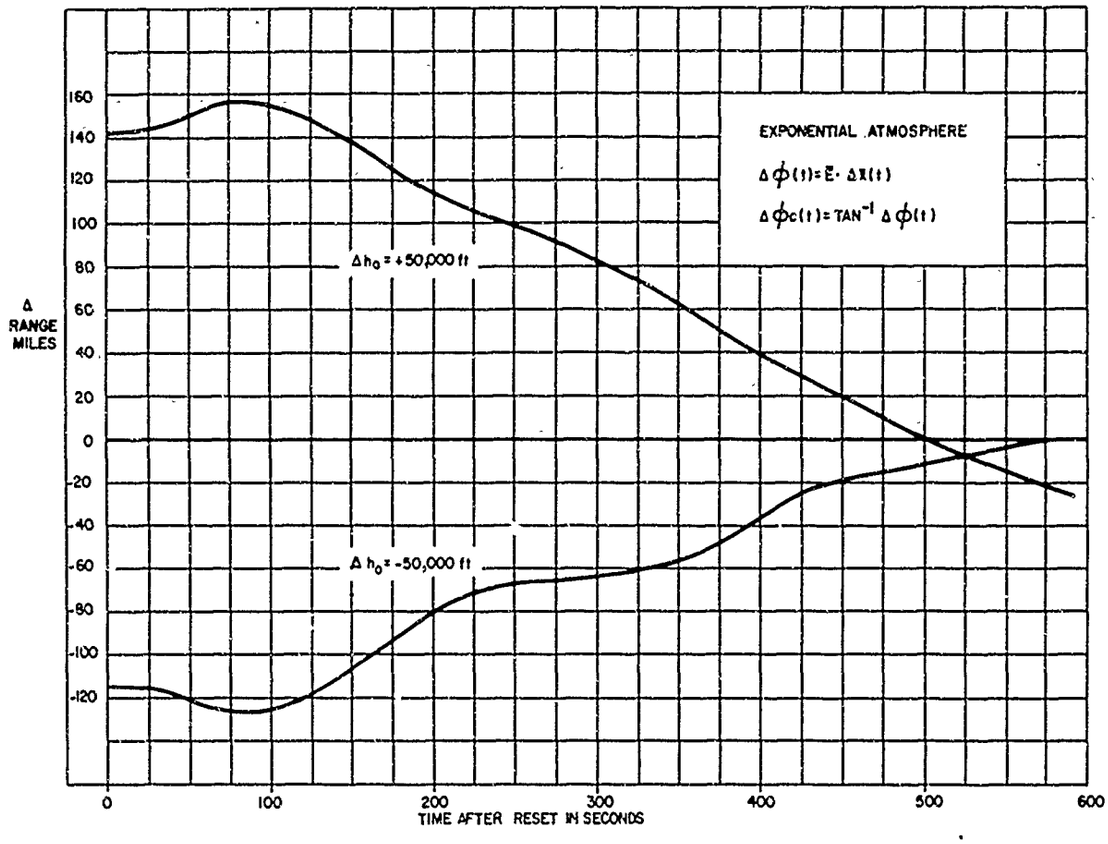

Figure 4-28. Closed-Loop Trajectory

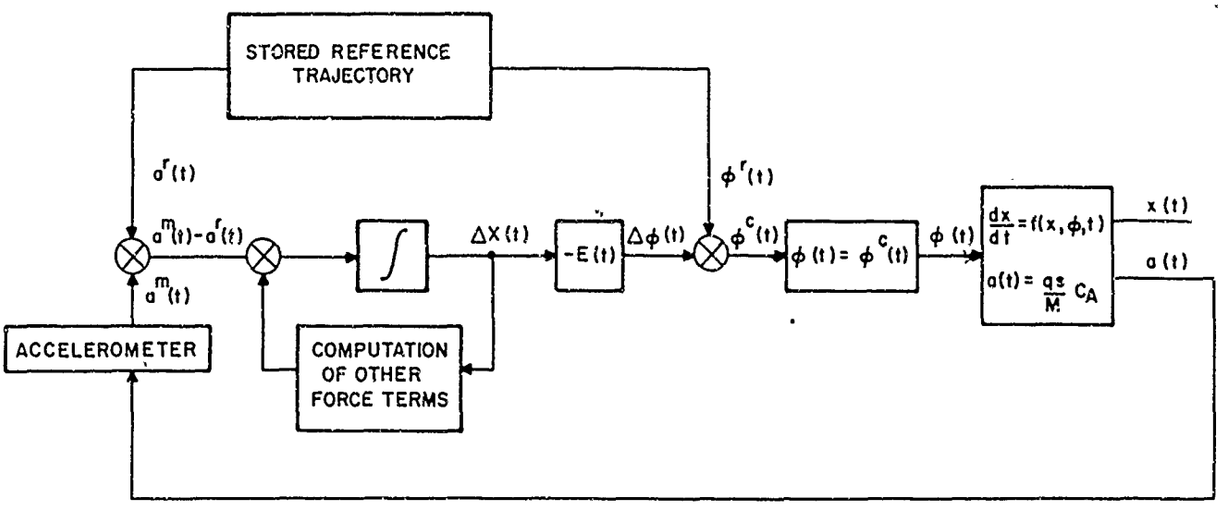

Figure 4-29. Closed-Loop System Showing Perturbational Navigation System

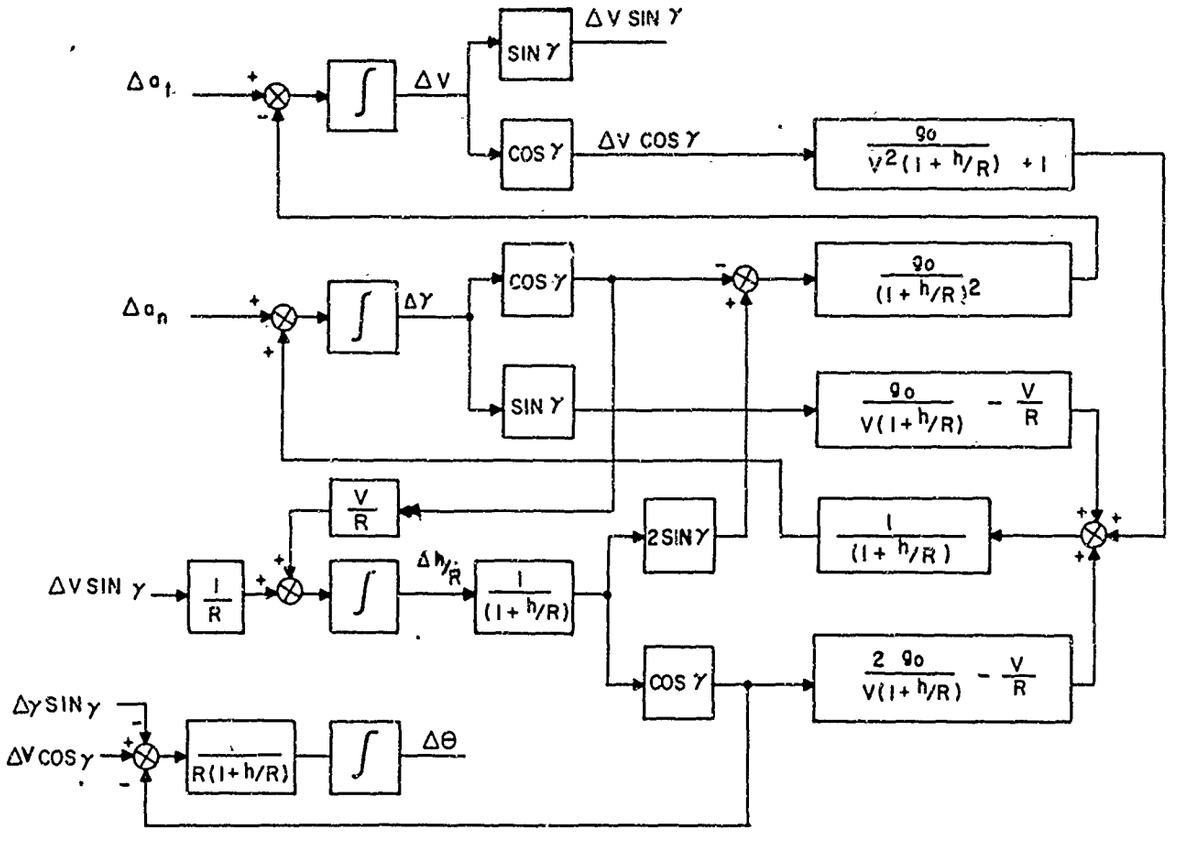

Figure 4-30. First-Order Navigation System for a Two-Dimensional Trajectory - Fixed Reference

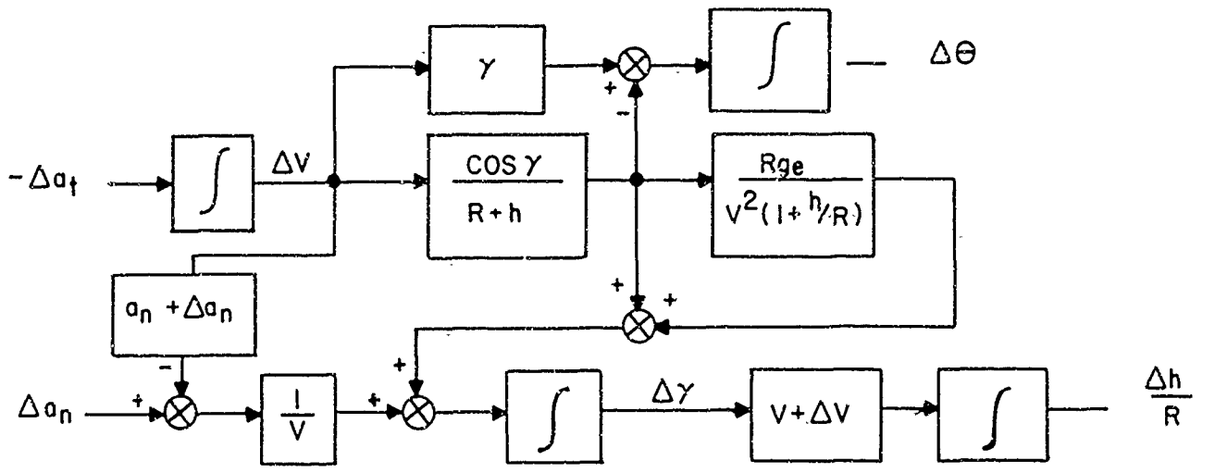

Figure 4-31. Approximate Navigation System for a Two-Dimensional Trajectory - Fixed Reference Frame

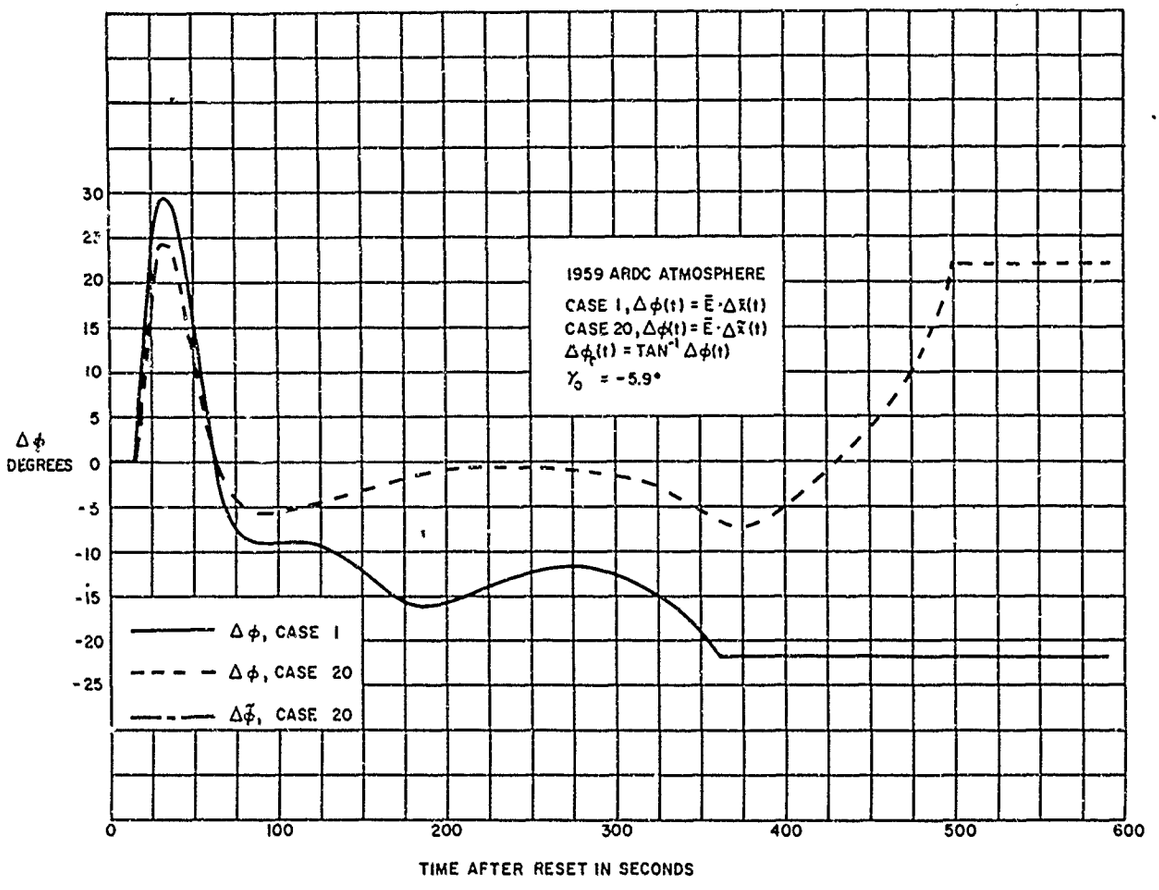

Figure 4-32. Closed-Loop Trajectory

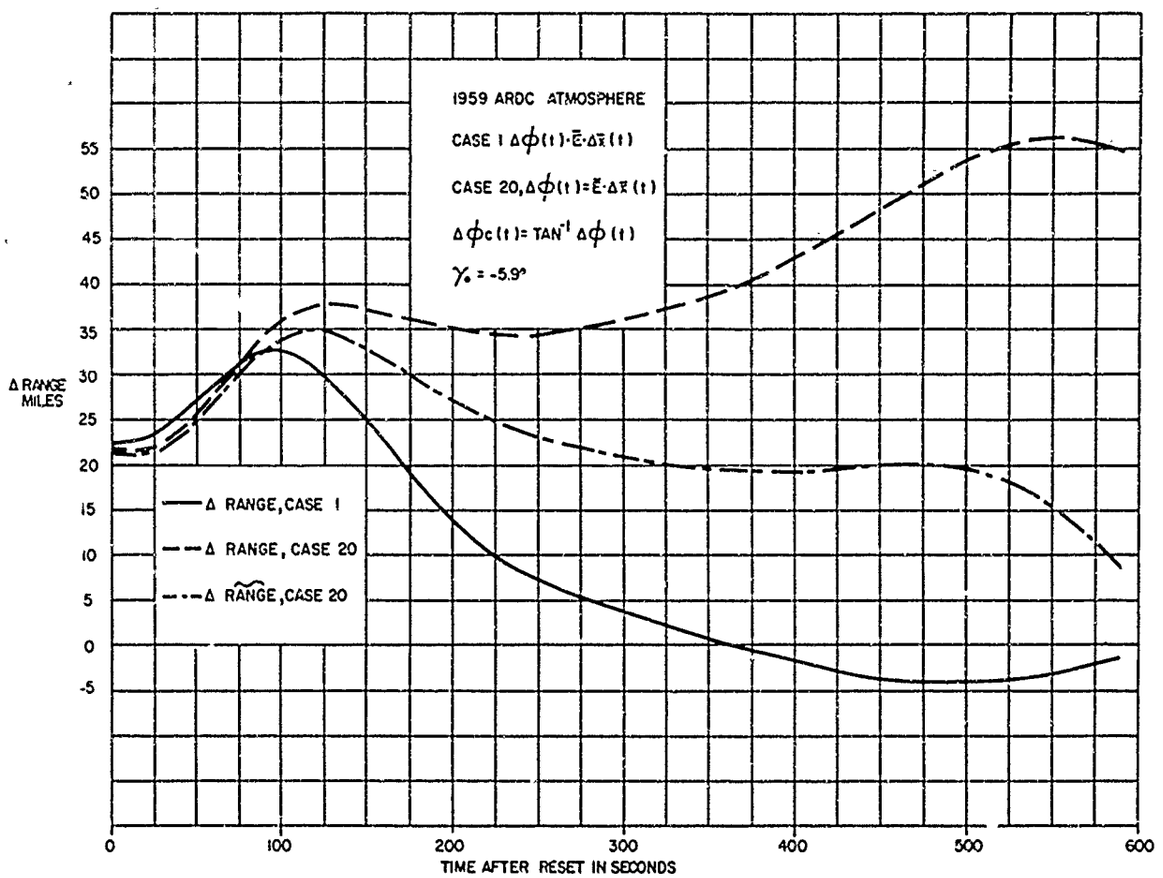

Figure 4-33. Closed-Loop Trajectory

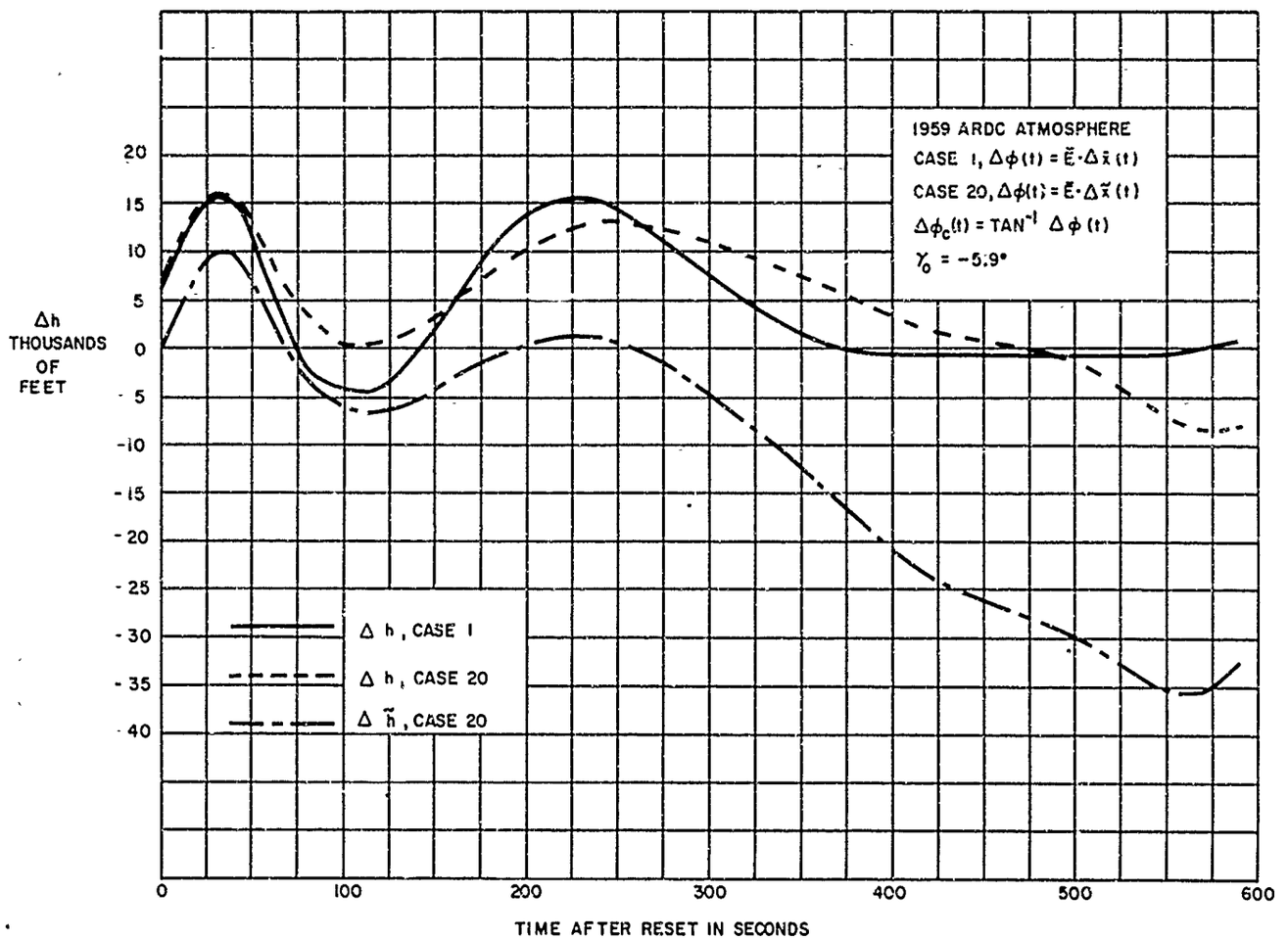

Figure 4-34. Closed-Loop Trajectory

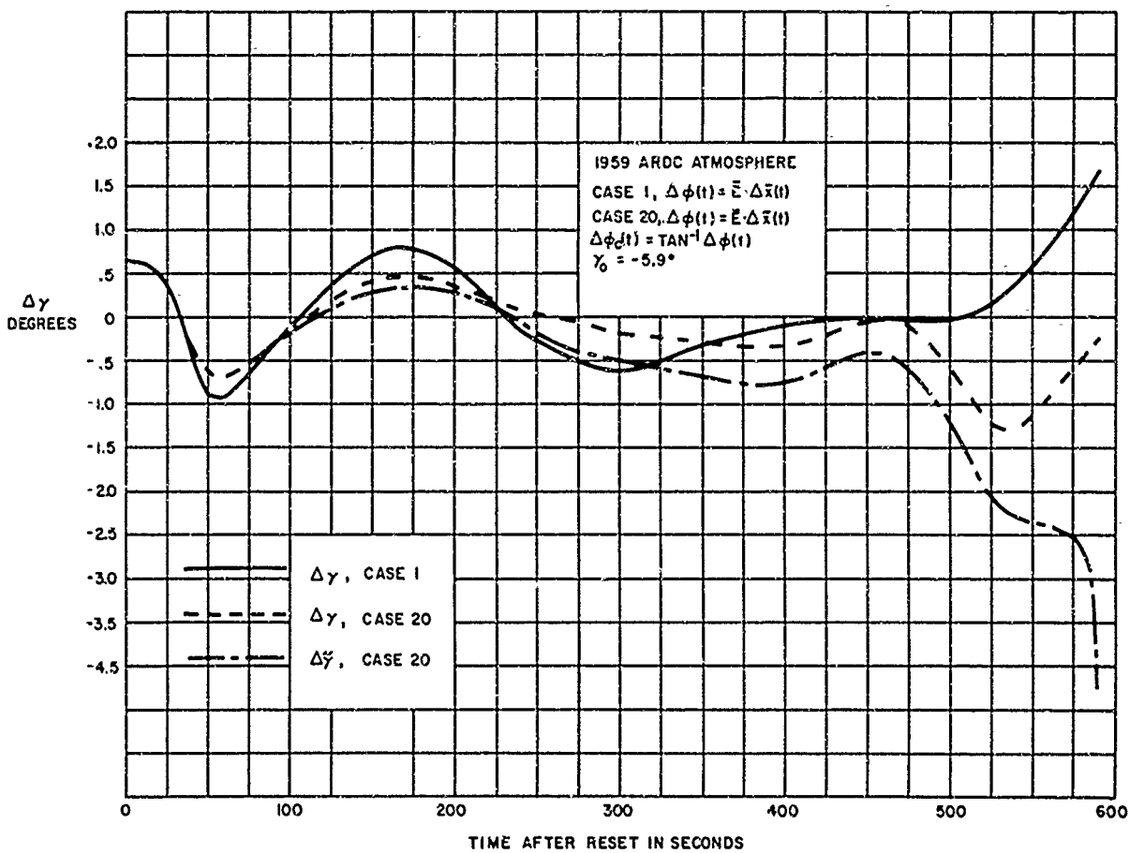

Figure 4-35. Closed-Loop Trajectory

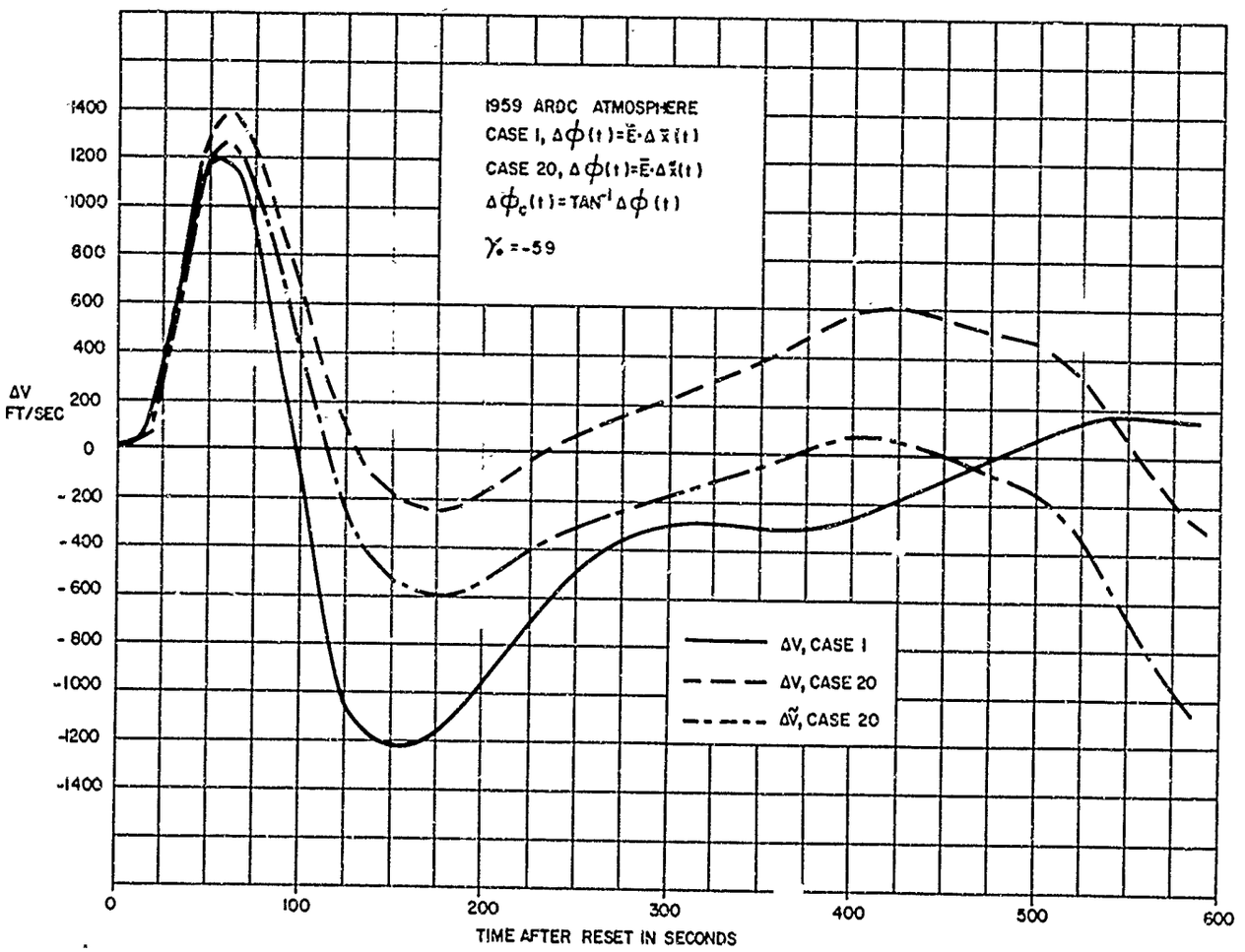

Figure 4-36. Closed-Loop Trajectory

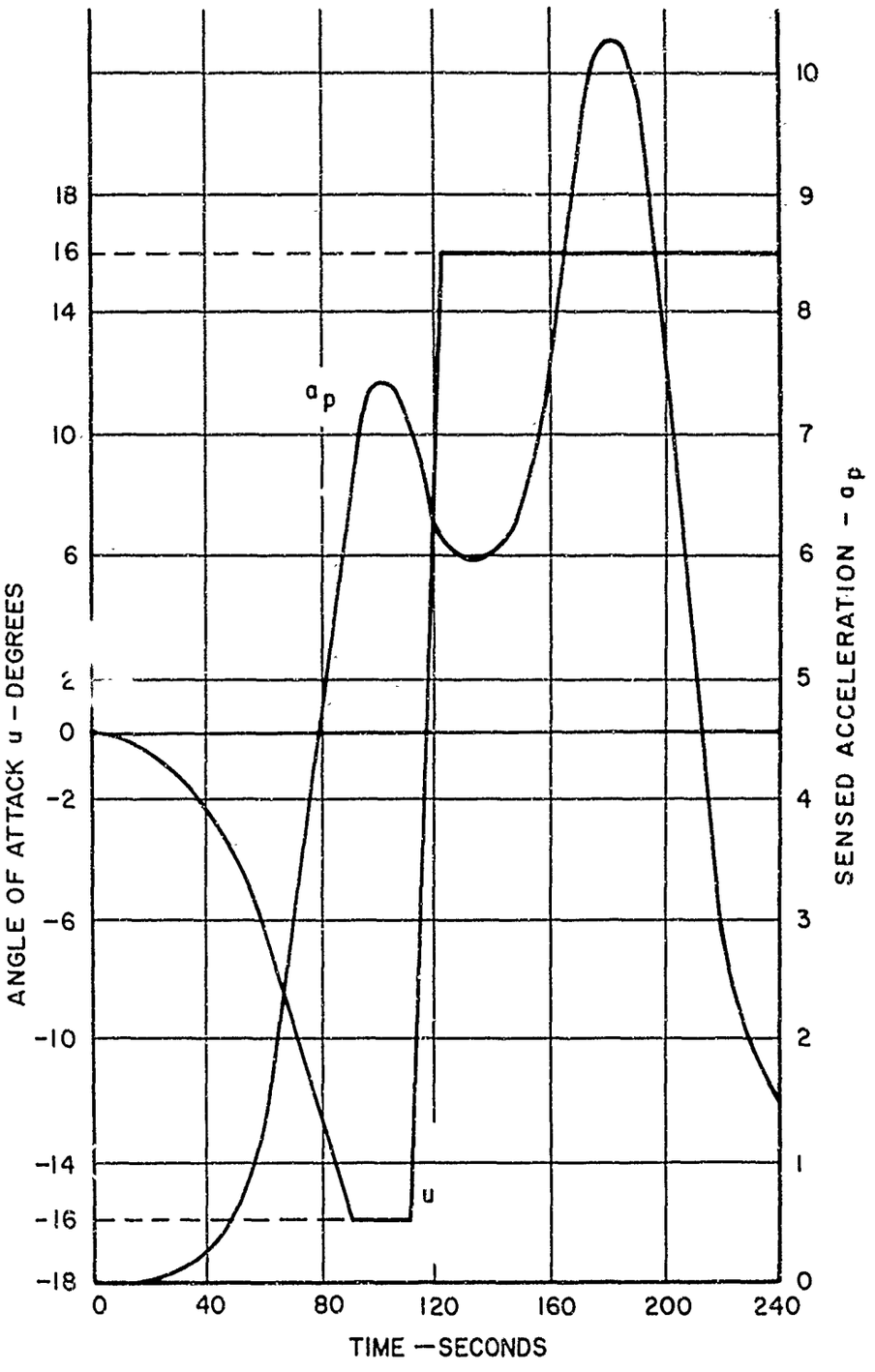

Figure 4-37. Extremal Reference Control

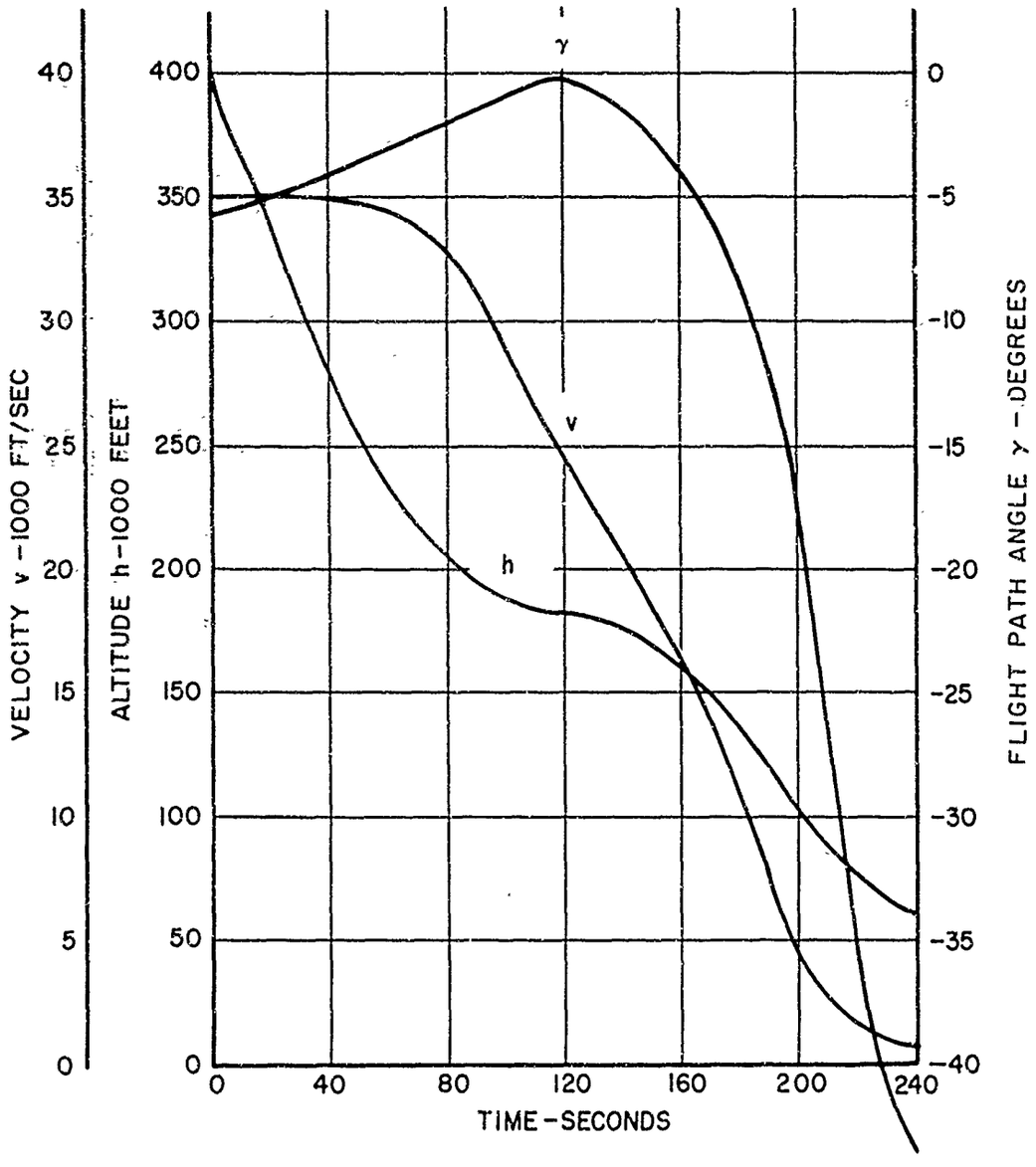

Figure 4-38. Extremal Reference Trajectory

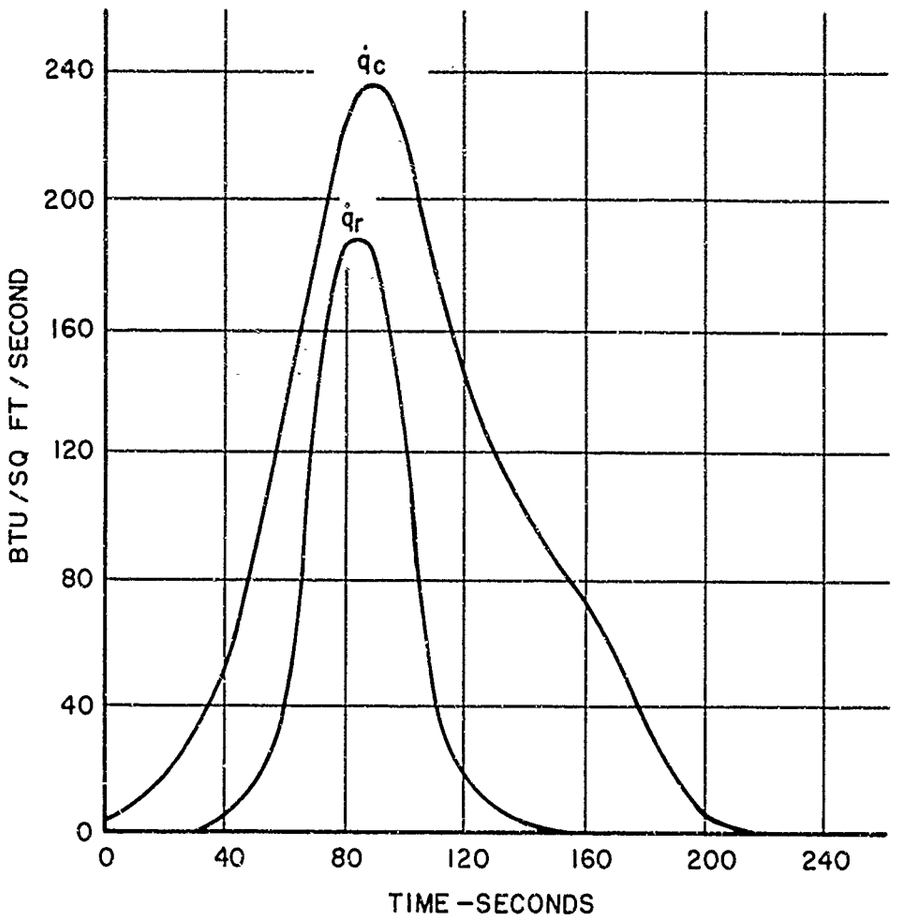

Figure 4-39. Extremal Reference Trajectory Heating

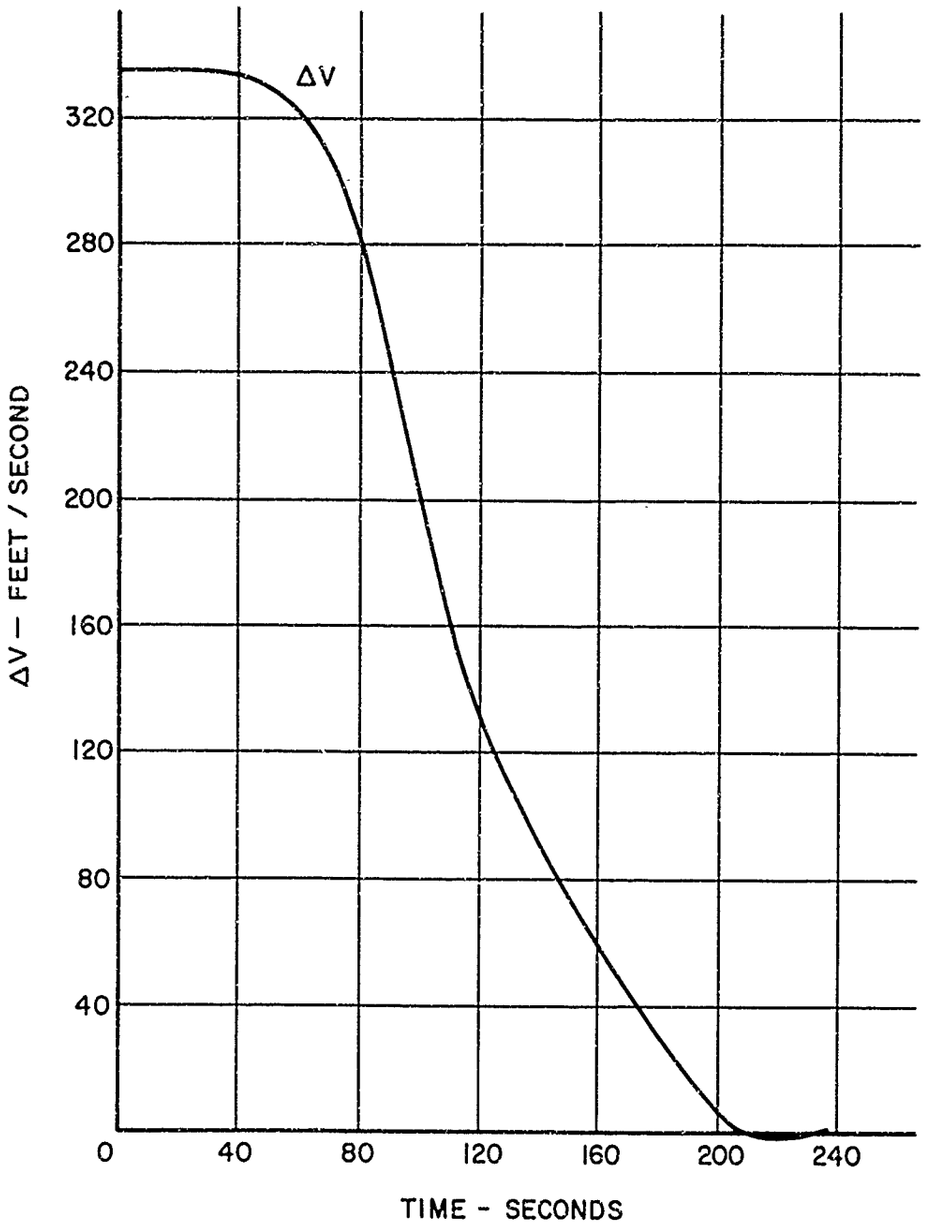

Figure 4-40. Velocity Sensitivity for Extremal Reference Trajectory

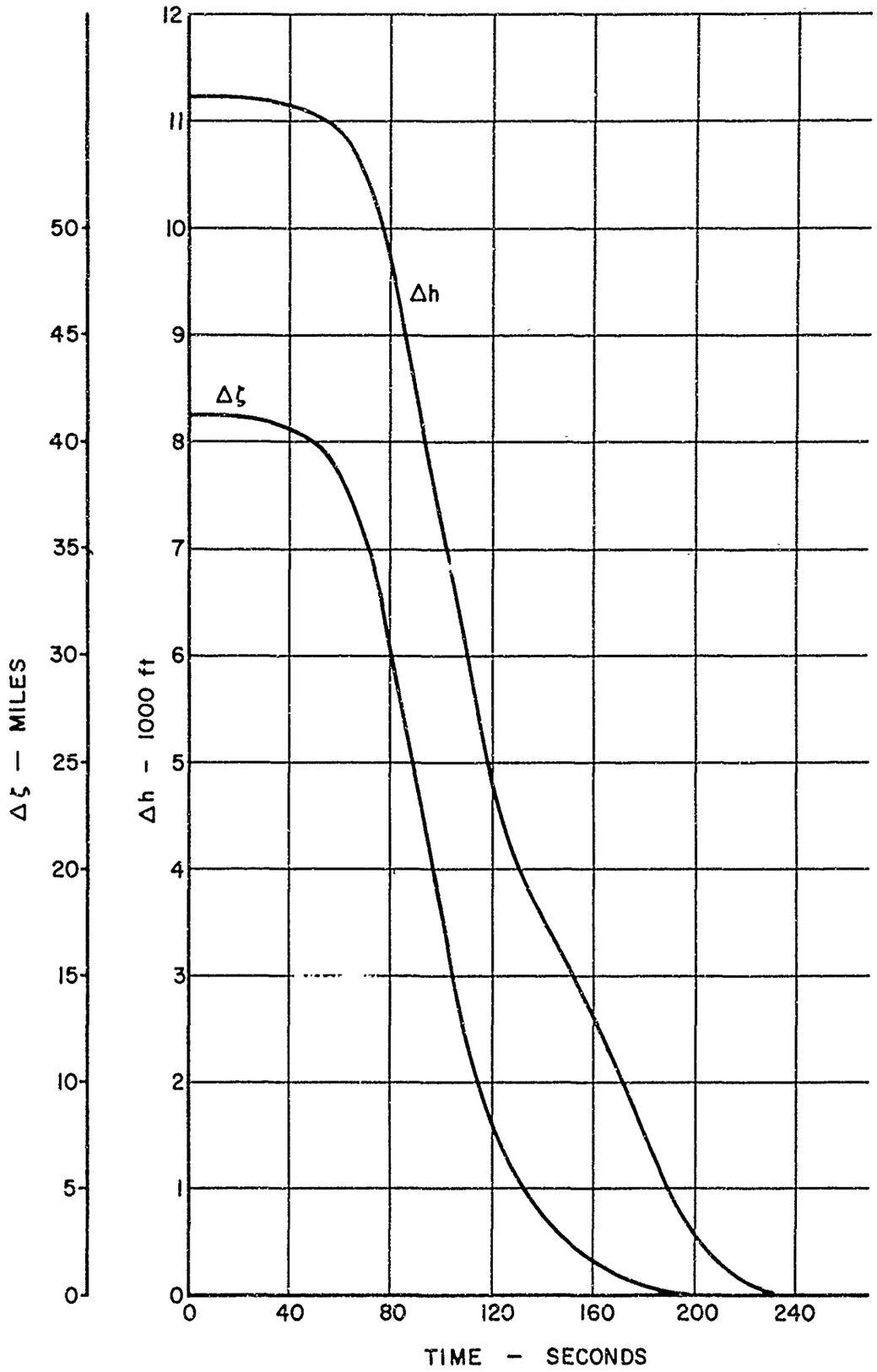

Figure 4-41. Range and Altitude Sensitivity for Extremal Reference Trajectory

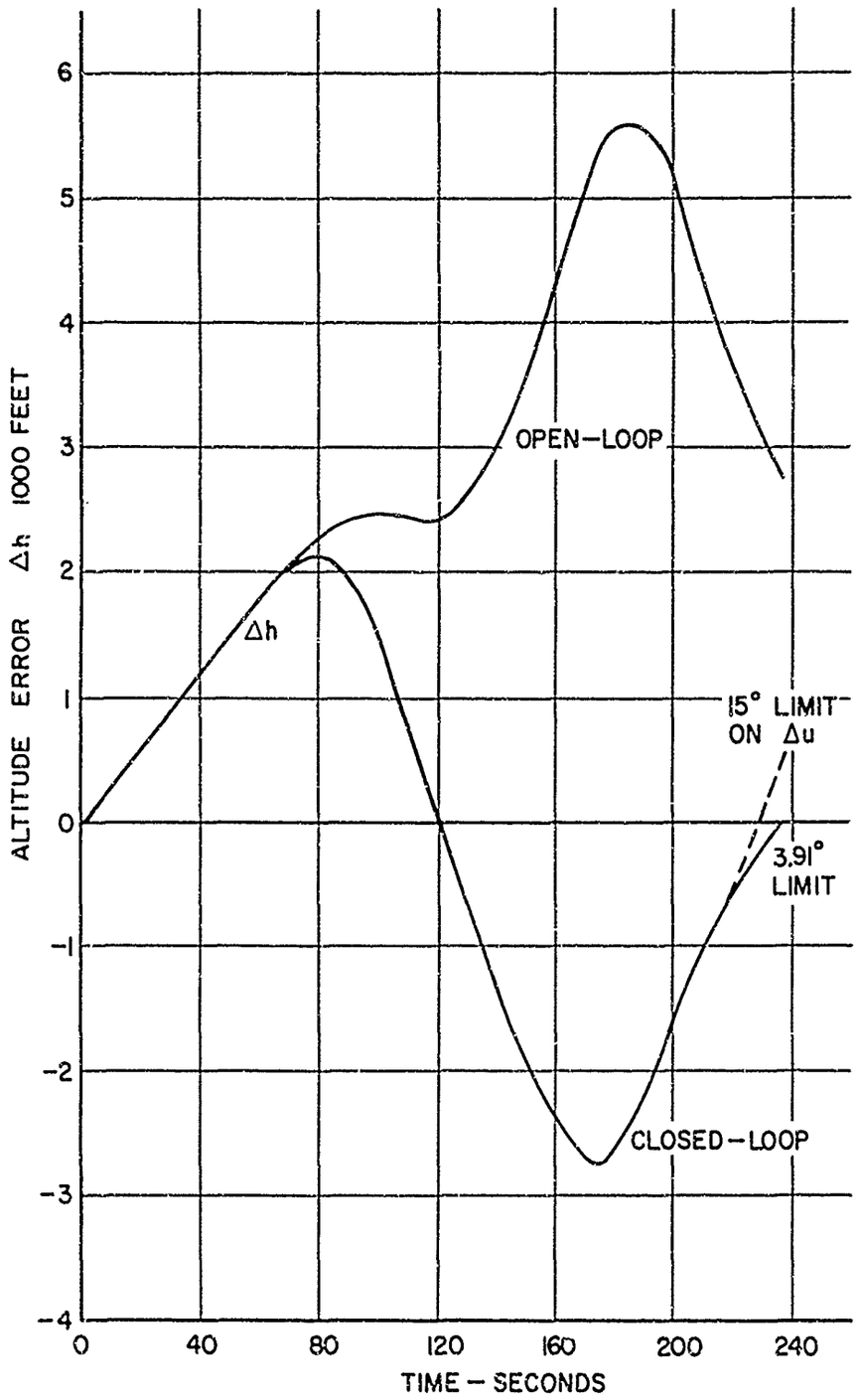

Figure 4-42. Open- and Closed-Loop Errors, Altitude Case: Initial Perturbation $\Delta\alpha_o$ = 0.05 degree

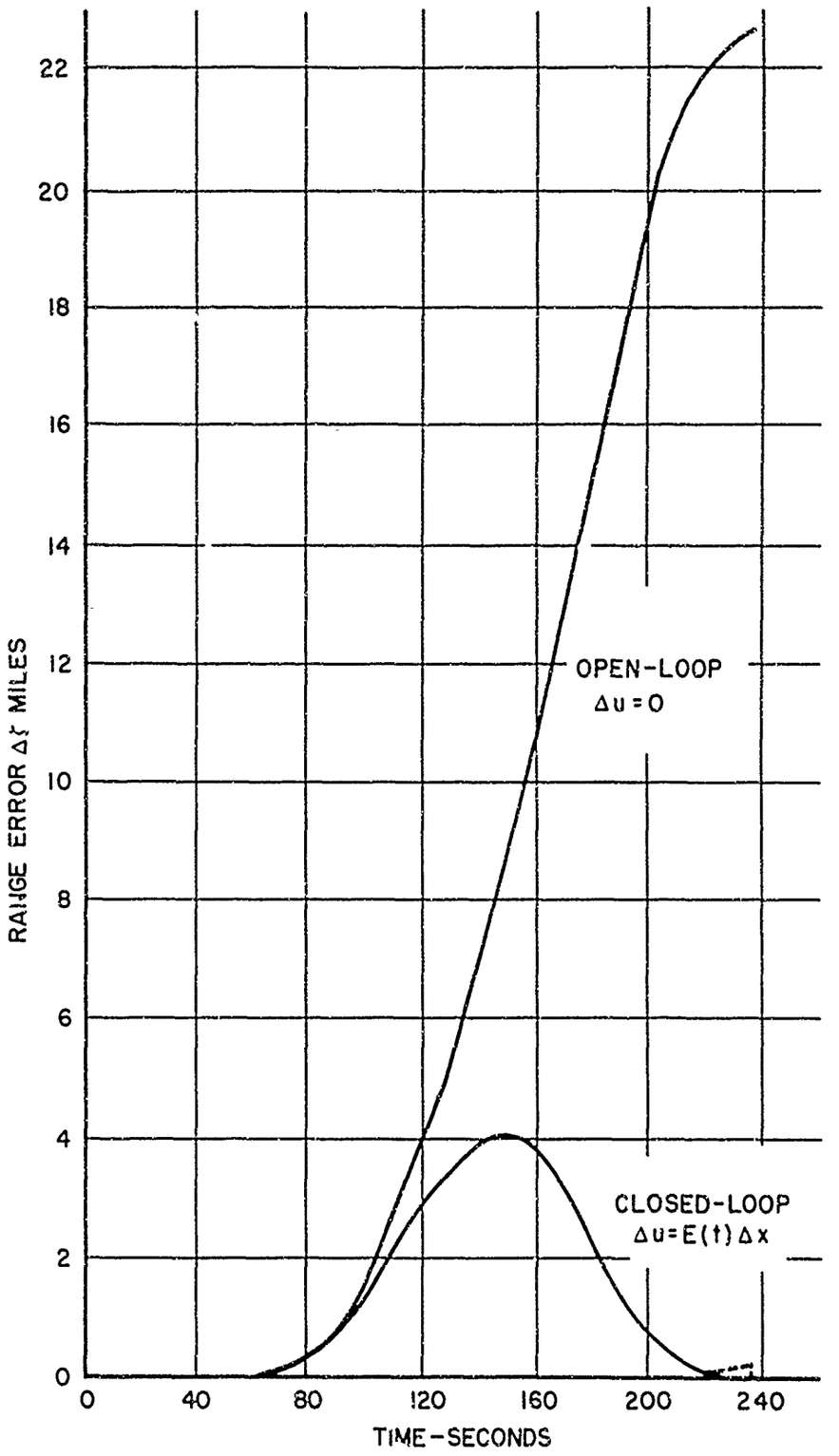

Figure 4-43. Open- and Closed-Loop Errors, Range Case: Initial Perturbation $\Delta\alpha_o$ = 0.05 degree

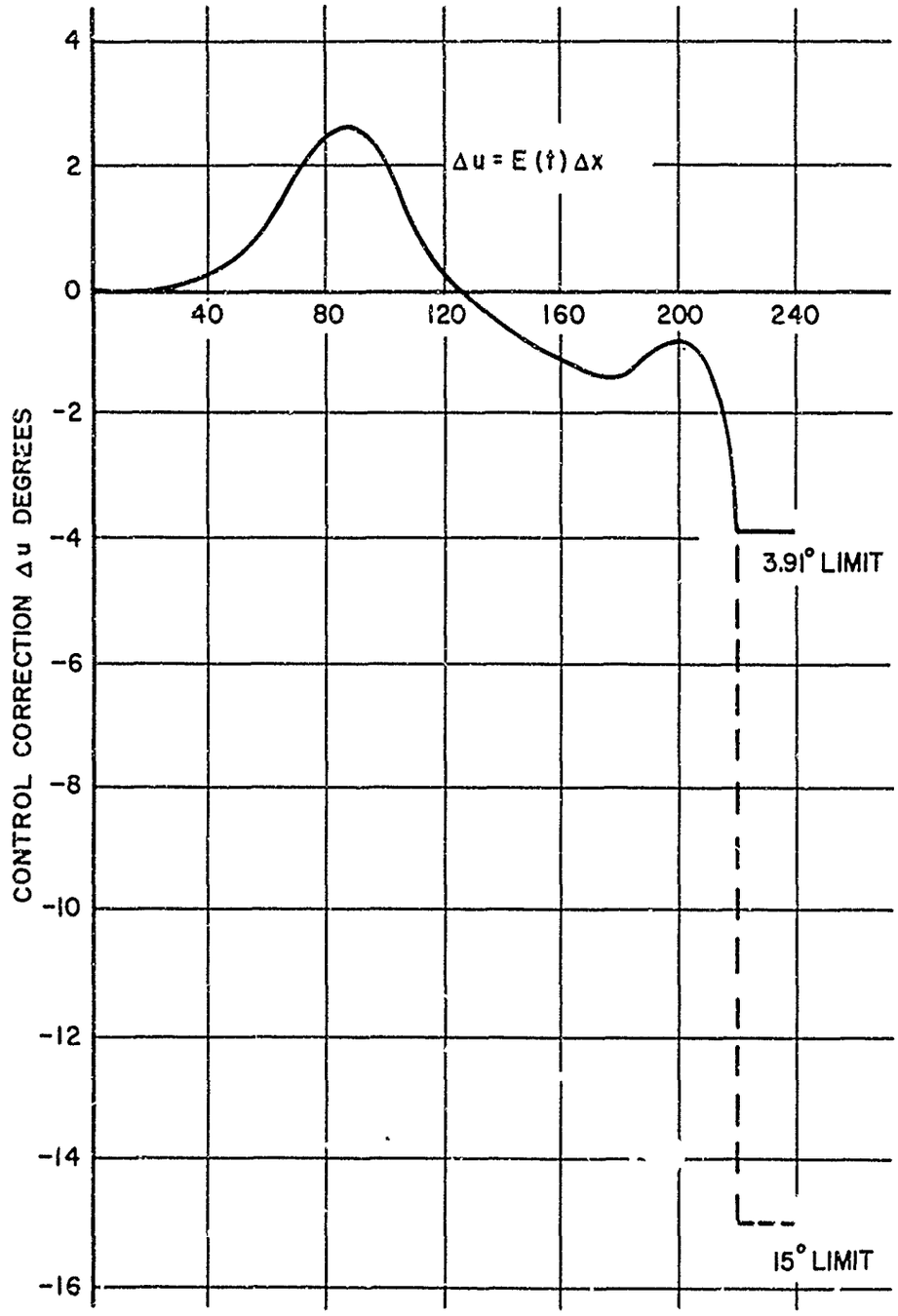

Figure 4-44. Control Correction Case: Initial Perturbation $\Delta\alpha_o$ = 0.05 degree

ERRATA SHEET FOR FDL-TDR-64-13, VOLUME I,

FEASIBILITY STUDY OF NEW TECHNIQUES FOR CONTROL OF RE-ENTRY VEHICLES

1296 28 136

page 8, Equation (2.1), should read

$$J = g(T,x(T)) + \int_0^T f_o(x,u)d\tau$$

page 21 line 6 from bottom - first word is Equations

page 23 line 5 from bottom - first word is Variables

page 26 The off-diagonal terms in matrix at bottom of page are $\nabla_{p_o} \dot{J}$ and $\nabla'_{p_o} \dot{J}$ respectively.

page 27 last equation is numbered (2.71). Also, the g in the last term should be Ψ_i.

page 31 Equation (2.92) requires brackets as in equation (2.91).

page 32 line 2, (A28) should be (A.28)

Equation (2.96) should read

$$(\nabla_{p_o} x_{n+1})_1 = \nabla_{p_o} x_{n+1}(t_1) + [x^-_{n+1}(t_1) - x^+_{n+1}(t_1)]\nabla_{p_o} t_1$$

page 34 - line 10 from bottom - capital P should be lower case for page

page 35 delete lines 9 and 10 from bottom

page 46 Equation (3.41) p should be p' (transposed, or row vector).

page 48 line 8, a^2+2 should be $\sqrt{a^2+2}$

page 52 line 8 from bottom - the a should be α

After line 6 add the following: The minimum principle is satisfied by the rules at the top of page 49. A corner exists at a point where p_2 passes through zero. Integrations must be restarted at such a point with $\alpha_{NEW} = \pi - \alpha_{OLD}$, provided that $\dot{p}_2 \neq 0$.

page 53 line 8 from bottom - α_1 should be α.

page 59 Equation (3.67) - $\frac{\partial q}{\partial x_3}$ in the third equation should be $\frac{\partial \dot{q}}{\partial x_3}$.

equation (3.68), last term - u_2 is μ_2.

page 60 line 8, the first term of the vector is $p_1 v C_{DL}$.

page 61 line 3, the 3rd and 4th words should be "when either"

line 7 from bottom - u_1 should be μ_1.

page 63 equation (3.79) should read $-|u| < \phi < |u|$

equation for μ_2 is numbered (3.80), and should read

$$\mu_2 = -\frac{g_o}{v}\sqrt{\frac{[C_L^2 + C_D^2][(C_{LO}p_2)^2 + (C_{DL}p_1 v)^2]}{(b^2 - ac)}}\ \frac{\sin(u-\phi)}{\sin u} \qquad (3.80)$$

line 10 should read ...and $\mu_2 = 0$ with $\dot{\mu}_2 \neq 0$,....

Equation (3.81) - the first column elements should have dots above them (except for the zero) to indicate time derivatives, i.e., $\dot{v}(T)$, etc.

page 64 Equation (3.82) - the first element of the matrix is $-\dot{p}'(T)\dot{x}(T)$ and the third element is $-\nabla'_{p_o} x(T)\dot{p}(T)$.

page 65 Equation (3.84) The left-hand side should be the same as that for equation (2.35) on page 17.

Expression (3.85) should read

$$(\nabla'_y \psi_2)^{-1} \nabla^2_y J (\nabla_y \psi_2)^{-1}$$

Equation (3.86) - The first column elements of the inverted matrix should have dots over them to indicate time derivations.

Line 4 from bottom - (3.85) should be (3.86)

page 66 line 2 - "completed" should be "computed".

page 70 - equation (4.7) should read

$$\dot{\Delta x} = [\nabla_x f + \nabla_u f\, E]\Delta x$$

page 72 equation (4.11) - the arguments t_o in the second terms should be "a".

page 73 equation (4.14) - the a_o's should all be a's.

the dimension of Λ' should be $((n-q)xn)$

page 74 - line 6 from bottom - range on t should be $a \leq t < T$.

page 75 equation (4.22) should read $\rho = \rho_o e^{-\beta R\xi}$

page 76 line 2 - the atmosphere coefficient should be 1/23500.

line 4 from bottom: $\gamma_o = -6.4$ degrees.

page 79 last line... the 10-g acceleration limit.

page 94 line 3 - the last word is "law"

page 95 line 4 - α should be γ

page 110 Reference 6 - replace "Report" by TR-R-

Reference 7 - "Atmosphere" should be "Atmospheres"

replace "Report" by TR-

Reference 9 - Replace "Report" by TR-

page 111 Reference 19 - the original paper number is 61-6

page 112 Reference 27 - add (1961)

page 113 the right-hand side of equation (A.1) should be $-\dot{p}'$

Equation (A.4) should read $0 \geq \mu$

page 119 the initial condition for equation (A.36) is $x_{n+1}(0) = 0$

the lower limit for the integral of equation (A.37) is 0.

page 122 delete the last sentence of the first paragraph